Synthesis and characterisation of high performance flocculants and superabsorbents from chemically modified starch and glycerol

AD Mohammed

23946822

Thesis submitted for the degree *Philosophiae Doctor* in Chemistry at the Potchefstroom Campus of the North-West University

Promoter: Prof DA Young

Co-promoter: Prof HCM Vosloo

October 2015

Abstract

Keywords: Starch acrylates, Gliserol acrylates, polymerization, super absorbents, xanthates, heavy metal removal

Superabsorbent polymers from chemically modified starch and glycerol have been prepared by acryloylation of starch followed by grafting with acrylic acid (AA) using Fenton's initiation system (Fe^{2+}/ H_2O_2). Fourier-transform infrared spectroscopy (FTIR) analyses provided evidence of starch ester formation and grafting of AA onto its backbone. Further characterisation of the product was carried out using X-ray diffraction (XRD), scanning electron microscopy (SEM) and thermogravimetric (TGA) techniques. The number of acryloyl groups per starch molecule and degree of neutralisation determine the superabsorbent behaviour of the samples. Under all the experimental conditions studied, polymer samples with improved grafting percentage, ratio, efficiency and low amount of homopolymer with excellent water retention ability and remarkable absorbency under load were obtained. Furthermore, glycerol acrylate (GA) was synthesised by acryloylation reaction with acryloyl chloride. The ester was used as cross-linking agent at varying proportions in the synthesis of poly(acrylic acid) (PAA) and acryloylated starch-*g*-poly(acrylic acid). The amount of cross-linking density in the products and the degree of neutralisation determine the absorbency of the polymer samples. The use of the cross linker enhances the absorbency of the samples up to a level when excessive cross-linking produces a rigid and a tightly-framed structure that limits the absorption of water within the polymer network. Moreover, the thermal behaviour of the samples was affected by the chemical processes involved.

Alternatively, starch grafted with poly(acrylic acid) (starch-*g*-PAA) was synthesised via free radical polymerisation using a new radical initiator. Oxy-catalyst, which is a $^{\cdot}OH$ generating catalyst from H_2O_2, was used for the first time as the initiator with aluminium triflate as co-catalyst. The percentage add-on (% add-on) and the grafting efficiency (GE %) were dependent to a degree on the amount of co-catalyst, temperature, starch to monomer ratio and time of the reaction.

Starch and glycerol xanthates were also synthesised and used for metal scavenging activities.

Xanthates from both glycerol and insoluble starch are synthesised and effectively used in the removal of Pb, Cd and Cu from aqueous solutions. The insoluble metal complex formed

between the sulphur atoms in the xanthates and the heavy metals easily separated. Moreover, use of glycerol xanthate requires no pH adjustment to give a 100 % heavy metal removal within the range of the detection limit. Butyl xanthate was also synthesised to allow a good comparison with the glycerol and insoluble starch xanthate. The latter was proven to be more effective in metal scavenging activities. FTIR was used to prove evidence of xanthation. In addition, ^{1}H and ^{13}C NMR were used to characterise the glycerol xanthate.

The chemical modification of the two sustainable resources find application in other areas such as capping agents of nanoparticles and as sulphur donor species in complex reactions for the synthesis of nanoparticles.

Opsomming

Sintetisering en karakterisering van hoë werkverriging flokkulante en superabsorberendepolimere vanaf chemies-gemodifiseerde stysel en gliserol

Sleutelwoorde: styselakrilaat, gliserolakrilaat, polimerisasie, superabsorbeerders, xantate, swaarmetaal verwydering

Superabsorberende polimere is vanaf chemies-gemodifiseerde stysel en gliserol deur akriloïlering van stysel berei, gevolg deur inenting met akrielsuur (AA) deur gebruik van Fenton se inisiasiesisteem (Fe^{2+}/ H_2O_2). Fourier-transformasie-infrarooispektroskopie (FTIR) analises het styselestervorming en inenting van AA op die ruggraat bewys. Verdere karakterisering van die produk is uitgevoer dmv X-straaldiffraksie (XRD), skandeer-elektronmikroskopie (SEM) en termogravimetriese (TGA) tegnieke. Die aantal akriloïelgroepe per styselmolekuul en die graad van neutralisasie bepaal die superabsorpsiegedrag van die monsters. Deur middel van eksperimentele kondisies wat bestudeer is, is polimeermonsters met verbeterde inentingspersentasie, -verhouding en -doeltreffendheid gesintetitseer. Slegs lae hoeveelhede homopolimeer is in die proses gesintetiseer. Die polimere het uitstekende waterretensievermoë en merkwaardige absorbering onder las aangetoon. Verder is gliserolakrilaat (GA) gesintetiseer deur 'n akriloïeleringsreaksie met akriloïelchloried. Hierdie ester is aangewend as kruisbindingreagens by verskillende verhoudings in die sintese van poli(akrielsuur) (PAA) en geakriloïeleerde, ingeënte stysel-*g*-poli(akrielsuur). Die mate van kruisbindingsdigtheid in die produkte en die graad van neutralisasie bepaal die absorbeervermoë van die polimeermonsters. Die gebruik van die kruisverbinder bevorder die absorbeervermoë van die monsters tot 'n vlak waar totale kruisbinding 'n rigiede en digte struktuur lewer wat die absorpsie van waterige verbindings binne-in die polimeernetwerk beperk. Verder word die termiese gedrag van die monsters beïnvloed deur die betrokke chemiese prosesse.

Alternatiewelik is stysel ingeënt met poli(akrielsuur) (stysel-*g*-PAA), gesintetiseer via vryradikaalpolimerisasie met gebruikmaking van 'n nuwe radikaalinisiëerder. 'n Oksikatalisator, wat 'n ˙OH-genererende katalisator vanaf H_2O_2 is, is vir die eerste keer gebruik as die inisiëerder met aluminiumtriflaat as ko-katalisator. Die persentasie toevoeging

(%toevoeging) en die inentingsdoeltreffendheid (GE %) was tot ’n mate afhanklik van die hoeveelheid ko-katalisator, temperatuur, stysel-tot-monomeerverhouding en reaksietyd.

Stysel- en gliserolxantate is ook gesintetiseer en gebruik vir metaalherwinning. Xantate vanaf beide gliserol en onoplosbare stysel is gesintetiseer en effektief gebruik in die herwinning van Pb, Cd en Cu vanuit waterige oplossings. Die onoplosbare metaalkompleks, gevorm tussen die swawelatome in die xantate en die swaarmetale, is maklik geskei. Voorts vereis die gebruik van gliserolxantaat geen pH-verstelling om ’n 100% swaarmetaalvewydering tot onder die deteksielimiet te bereik nie. Butielxantaat is ook gesintetiseer met die oog op ’n geldige vergelyking met die gliserol- en onoplosbare styselxantate. Laasgenoemde het geblyk meer effektief te wees ten op sigte van metaalherwinning. FTIR is gebruik om xantatisering te bewys. Verder is ^{1}H en ^{13}C KMR gebruik om gliserolxantaat te karakteriseer.

Die chemiese modifikasie van die twee volhoubare bronne vind toepassing op ander gebiede, soos bv. as blokkeringsreagense by nanopartikels en as swaweldonorspesies in kompleksreaksies vir die sintese van nanopartikels.

Dedication

I dedicate this work to my Mother, Maimunat, for her unceasing support and love.

Acknowledgements

Thanks and glory is to Allah, the most merciful who gave me the power and courage to carry out this work.

I wish to express my profound gratitude to Prof. Desmond A. Young for his useful advice and guidance throughout the period of this work. I am also glad to express my sincere gratitude to Prof. HCM Vosloo for his valuable suggestions and patience in going through the work.

I would also like to thank the following people and organisations for their contributions to this project:

Dr DC Onwudiwe and Prof. Christien Strydom for their immense assistance in this project.

Dr Frans Marx for his input in the preparation of the manuscript.

Dr LouwrensTiedt, Dr Anine Jordaan of the Laboratory for Electron Microscopy and Belinda Venter, North-West University, for the SEM and XRD analyses, respectively.

Mr André Joubert for the NMR analyses

NRF and Sasol for funding and supply of chemicals for the project.

The following people: Dr Ismael Amer, Dr Modupe Ogunrombi, Hestelle Stoppel, Nisha Brock, Grogory Okolo and all the students in the synthesis and catalysis group for their help and being friendly.

Lastly and not the least, I thank all my family and friends who have rendered their support and encouragement throughout the period of the project.

Table of contents

Chapter 1

Introduction and objectives

Chapter 2

Historical and theoritical background

Chapter 3

Synthesis and characterisation of superabsorbents from starch grafted with acrylic acid

Chapter 4

Synthesis of high performance superabsorbent glycerol acrylate-cross-linked poly (acrylic acid)/poly (acryloylated starch copolymers)

Chapter 5

Graft copolymerisation of acrylic acid onto starch using oxy-catalyst/aluminium triflate as intiators

Chapter 6
Synthesis of xanthates from glycerol and starch for removal of heavy metals ions

Chapter 7

Miscellenous applications

Chapter 8

Conclusions and recommendations

Appendices

List of publications

- ✓ Aliyu D. Mohammed, Desmond A. Young, Hermanus C.M. Vosloo. Synthesis and Study of Superabsorbent Properties of Acryloylated Starch Ester Grafted With Acrylic Acid. Article Starch/Starke 2014, 66:1–7.

- ✓ Aliyu D. Mohammed, Damian C. Onwudiwe, Desmond A. Young, Hermanus C. M. Vosloo. "Synthesis of Highly-Confined CdS Nanoparticle by Copolymerisation of Acryloylated Starch. Materials Letters, 2014, 114:63-67

- ✓ Damian C. Onwudiwe Aliyu D. Mohammed, Christien A. Strydom, Desmond A. Young, Anine Jordaan Colloidal synthesis of monodispersed ZnS and CdS nanocrystals from novel zinc and cadmium complexes Superlattices and Microstructures 2014, 70:98–108

List of Abbreviations

φ	Degree of swelling
AA	Acrylic acid
ACE	Associated chemical enterprise
ACN	Acrylonitrile
AGU	Average glucose unit
AM	Acrylamide
AS	Acryloylated starch
AS-g-PAA	Acryloylated starch graft poly(acrylic acid)
AS-g-PAA-GA	Acryloylated starch graft poly(acrylic acid) cross-linked
ATRP	Atom transfer radical polymerisation
AUL	Absorbency under load
CAN	Ceric ammonium nitrate
CAS	Cross-linked acryloylated starch
CAS-g-PAA	Cross-linked acryloylated starch graft poly(acrylic acid)
DIC	Diisopropylcarbodiimide
DMA	N,N′-Dimethyl acetamide
DMAP	4-Dimethyl amino pyridine
DMF	N,N'-Dimethylformamide
DMSO	Dimethylsulfoxide
DS	Degree of substitution
DSC	Differential Scanning calorimetry
DTG	Derivative thermogravimetric
EPI	Epichlorohydrine
FAS	Ferrous ammonium sulphate
FTIR	Fourier transform infra-red microscopy
GA	Glycerol acrylate
GA-PAA	Glycerol acrylate poly(acrylic acid)
GE	Grafting efficiency
GR	Grafting ratio

GX	Glycerol xanthate
HP	Homopolymer
HSAB	Hard Soft Acid Base
ICP-MS	Inductively coupled plasma mass spectroscopy
ISX	Insoluble starch xanthate
KPS	Potassium persulfate
ND	Not detected
NMR	Nuclear magnetic resonance spectroscopy
PAA	Poly(acrylic acid)
PAS	Poly acryloylated starch
PEP	Phosphoenolpyruvate
PG	Percentage grafting
PMMA	Polymethylmethacrylate
SEM	Scanning electron microscopy
SME	Specific mechanical energy
Soln	Solution
TEM	Transmission electron microscopy
Temp.	Temperature
TGA	Thermogravimetric analysis
XRD	X-ray diffraction analysis

Chapter 1

Introduction and Objectives

1.1 Introduction

Scientific knowledge has become a useful tool for handling the menace of human overpopulation and environmental offensives from technological growth of the world today. The daunting problems of global climate change, ozone depletion, pollution, resource exhaustion and population growth are factors to reckon with in our world today. Their effective control and solutions are quite relevant for the survival of the human race on earth [1]. Environmental and economic conditions are always considered in implementation and execution of the scientific approach in problem-solving of grave issues that threaten the ecological and overall stability of our planet.

Synthetic products have gained a wide application in different industries due to the fear of depleting the availability of natural materials. Additionally, they have unique features and advantages such as being easily tailored and processed to the desired property. However, unlike natural materials, synthetic products are often associated with toxicity, high cost and non-biodegradability. These considerations cause the world to focus on environmentally friendly and low economic demand techniques and the usage of natural materials with little or no ecological and economic damages in controlling the harmful effects and incessant demands of high population. However, persistent usage of natural and non-synthetic materials could lead to a compromise to their availability for future usage. Hence the need for the use of sustainable resources becomes a fundamental approach in our world today.

1.2 Sustainable resources

Sustainable resources have attracted much attention from different industries for the manufacture of simple household wares to pharmaceutical and agricultural applications. These include materials from agricultural crops such as starch, cellulose, rubber and other materials that could be replenished quickly without total exhaustion of the global reserve. Apart from being renewable; the resources are nature-based and therefore abundantly available, have limited pollution effects on the environmental setup and are cost effective. This research focuses on the effective utilisation of naturally occurring and related materials which could be chemically modified to find applications as superabsorbent, heavy metal scavengers and other applications.

1.3 Chemical modification of the resources

Chemical processing of starch and similar materials from natural sources are often met with some limitations in various applications. For example, the limitations include poor adaptability, inferior properties and the need for high quantity of the product for a desired application. These limitations of nature-based materials are checked by chemical modification of the materials, as this imparts new and improved properties into the starting material; hence, making them more satisfactory to use. More importantly, the chemical treatments add some new features without inhibiting the desired properties of the starting material. The standard techniques used in the chemical industry for modification of nature-based materials include esterification, etherification, graft copolymerisation and oxidation.

1.4 Superabsorbents

Superabsorbents are materials that can absorb and retain water such as water, human urine and blood, several times their weight. They are usually made up of cross-linked, three-dimensional flexible networks of polymer chains containing hydrophilic groups like hydroxyl, carboxyl, amine or imide groups in their structure [2]. Furthermore, typical absorbents (such as tissue papers, polyurethane foams, wood pulp, and domestic sponges) quickly loose the water under application of slight pressure. Conversely, superabsorbents have a remarkable ability to retain the water even under pressure. Because of this impressive ability, superabsorbents find a wide range of application in agriculture [3], drug delivery [4] and dew-preventing coatings [5].

1.5 Metal scavenging

Water-soluble salts of heavy metals, such as lead, cadmium, mercury and copper have become one of the biggest challenges of the human population today. The prevalence of the metals in water and their lethal effects call for general attention to the purification of water, by removing the harmful metals thereby making the water fit for drinking. Among the chemical processes that have been employed are chemical precipitation, oxidation and reduction processes, ion exchange, reverse osmosis, evaporative recovery and electrochemical treatment [6]. Newer and more efficient techniques used today are the graft

copolymers of starch and vinyl monomers (acrylics) and xanthates. Starch grafted with acrylamide [7] and poly(MAA) [8] have been extensively used as heavy metal scavengers. Alkyl xanthates such as ethyl xanthates are also used effectively in trapping copper metal ions from wastewater [9]. Soluble starch xanthates [10] and insoluble starch xanthate [11] are experimentally proven to remove heavy metals from waste water.

1.6 Objectives

The aim of this work is to study the properties and applications of chemically modified starch and glycerol without sacrificing their desired native properties. Since both substances contain polar hydroxyl groups at more than one position in their structures, chemical transformations at these sites become quite a straightforward process in the formation of chemically modified products with enhanced quality and efficiency in application. The superabsorbency of grafted starch poly(acrylic acid), heavy metal removal from waste water using starch and glycerol xanthates and miscellaneous applications were investigated.

The objectives of the study are as follow:

1. Investigate the cross-linking and acryloylation of starch with acryloyl chloride and grafting with acrylic acid using Fenton's initiation system.
2. Study the superabsorbency of the polymers in water, saline solution and under pressure.
3. Study the copolymerisation of starch with acrylic acid using glycerol acrylate as cross-linking agent. Varying the cross-linking densities would determine the effect on the physico-chemical properties of the product.
4. Synthesis of polyacryloylated starch and its application as capping agent of CdS nanoparticles
5. Study the grafting parameters of copolymerisation of starch with acrylic acid using an oxy-catalyst initiator. Oxy-catalyst, like Fenton's reagent, is a hydroxyl generating radical and is used for the first time to initiate graft-copolymerisation of starch with acrylic acid, instead of ferrous ammonium sulphate with hydrogen peroxide.
6. Synthesis of starch and glycerol xanthates and their metal scavenging activity on lead, cadmium and copper II ions from waste water.
7. Miscellaneous applications of xanthates. For instance, as sulphur donor species in the production of nanoparticles.

1.7 Layout of the Thesis

The research work is composed of seven chapters. Chapters 3–7 describe the experimental work on the chemical modification of the sustainable resources (in this case starch and glycerol). Furthermore the characterisation of the products and applications of the modified products as superabsorbents, capping agents of nanoparticles and as heavy metal scavengers are also discussed.

The layout is as follows:

Chapter 1: Introduction and objectives

Chapter 2: Historical and theoretical background

Chapter 3: Synthesis and characterisation of superabsorbents from starch grafted with acrylic acid.

The chapter is about the synthesis of acryloyl chloride followed by its reaction with starch to produce acryloylated starch ester, which was then grafted with acrylic acid to form starch-g-PAA polymer. Another polymer was also synthesised by cross-linking of starch followed by the formation of starch ester (acryloylation) and then grafted with acrylic acid. The polymer samples obtained in each procedure were characterised and tested for superabsorbency in water, saline solution and absorbency under load.

Chapter 4: Synthesis of high performance superabsorbent glycerol acrylate-cross-linked poly(acrylic acid)/poly(acryloylated starch) copolymers

The chapter describes the synthesis of glycerol acrylate and its application as a cross-linking agent in the synthesis of superabsorbents poly(acrylic acid) and acryloylated starch poly (acrylic acid). The effect of cross-linking density and other reaction conditions on the grafting parameters were studied.

Chapter5: Graft copolymerisation of acrylic acid onto starch using oxy-catalyst/Aluminium triflate as initiators

The chapter discusses the grafting of starch with acrylic acid using oxy catalyst as initiator instead of ferrous ammonium sulphate. The grafting parameters were studied to assess the suitability of the new catalyst in grafting vinyl monomers such as acrylic acid onto starch.

Chapter 6: Synthesis of xanthates from glycerol and starch for removal of heavy metal ions

The chapter describes the synthesis and characterisation of starch and glycerol xanthates and their application in the removal of lead, cadmium, copper metal ions from wastewater.

Synthesis of butyl xanthate is discussed in this chapter and its application as sulphur-donor group in the production of CdS nanoparticles

Chapter 7: Miscellaneous applications

This chapter covers the synthesis of poly (acryloylated starch) and its application as capping agent of nanoparticles from CdS in an *in situ* process. It also includes the use of butyl xanthate (which is commercially used) as sulphur donor group in metal complex formation for generating nanoparticles.

Chapter 8: Conclusions and recommendations for further work

1.8 References

[1] Swisher S. *The Park Place Economist*, 2006, 14:88 – 95.

[2] Kiatkamjornwong S. *Sci. Asia* 2007, 33:39–43

[3] Po R. *J. Macromol. Sci., Rev. Macromol. Chem. Phys.* 1994, 34:607–661

[4] Kikuchi A., Okano T. *Adv. Drug Delivery Rev*. 2002, 54:53–77

[5] Chen J., Zhao Y. *J. App. Polym. Sci.* 1999, 74:119–124

[6] Wing E.A., Swanson C.L., Doane W.M., Russell C.R.J. *Water Pollution Control Federation*, 1974, 46:2043–2047

[7] Tripathy T., De B.R. *J. Phys. Sci.* 2007, 11:139–146

[8] Mostafa K.M., Samarkandy A., El-Sanabary A.A. *J. App. Polym. Sci.* 2009, 112:2838–2846

[9] Chang Y., Chang J., Lin T., Hsu Y. *J. Hazard Mater.* 2002, 94:89–99

[10] Chaudhari S., Tare V. *J. App. Polym. Sci.* 1999, 71:1325–1332

[11] Chang Y.K., Shih P.H., Chiang L.C., Chen T.C., Lu H.C., Chang J.E. *Environ. Informa. Archives,* 2007, 5:684–689

Chapter 2

Historical and Theoretical Background

2.1 Starch

Starch is one of the naturally occurring reserves of polysaccharides that are nontoxic, biodegradable and inexpensive. Starch is found naturally in the seeds, roots or tubers of different plants, such as corn, maize, wheat, rice, potato and cassava [1,2]. It is widely produced for industrial exploitation around the globe. In the year 2003, the total worldwide production was approximately around 66 million tonnes [3]. It is noteworthy that the industrialised countries produce more starch than others. USA is the highest producer followed by countries in Europe and Asia [4,5].

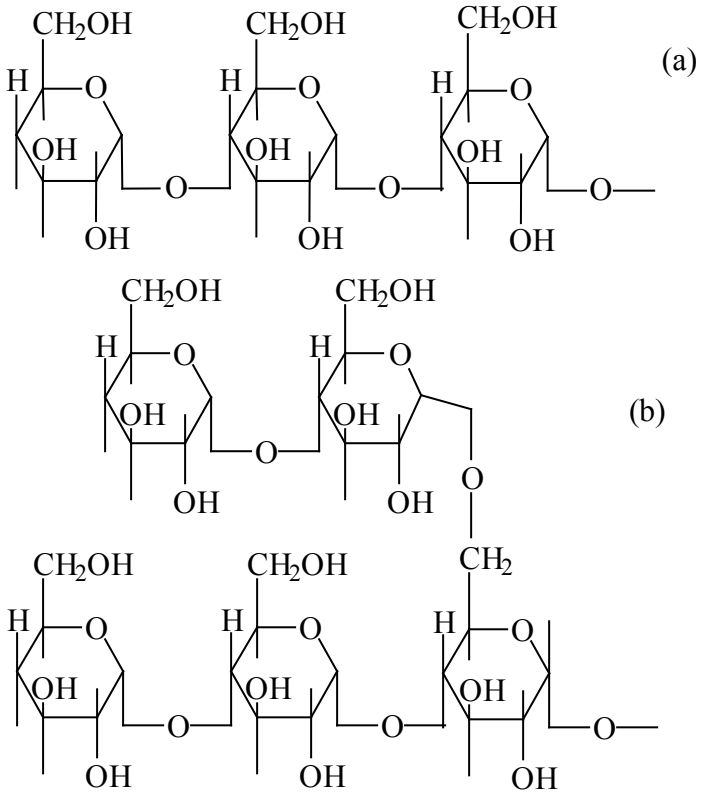

Figure 2.1 Structures of (a) amylose and (b) amylopectin

Starch primarily consists of two polymeric components: amylose and amylopectin. Amylose is a linear component of starch with the polymer units connected through α-D-(1,4)- glucosidic linkages. The percentage composition of amylose is typically in the range of 18 – 28 % [1]. Amylopectin is the branched polymer component with the units linked together through α-D- (1,6)-glucosidic bonds [1]. Fig. 2.1 shows the structures of amylose and amylopectin; the molecules of amylopectin are generally larger and present in a higher

percentage than amylose and the ratio depends on the starch source. Each component and its percentage ratio determine the functionality and overall properties of the starch, such as crystallinity, solubility, viscosity, swelling ability and gelatinisation [6].

2.1.1 Uses of starch

Starch has been considered a useful material in industries, mainly because of its biodegradability, availability, non-toxicity, high purity and low-cost [7].

Table 2.1 Various applications of starch in different industries [8].

Industry	Application
Pharmaceutical	Soap filler/extender, dusting powder make-up face creams, pill coating, tablet binder/ dispersing agent
Metallurgical	Sintered metal additive, sand casting binder, foundry core binder
Paper	Internal sizing, filler retention, paper coating, paper stilt material, surface sizing, disposable diapers,
Textile	Warp sizing, fabric finishing, printing
Construction	Fire resistant wall board, asbestos clay/limestone binder, plywood/ chipboard adhesive, concrete block binder, gypsum board binder
Mining	Ore floatation, ore sedimentation, oil well drilling muds
Adhesives	Hot melt glues, stamps, book binding, wood adhesives, laminations, corrugation, paper sacks, engineering pressure-adhesives, envelop labels.
Miscellaneous	Wide range binding agents, biodegradable plastic film, dry cell batteries, printed circuit boards, leather finishing, match head binder.

2.2 Glycerol

Glycerol and other renewable carbon sources have attracted attention in different industries due to the rising concern of fossil resources in terms of cost, sustained availability and environmental pollution [9]. The abundance of glycerol from both synthetic and natural sources enhances its immeasurable importance in the pharmaceutical and biodiesel industries. It occurs abundantly as the main structural components of many lipids [10], and it is also the

principal by-product obtained from trans-esterification reactions of vegetable oils and animal fats [11,12]. Fig.2.2 shows the production of glycerol from different routes in the oil and fats processing industry. The structural feature of glycerol favours easier chemical conversions to obtain desired products in industries. For instance, Dharmadi *et al.* [13] reported that glycerol exhibits a greater degree of reduction than sugars. Thus glycerol offers a higher opportunity to obtain reduced chemicals at higher yields such as succinate, ethanol, xylitol, propionate, and hydrogen than from sugars. For example, the conversion of glycerol to glycolytic intermediates, phosphoenolpyruvate (PEP), produces twice the amount of reducing equivalents produced by the metabolism of glucose or xylose [14].

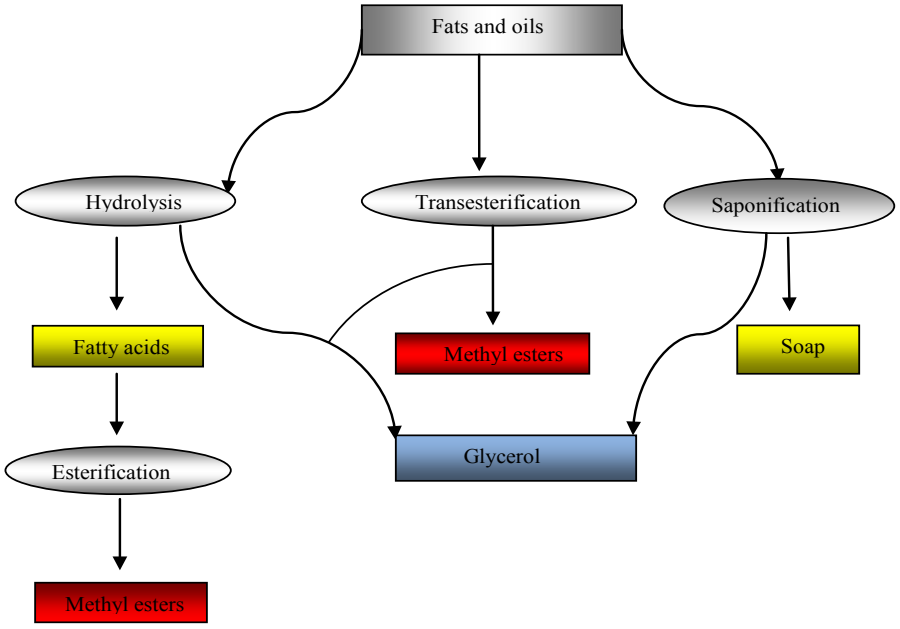

Figure 2.2 Schematic diagram showing the production of glycerol from fats and oils [15].

2.3 Xanthates

The use of xanthates in heavy metal scavenging activity is considered a promising technique [16] and involves a low-cost operation. The efficiency of the technique lies in the formation of insoluble complexes with the heavy metal ions. Unlike in the sulphide precipitation technique, use of xanthates is not associated with the problem of residual

sulphide in the treated water [17]. Different kinds of xanthates are used industrially in the treatment of wastewater to get rid of unwanted and harmful metal ions. Starch xanthate, like other forms of xanthates, has been reported to have an impressive efficiency in metal scavenging activity [16–20]. Glycerol polyhydroxy sodium xanthate has been used as a depressing agent in the separation of minerals due to its structural features [20].

2.4 Chemical modification of starch

Starch, as a natural polymer, is modified physically, chemically or enzymatically in order to overcome some of the limitations encountered in its applications such as high water sensitivity, poor mechanical strength and instability of its gels over time [21]. In otherwords, the modification enhances its desirable properties, such as thickening, gelling, binding, adhesion and film forming properties. The chemical modification is done to enhance its suitability and efficiency for grafting with vinyl monomers. It is expected that ester derivatives of starch would provide more sites for the grafting monomers to be bonded on the starch trunk.

Dzulkefly *et al*. [22] are reported to have carried out an esterification reaction of sago starch with fatty acid chlorides, but without any solvent. The sago starch was dried for two hours at 105 °C prior to esterification; formylation of the dried starch was done by reacting 2.5 g with formic acid (2.0 – 9.5 eq/glucose) at 25 °C for five minutes with constant stirring. This process was done to activate the glucose ring of the starch. Fatty acid chloride (2.0 – 10.0 eq/glucose) was then added drop wise, followed by heating in a three-necked round bottomed flask at 90 °C for 40 min with constant stirring. After the precipitation of the sago starch ester by the addition of 150 mL absolute ethanol, the mixture was centrifuged at 3000 rpm. The maximum yields of 80% and 73% with the same degree of substitution (DS) of 1, 2 for octanoate and lauroate sago ester were obtained respectively. The presence of the ester carbonyl group in the FTIR spectra of the ester product showed that the sago starch had been esterified. The intensities of carbonyl and methyl peaks decreased with the increase in the degree of substitution (DS) [22]. A similar chemical process was reported [23], whereby thermoplastic starch was subjected to a trans-esterification reaction with poly(vinyl acetate) and poly (vinyl acetate-co-butyl acrylate). In the procedure, wheat starch was reacted with the above-mentioned copolymers in an internal mixer at 150 °C in the absence of catalyst but in the presence of sodium carbonate, zinc acetate and titanium (IV) butoxide. The resulted

blends were characterised by the proton and carbon-13 nuclear magnetic resonance (^{1}H-NMR and ^{13}C-NMR) spectroscopy, DSC, DMTA, TGA and water absorption. It was confirmed that partial trans-esterification took place between the starch and the polymers from the^{1}H-NMR and ^{13}C-NMR spectroscopy result.

An alternative approach to starch esterification is based on biocatalysis, in which the polysaccharides are subjected to enzymatic action to give the starch ester. Lukasiewicz [24] outlined a chemical procedure to obtain the starch ester by enzymatic action. Maize starch was treated with an acylation agent (carboxylic acid with different aliphatic chains), at various temperatures, solvent and substrate/enzymes ratio. In this case, lipase was used. The product (esters) was analysed according to the degree of substitution that, however, showed that the technique could be used to obtain high substituted starches.

Similar research work was reported by Rajan *et al*. [25] whereby esterification of starch using recovered coconut oil by enzymatic action, produced a substituted starch ester derivative. The same enzyme, Lipase, was used in the process for complete hydrolysis of the fatty acids present in the recovered oil. Three (3) different esterification techniques were employed on the cassava and maize starch, and in each case the feasibility of the reaction was noticed based on the DS. Among the three (3) techniques reported, microwave esterification yielded a product with a higher DS compared to the solution and semi-solid state esterification. Lukasiewiz [24] reported the effective use of DMF as a solvent in solution state esterification and highlighted the limitation of DMSO as solvent. Similarly, Rajan *et al.* have observed the same limitation and non-effective use of DMSO for the esterification of cassava starch.

Starch can be chemically modified via esterification by using various acid anhydrides to give the substituted ester derivative. Jerachaimongkol *et al.* [26] reported a successful experimentation of cassava starch with different acid anhydrides; acetic anhydride, propionic anhydride, and butyric anhydride at 10, 20, and 40% w/w of the dried starch. The DS of the products showed a high correlation with the amount of esterifying agent. Another important parameter observed was the decrease in hydrophilicity of the starch ester, which further confirmed the substitution of hydrophilic hydroxyl groups (OH) with hydrophobic ester groups in the starch molecule.

A different technique was reported by Miladinov and Hanna [27], whereby starch esters were synthesised by extruding 70% amylose-starch with fatty acid anhydrides and sodium hydroxide (catalyst) in a single screw extruder. Acetic, propionic, heptanoic, and palmitic acid anhydrides were used at 0.01, 0.02, and 0.03 mol levels to obtain different degrees of

substitution (DS) in the starch. Like the works reported earlier, there was no significant difference in DS between the various acid anhydrides, but could only be observed when the amount of the fatty acids was varied. The lowest DS was obtained with the 0.03 mol level. The study agreed with the finding of Jerachaimongkol *et al*. [26]. Unlike the conventional methods of synthesising starch esters (i.e. in an aqueous medium), an extrusion technique was carried out in a short space of time. The extrusion technique has a range of applications in the polymer industry (in starch modification). For instance, starch-based novel micro-encapsulating agents were prepared using a reactive extrusion process [28]. The technique was, however, characterised by low specific mechanical energy (SME), which was an index of the relative ease with which a material could be extruded and the relative cost of the extrusion technique. The longer chain acid anhydrides, in this case, heptanoic and palmitic acid anhydride were less soluble in water and formed separate phases and therefore acted as lubricants between the extruder barrel and the viscous gelatinised starch. On the other hand, the long-chain fatty acids used in esterifying the starch reduced the molecular interaction between the starch molecules by sterically hindering hydrogen bonding. Less interaction between the molecules resulted in lower viscosity of the extrudate. These effects are expected to accumulate with increase in anhydride concentration. The net result is the decrease in SME for higher doses of long-chain fatty acids anhydride treatments [27].

Another approach to starch esterification was reported by Biswas *et al.* [29], whereby the esterification reaction was carried out using iodine as a catalyst in the presence of acetic anhydride. The reaction was conducted at 100 °C without the use of additional solvent. Starch derivatives (acetate) were produced in the experiment by using both conventional and micro-wave heating. The reaction was found to be much faster with a microwave heating source than with a conventional heating technique. The DS of the product increased with higher concentrations of iodine and acetic anhydride, up to a certain point where after the yield decreased with an increase in the concentration level of iodine and acetic anhydride. The use of iodine as catalyst had to be conducted with care, because excessive levels of acetic anhydride and iodine could cause acid hydrolysis and lead to the formation of peracetylated oligomers with high DS, with the product becoming plasticised and the physical properties affected [29].

Another route to a starch derivative is the procedure reported by Auzely-Velty and Rinauda [30]. In their work, starch esters with hydrolysable cationic groups were synthesised by reacting starch compounds with betain derivatives in the presence of diisopropylcarbodiimide (DIC) and 4-dimethylamino pyridine as coupling reagents in an aprotic solvent. Nevertheless,

owing to the low reactivity of DIC, it is more commonly used in an activated form, such as an acid chloride. This reaction was met with many problems which included non-completion of the reaction, non homogeneity of the starch ester molecules and the formation of extremely unstable betain acid chloride. These limitations necessitated the duo to devise a procedure for convenient esterification that could lead to homogenously substituted compounds. They outlined a procedure whereby the starch was dissolved in dimethyl sulfoxide (DMSO). The polymer was then reacted with N,N′-dimethyl glycine that was activated *in situ* by the addition of N,N′-diisopropylcarbodiimide (DIC) and 4-dimethyl amino pyridine (DMAP). The reaction proceeded smoothly at room temperature to give poly(N,N′-dimethyl glycyl) ester of starch in 74% yield. The NMR was carried out in D_2O. Digital integration of the NMR signals arising from the anomeric protons of starch and the methyl groups of N,N′-dimethyl glycine gave an average substitution of 0.3, indicating that the esterification reaction proceeded efficiently. IR spectroscopy was used to confirm the ester bond (1747cm^{-1}). The quarternisation of the ester amines was carried out with methyl iodide in DMSO at room temperature. After an ultra filtration process, the reaction was completed in a few hours to form starch betainate in chloride form with 89% yield.

2.4.1 Cross-linking

Cross-linking of native starch is aimed to add chemical bonds at random locations within the granules, thereby strengthening and stabilising the relatively tender swollen starch granules [31]. It also reinforces the granules to be more resistant towards acidic media, heat and shearing, which arises from the reduced mobility of the amorphous chains in the starch granules as a result of intermolecular bridges [32]. There are various chemical species that are used as cross-linking agents. These include sodium trimethaphosphate, sodium tripolyphosphate, epichlorohydrin, and phosphoryl chloride. Each of these compounds acts as a cross-linking agent by forming ether or ester intermolecular linkages between the hydroxyl groups on the starch molecule [33]. The cross-linking reactions take place either by intramolecular or intermolecular bonds between the polymer matrices. Fig. 2.3 shows the two modes of cross-linking reaction.

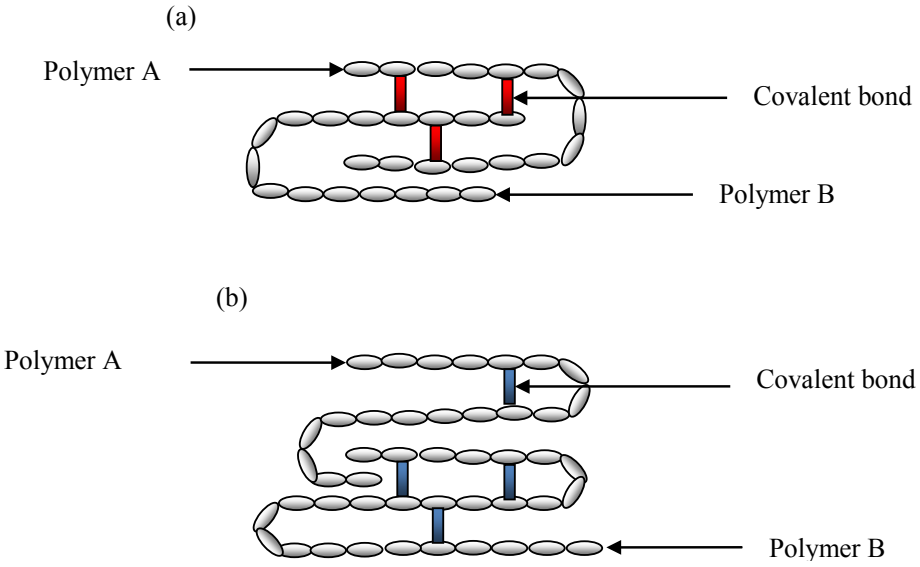

Figure 2.3 Schematic diagram showing (a) Intermolecular cross-linking and (b) Intramolecular cross-linking [34].

Cross-linking of starch prior to grafting with vinyl monomers is one of the other chemical techniques used to improve the physico-chemical properties of both the starch and the graft copolymer. Properties associated with native starch, such as poor freeze-thaw stability, resistance to shear and fair-to-poor stability to retrogradation [35] are improved via chemical cross-linking of starch molecules.

2.4.2 Acetylation

Starch acetate can be prepared by the reaction of starch with acetic acid [36], acetic anhydride [37,38], vinyl acetate [39], acetyl chloride and diketene [40]. The three free hydroxyl groups on C_2, C_3 and C_6 of the starch molecule can be substituted with acetyl groups during Acetylation. C_2 and C_3 are the carbon atoms containing the secondary –OH while C_6 is the carbon atom containing the primary –OH at the exterior surface. C_2 and C_3 are less reactive than C_6. Therefore, the theoretical maximum DS is 3. Pyridine is a good catalyst in the preparation of starch acetate with high DS because, apart from enhancing a complete esterification reaction, it also does not cause starch degradation during the reaction [41]. Scheme 2.1 shows acetylation reaction of starch with acetic anhydride. Chemical modification of starch via acetylation plays a fundamental role in limiting the retrogradation

property of starch especially in the food industry. It also enhances the desirable properties such as food safety and economic stability [40].

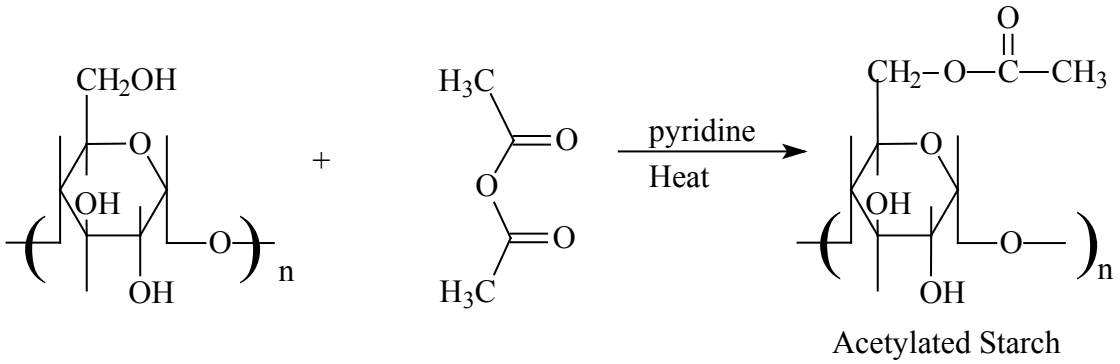

Scheme 2.1 Acetylation of starch using acetic anhydride.

2.4.3 Acryloylation

The introduction of acryloyl groups onto the backbone of chemical substrates, for instance starch and glycerol, improves the grafting parameters such as grafting efficiency and percentage add-on. The values of these parameters determine the effectiveness and economic viability of graft copolymerisation in polymer industries. The acryloylation of the substrates (starch and glycerol) increases the number of active sites ready for free radical polymerisation, as the number of double bonds that would react with the vinyl monomers is readily available on the backbone. In other words, the number of active propagating chains is increased in the grafting process, thus limiting the amount of homopolymers produced along the copolymer. Acryloylation of substrates like starch prior to copolymerisation improves the physico-mechanical properties of the copolymer, such as superabsorbency and adhesion-to-fibres [42]. Scheme 2.2 shows the chemical steps in the synthesis of acryloylated starch from acryloyl chloride and the grafting reaction with acrylic acid to produce the starch poly(acrylic) acid graft copolymer.

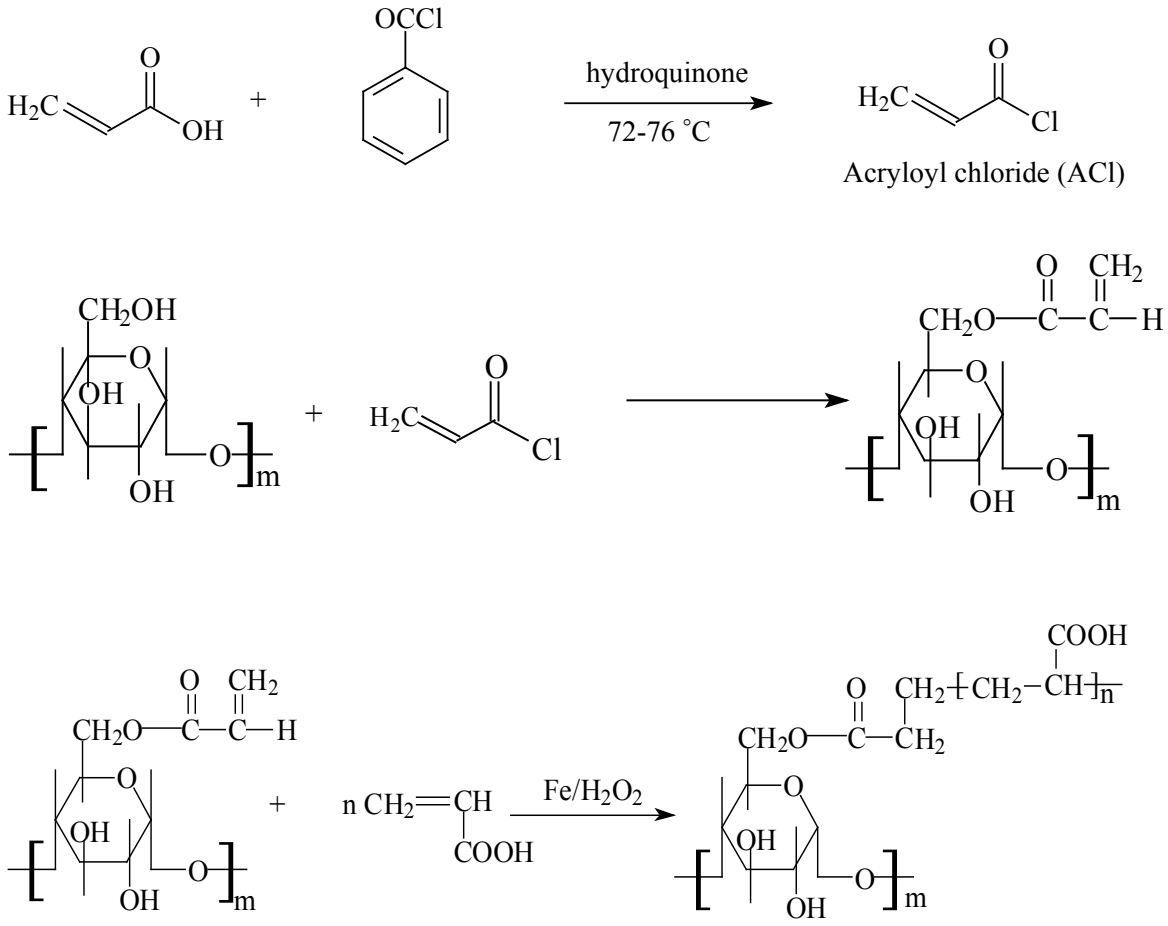

Scheme 2.2 **Acryloylation reaction of starch with acryloyl chloride. The structural features of starch allow a facile control of the degree of substitution (DS) on the acryloylated product.**

2.4.4 Xanthation

Xanthation is a process whereby chemical substances are mixed with carbon disulphide in alkaline conditions. The products (xanthates) are effectively used in the treatment of waste water from industrial effluents and domestic usage. The efficiency of the technique lies in the formation of insoluble complexes with the heavy metal ions that could be easily separated. The process is, however, not associated with the problem of residual sulphide in the treated water as was discovered with sulphide precipitation technique [43].

2.4.5 Free radical grafting onto starch and glycerol with vinyl monomers

Starch, other polysaccharides and chemical compounds like glycerol are chemically modified by generating free radicals on the substrate by the initiator. They then react with the monomers to produce a copolymer with added desirable properties. Many techniques are used in free radical grafting onto chemical substrates, such as starch and glycerol. These include: (i) chemical techniques, (ii) radiation (iii) photochemical and (iv) enzymatic processes. However, the techniques that are frequently used are the chemical and radiation processes.

2.4.5.1 Fenton's initiation

Fenton's initiation system is one of the chemical techniques that are widely used in free radical polymerisation. This is because the technique is identified with the availability of the reagents and the ability of the grafting process to be run at low temperatures without decomposing into harmful and toxic substances as is found with azo initiators [44]. The initiation step in these methods involves decomposition of the peroxide to form a hydroxyl radical that attacks the vinyl double bond producing the macro radical in the propagation step.

The Fenton reaction system involves generating of $^{\cdot}OH$ from the chemical interaction of hydrogen peroxide and ferrous ammonium sulphate. The Fenton redox initiation is postulated to follow the following steps (Scheme 2.3) [45].

$$Fe^{2+} + H_2O_2 \longrightarrow Fe^{3+} + {}^{\cdot}OH + OH^-$$

$$^{\cdot}OH + Fe^{2+} \longrightarrow Fe^{3+} + H_2O_2$$

$$^{\cdot}OH + H_2O_2 \longrightarrow H_2O + {}^{\cdot}OOH$$

$$^{\cdot}OOH + H_2O_2 \longrightarrow {}^{\cdot}OH + H_2O + O_2$$

Scheme 2.3 Free radical generation from Fenton's initiation system.

The reaction is easily controlled by adjusting the concentration of ferrous sulphate and hydrogen peroxide. Although chemical compounds like KPS are found to be efficient thermal initiators in aqueous medium, as reported [46], the $^{\cdot}OH$ species produced from Fenton

initiation system is highly electronegative and stronger than other radicals generating species such as $SO_3^{\cdot-}HSO_4^{-\cdot}$. In addition, it easily abstracts a proton to form a starch macro radical which facilitates a high grafting efficiency and ratio [47].

2.4.5.2 Ceric ammonium nitrate (CAN)

Ceric ammonium nitrate is a common chemical species used in free radical initiation in graft copolymerisation. The Ce^{4+} leads to the cleavage of the C-C bond or by the abstraction of proton from the hydroxyl groups in polysaccharides thereby facilitating grafting reactions resulting in the formation of ether linkages [48,49]. In some cases, the Ce^{4+} attacks the monomer to form a radical which results in homopolymer formation. Han *et al.* [50] proposed the following mechanism (Scheme 2.4) for graft copolymerisation of starch with vinyl monomers using a CAN initiator.

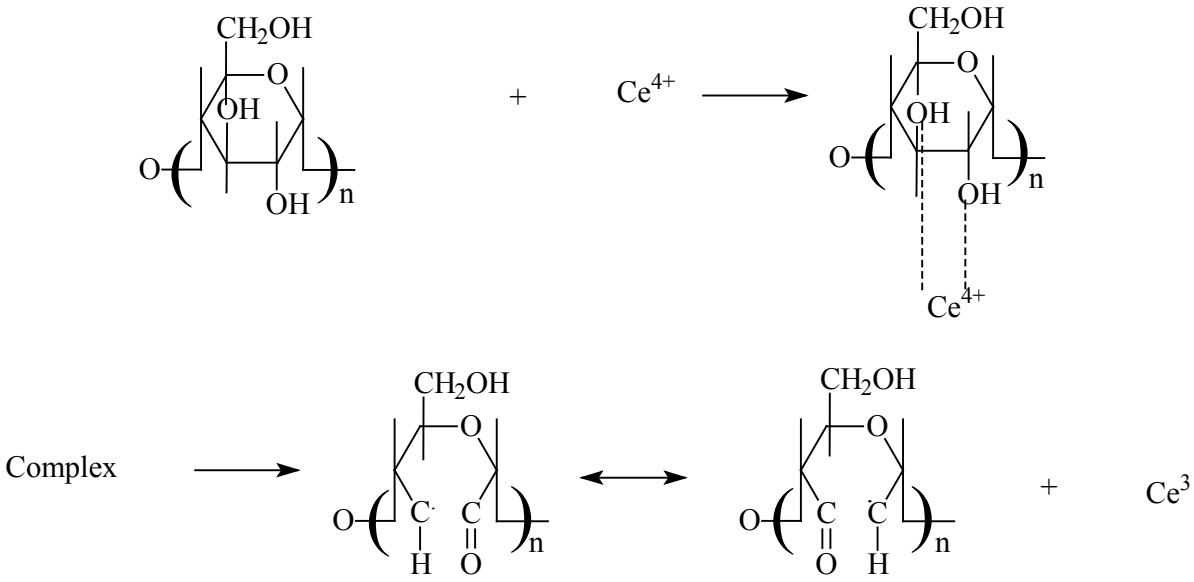

Scheme 2.4 **Free radical initiation system using CAN [49].**

CAN was found to be the most efficient initiator in free radical grafting of vinyl monomers onto starch in terms of a high yield and the least amount of homopolymers [47,51]. The technique involves a direct formation of starch macro radical before the propagation step. Apart from Ce^{4+} other transition metals are directly used via oxidation of the polymer backbone to generate free radicals; and these metal ions include Cr^{6+}, V^{5+} and Co^{3+} [52].

CAN is reported to have a useful role as initiator in the graft copolymerisation of vinyl monomers such as methyl methacrylate and other alkyl methacrylates onto polyacrylonitrile with carbohydrate end groups and starch grafted with acrylonitrile or starch acrylonitrile in conjunction with styrene. It was, however, reported to have some limitations as initiator in graft polymerisation of styrene, α-methyl styrene, 4-vinyl pyridine and ether vinyl ether onto starch. Moreover, water soluble monomers such as acrylamide, methacrylamide, acrylic acid, and methacrylic acid produce polymers with a low grafting percentage when CAN is used as the initiator [53].

2.4.5.3 Other chemical techniques used in graft copolymerisation

2.4.5.3.1 Controlled free radical polymerisation (Living polymerization).

This is one of the methods that have been developed to provide potential for grafting reactions, as it combines features of conventional free radical and ionic polymerisations and has the necessary function of generating a polymer having the ability to propagate for a very long time to the desired molecular weight [52]. Living polymerisation techniques are utilised for the production of polymers with predictable molecular weight and narrow molecular weight distribution. A typical example of living polymerisation is atom transfer radical polymerisation (ATRP) of styrene and various methacrylates using various catalytic systems. Dormant chains are capped by halogen atoms which are reversibly transferred to metal complexes in the lower oxidation state. In this process a transient growing radicals and complexes in the higher oxidation states are formed [54].

2.4.5.3.2 Ionic grafting.

This technique goes via two processes, (a) Lewis base liquid containing alkali metal suspension, whereby organometallic compounds and sodium naphthalenide are used as initiators or by using cationic catalyst BF_3(b) Anionic mechanism, whereby the sodium-ammonia or the methoxide of alkali metals form the alkoxide of the polymer (PO^-Na^+), which reacts with monomer to form the graft copolymer.

2.4.5.4 Grafting initiated by radiation technique

2.4.5.4.1 Free radical grafting.

This technique requires irradiation of the macromolecule to undergo homolytic scission. In this process, an initiator is not essential as the fission process leads to the formation of free radicals on the polymer.

A comparison in terms of advantages of the processes shows the following: while homopolymerisation is very unlikely to occur with the pre-irradiation technique, (since the monomers are not exposed to radiation, which occurs in a mutual irradiation process), the pre-irradiation technique, on the other hand, involves scission of the base polymer due to its direct irradiation, and this can lead to the formation of block copolymers [52].

2.4.5.4.2 Ionic grafting.

The process involves the formation of ions as a result of irradiation, instead of free radical formation. The polymer is irradiated to form ions, which could be cations or anions, depending on the polymer type. The potential advantage of this technique is the high reaction rate. In other words, small radiation doses are sufficient to bring about the requisite grafting [54].

2.5 Superabsorbency

The ability of polymer materials to absorb large quantities of water several times their own weight is called superabsorbency. Superabsorbent polymers are mostly cross-linked hydrophilic polymers synthesised from direct grafting of the monomers onto the backbone of the substrate with the aid of cross-linking agents [51,53,55]. Because of their ionic nature and interconnected structure, they absorb large quantities of water and other aqueous solutions without dissolving by solvation of water via hydrogen bonds [56]. This remarkable ability to retain aqueous solutions results in superabsorbent polymers with a range of applications in agriculture [57], pharmaceutical industries for drug delivery and personal hygiene products [58]. The abundance, non-toxicity and inexpensive nature of polysaccharides make them suitable for application as superabsorbent to wholly or partially replace the synthetic superabsorbents. Starch, cellulose, chitin and natural gum are some of the most important polysaccharides that are widely used in different applications. The polysaccharide-based

superabsorbents are either used by direct cross-linking of the backbones or by graft copolymerisation of suitable vinyl monomer(s) on the polysaccharide in the presence of cross-linker [59]. The common techniques employed in the production of superabsorbent polymers of starch-poly(acrylic acid) (starch-g- PAA) involve the use of direct grafting of acrylic acid onto starch backbone with the aid of cross-linking agents [51,60,61]. In some cases, the process involves an indirect technique whereby acrylonitrile (ACN) is grafted onto the starch backbone followed by hydrolysis [51,53]. The cross-linking of the graft copolymers yields the formation of an interconnected structure which allows trapping of large amounts of water without being dissolved. On the other hand, chemical modifications of starch or glycerol, such as acryloylation of the starch before grafting, produce a polymer structure with long comb-like chains that can allow water to be trapped within the network of the polymer structure [42]. Acryloylation of starch or glycerol followed by grafting, yields a superabsorbent polymer with adequate granular swelling, improved shear resistance and improved absorbency under load (AUL). The products could find application in some areas such as in pharmaceutical applications for drug delivery (as it was discovered to have a prolonged drug release and well controlled burst release) [62], infant diapers, paper towels, medical sponges, and sealing properties to products e.g. underground wires and cables [63].

2.6 Capping agent of nanoparticles

Polymers with specific functional groups have found great application in nanomaterials synthesis. One of the recent trends in nanomaterials research is the control of particle morphology and size. The shapes of semiconductor nanocrystals have significant effects on their electronic, magnetic, catalytic, and electrical properties [64]. However, the synthesis of nanoparticles is uncontrollably followed by the agglomeration of the particles, which hampers the overall properties and uses of nanomaterials. Polymers are usually used as capping agents to modify and immobilise the nanoparticles, or in the preparation of polymer nanocomposites. Moreover, the functional groups present in the polymer affect the physical and electronic properties of the nanomaterial. Desirable properties of nanocrystals such as stability, luminescence, solubility, etc., are greatly enhanced by the functional groups of the polymer as well [65]. Presence of covalent bonds between the polymer as capping and passivating agent with the nanoparticle surfaces allows the nucleation and growth of nanocrystals directly inside the matrix through precursor molecules dispersed inside the matrices of the monomeric ligand [65].

2.7 Heavy metal removal

2.7.1 Techniques of heavy metals removal

Methods of removal of solid particles suspended in liquids include gravity-techniques, whereby solid particles with higher densities than water are removed. However, fine particles with diameters of about 10μm will not settle out of suspension by gravity alone in an economically reasonable amount of time. Therefore, the technique has serious limitations because even in an emulsion, the particle sizes are within the range of 0.05–5μm; hence the removal of particles from emulsions (de-emulsification) is even more difficult. The second process, which is widely used, is coagulation. The process involves destabilization of colloidal suspensions, which occurs by neutralizing the electric forces that keep the suspended particles separated.

The aggregates formed in the coagulation process are small and loosely bound; their sedimentation velocities are relatively low, thus limiting the efficacy of the technique. It is, however, relatively higher than for gravity separation [66].

Due to the limitations of the processes mentioned above, flocculation has become a common technique used in domestic waste water and effluent treatment. Flocculation in water treatment simply refers to an essential phenomenon where by particles of dispersion, through a process of contact and adhesion, form large size clusters. In other words, flocculation is synonymous with (particle) aggregation. The larger size particles called ‘flocs’ may then float to the top of the liquid water or settle to the bottom of the liquid so that it can be readily filtered.

2.7.2 Soluble and insoluble starch xanthate

Grafting of synthetic vinyl monomers onto natural polymers such as polysaccharides is one of the effective techniques used in the production of flocculants. Vinyl monomers, such as acrylamide, are grafted onto the backbone of the polysaccharides to form a copolymer with improved scavenging activity on the heavy metal. On the other hand, the poor resistance to degradation of the synthetic (vinyl) monomers is being controlled as well. Soluble and insoluble starch xanthates are reported to have been used in the removal of heavy metals from aqueous solutions [67,68]. The use of soluble starch xanthate is usually met with some

limitations, which is mainly the problem of separation of the metal starch xanthate precipitate complex from the aqueous phase. This is controlled by the addition of a cationic polyelectrolyte followed by simple settling or through high speed centrifugation [69]. The soluble starch xanthate forms a colloidal-metal interaction followed by coordination with the metal ion and the xanthate group. The insoluble starch involves the formation of unstable dispersion followed by heavy metal separation. Generally, the use of an insoluble starch xanthate in metal scavenging activity has more advantages of reliability and ease of operation, while the soluble starch xanthate process is relatively less expensive due to elaborate synthesis procedure required in the synthesis of insoluble starch xanthate.

2.7.3 Alkyl xanthates

Xanthates are a group of compounds that were first discovered in 1822 and have been used as flotation agents for the thiophilic minerals of the transition metals and as reagents for the separation and quantitative determination of many cations [70]. Alkyl xanthates are prepared by the reaction of alcohol with alkalis and carbon disulphide and have a wide range of applications, which include heavy-metal scavenging activity, adsorption in the flotation of metal sulphide minerals and flotation of metals, and in the synthesis and characterisation of luminescent gold (I) complexes [71]. Other alkyl xanthates, such as trifloroethyl xanthate are used for the analytical determination of gold [72]. Potassium ethyl xanthate is also used as a metal chelating agent and in the removal of metals such as copper from an aqueous medium [73].

2.7.4 Glycerol xanthate

The relative abundance and the structural features of glycerol warrant its chemical modification to form a wide variety of compounds for different applications. Glycerol xanthates, like alkyl and starch xanthates, are used in the trapping of heavy metals, while polyhydroxy sodium xanthate, due to its structural features, has been used as a depressing agent in the separation of minerals [74]. The metal scavenging activity of glycerol xanthate is enhanced by introducing more xanthate groups per molecule of the glycerol. This has become one of the advantages of glycerol over alkyl xanthates, since synthesis of a polyxanthate glycerol produces a molecule of glycerol with a large number of sulphur donor groups per molecule of the substrate. The structural feature of glycerol is found to play a fundamental role in easy complex formation with the heavy metals; hence, efficient removal. Although

starch xanthates could contain more than one molecule of xanthate per average glucose unit of starch (AGU), glycerol poly xanthates is a small molecular organic compound containing more exposed sulphide groups at spatial positions and without molecular hindrance that could be expected in starch xanthates in which the sulphur groups are attached to the bulky and polymeric structure of the glucose units.

2.8 References

[1]Young A.H. Fractionation of starch: Chemistry and technology. Academic Press, Inc., London, UK, 1984.

[2] Wurzburg O.B.: Introduction in modified starches: Properties and uses. CRC Press, Inc., BocaRaton, USA, 1986

[3] Holmes C.A.: Interactive European network for industrial crops and their applications, summary report for the European Union, 2000-2005, Agricultural and Rural Strategy Group, Central Science Laboratory, S, Hutton, York, UK, 2005, 22

[4] Bragança R.M., Fowler P., Industrial markets for starch, The Biocomposites Centre, University of Wales, Bangor, Gywnedd, UK, 2004

[5] Otey F.H., Doane W.M., Starch: Chemistry and Technology, 2nd Academic Press, Inc. 1984

[6] Jane J., Chen Y.Y., Lee L.F. McPherson A.E., Wong K.S., Radosavljevic M., Kasemsuwan T. *Cereal Chem.*1999, 76:629–637

[7] Lee S.J., Kim S.H., Kim M., *Food Eng. Progr.*1999, 3:141−157

[8] Yuryev V.P., Cesàro A., Bergthaller W.J. Starch and starch containing origins. Structure, properties and new technologies. New York: Nova Science Publishers, 2002

[9] Hansen A.C, Zhang Q, Lyne P.W.L. *Bioresour. Technol*. 2005, 96:277–85

[10] Silva G.P., Mack M., Contiero *J. Biotechnol. Adv.* 2009, 27:30–39

[11] Solomon B.O., Zeng A.P., Biebl H, Schlieker H, Posten C, Deckwer W.D. *J. Biotechnol.* 1995, 39:107–17

[12] Colin T, Bories A, Lavigne C., Moulin G. *Curr. Microbiol.* 2001, 43:238–43

[13] Dharmadi Y., Murarka A., Gonzalez R. *Biotechnol. Bioeng.* 2006, 94:821–9

[14] Behr A., Eilting J., Irawadi K., Leschinski J., Lindner F. *Green Chem*. 2008,10:13–30

[15] Yazdani S.S., Gonzalez R. *Curr Opin Biotechnol.* 2007, 18:213–219

[16] Chaudhari S., Tare V. *J. Appl. Polym. Sci.*1999, 71:1325–1332

[17] Chang Y.K., Shih P.H., Chiang L.C., Chen T.C., Lu H.C., Chang J.E. *Environ. Inform. Arch*. 2007, 5:684–689

[18] Guo L., Zhang S., Ben-ZhiJu B., Yang J., Quan X. *J. Polym. Res*. 2006, 13:213–217

[19] Wing R.E., Doane W.M., Russel C.R., *J. Appl. Polym. Sci.* 1975, 19:847–854

[20] Dao-ling X., Yue-hua H., Wen-qin Q., Ming-fei H., *J. Cent. South Univ. Technol.*2006, 6:678−682

[21] Takeda, Y., Takeda, C., Suzuki, A., Hizukuri, S. *J. Food Sci.* 1989, 54:177–182

[22] Dzulkefly K., Koon S., Kassim A., Sharif A., and Abdullah A., *M.J.A.S.* 2007, 11: 395–399

[23] Vargha V., Truter T., *Eur. Polym. J.* 2005, 41:715–726

[24] Lukasiewicz M., 14th International Electronic Conference on Synthetic Organic Chemistry (IECSOC-14) 1-30 November, 2010

[25] Rajan A., Prasad V.S., Abraham T.E., *Int. J. Biol. Macromol.* 2006, 39: 265–272

[26] Jerachaimongkol S., Chonhenchob V., Naivikul O., Poovarodom N. *Kasetsart J. (Nat. Sci).* 2006, 40:148–151

[27] Miladinov V.D., Hanna M.A. *Ind. Crop Prod.* 2000, 11: 51–57

[28] Murúa-Pagola B., Beristain-Guevara C.I., Martínez-Bustos F., *J. Food Eng.*2009, 91:380–386

[29] Biswas A., Selling G.S., Shogren R.L., Willet J.L., Buchanan C.M. and Cheng H.N. *Catalysis* 2009, 27:33–35

[30] Auzely-Velty R., Rinaudo M. *Int. J. Biol. Macromolecules* 2003, 31:123–129

[31] YizhiMeng Y., Rao M.A. *Carbohydr. Polym.* 2005, 60:291–300

[32] Xiao H.X., Qin-Lu Lin Q.L., Gao-Qiang Liu G.Q., Feng-Xiang Yu F.X. *Molecules* 2012, 17:10946–10957

[33] Koo S.H., Lee K.Y., Lee H.G. *Food Hydrocolloids* 2010, 24:619–625

[34] Battacharya A., Rawlings J. W., Ray P. Polymer grafting and cross-linking, John Wiley & Sons Inc., Hoboken, New Jersey, 2009

[35] Raina C.S., Singh, S., Bawa A.S., Saxena, D.C. *Eur. Food Res. Technol*. 2006, 223:561–570

[36] Clark H.T., Gillspie J.A. *J. Am. Chem. Soc.,* 1932, 54: 2076–2083

[37] Caldwell C.G., Starch ester derivatives. U.S. Patent 1949, 2461139

[38] Wolff I.A., Olds D.W., Hibert G.E. *J. Am. Chem. Soc.,* 1951, 73:346–349

[39] Jetten W., Stamhais E.T., Joosten G.E.H. *Starch/Starke* 1980, 32:364 –368

[40] Ogawa K., Hirai I., Shimasaki C., Yoshimura T., Ono S., Rengakuji S., Nakamura Y., Yamazaki I. *Bull.Chem. Soc. Jpn.*1999, 72:2785–2790

[41] Xu Y., Miladinov, V. Hanna M.A. *Cereal Chem.* 2004, 81:735–74

[42]Mohammed A.D., Young D.A., Vosloo H.C.M. *Starch/Starke* 2014, 66:1–7

[43]Kumar A., Rao N.N., Kaul S.N. *Biores. Technol.* 2000, 71:133–142

[44] Bianco G., Gehlen M.H. *J. Photochem. Photobiol. A*. 2002, 149:115–119

[45] Lagos A., Reyes J. *J. Appl. Polym. Sci.*: *Part A*: Polymer Chemistry, 1988, 26:985–991

[46] Mundargi, R.C., Agnihotri, S.A., Sangamesh A., Patil S.A., Aminabhavi, T.M. *J. Appl. Polym. Sci.*2006, 101: 618–623

[47] Li M., Zhu Z., Pan X. *Starch/Starke* 2011, 63:683–691

[48] Gaylord, N., *J. Polym. Sci.*:*Polym.Symp*. 1972, 37:153–173

[49] Iwakura Y., Imai Y. *J. Polym. Sci. Part A*. 1965, 3:1185–1193

[50]Han T.L., Kumar R.N., Rozman H.D., Noor G.M.A. *Carbohydr. Polym.*2003, 54:509–516

[51] Athawale V.D., Lele V. *Carbohydr. Polym*. 2000, 41:407–416

[52] Bhattacharya A., Misra B.N. *Prog. Polym. Sci.*2004, 29:767–814

[53] Athawale V.D., Rathi S.C. *Rev. Macromol. Chem. Phys.* 1999, 39:445–480

[54]Wang J.S., Matyjaszewski K., *Macromolecules* 1995, 28:7901–8001

[55] Takeda Y., Takeda C., Suzuki A., Hizukuri S. *J. Food Sci.* 1989, 54:177–182

[56] Kiatkamjornwong R., Wongwatthanasatein R. *Macromol. Symp.* 2004, 207:229–240

[57] Raju K.M., Raju M.P., Mohan Y.M. *Polym. Int.* 2003, 52:768–772

[58] Kikuchi A., Okano T. *Adv. Drug Delivery Rev.* 2002, 54:53–57

[59] Zohuriaan-Mehr M.J., Kabir K. *Iran. Polym. J.* 2008, 17:451–477

[60]LuS. J., Yao K., Lin S., Cao D., Chen Y. *Starch/Stärke*, 2003, 55:518–523

[61] Weaver M.O., Montgomery R.R., Miller L.D., Sohns V.E., Fanta G.F., Doane W.M. *Starch/Stärke* 1997, 29:410–413

[62] Ashish P.Y., Khanderao R.J., Deelip V.D., *Int. J. Pharm. Pharm. Sci*., 2013, 5, ISSN-0975–1491

[63] Kiatkamjornwong S., *Sci. Asia* 2007, 33, 39–43

[64] Yang S.Y., Li Q, Chen L, Chen S. *J. Mater. Chem.* 2008, 18:5603–5599

[65] Mohammed A.D., Onwudiwe D.C., Young D.A., Vosloo H.C.M. *Mater. Lett.* 114, 2014:63–67

[66] Bratby J. Coagulation and flocculation, Uplands press Ltd. Cryodon Cambridge, 1st Edition 1980

[67] Tare V., Chaudhari S. *Water. Res.* 1987, 21:1109–1118

[68] Jawed M., Tare V. *J. Appl. Poly. Sci.* 1991, 42:317–324

[69] Chaudhari S., Tare V. *J. Appl. Poly. Sci.*1999, 71:1325–1332

[70] Wing R. E., Doane W. M. U.S. Patent 1976, 695617

[71] Mohamed A.A., Kani I., Ramirez A.O., Fackler J.P. *Inorg. Chem.* 2004, 43:3833–3839

[72] Moran M., Cuadrado I., Masaguer J.R., Losada J., Foces-Foces C., Cano F.H. *Inorg. Chim. Acta* 1988, 143: 59–70

[73] Chang Y., ChangJ., LinT., HsuY. *J. Hazard Mater.*2002, 94:89–99

[74] Dao-ling X., Yue-hua H., Wen-qin Q., Ming-fei H. *J. Cent. South Univ. Technol.*2006, 6:678−682

Chapter 3

Synthesis and Characterisation of Superabsorbents from Starch grafted with Acrylic acid

Part of this chapter has been reported in: starch/stärke,(66) 2004,1-7

3.1 Introduction and Objectives

3.1.1 Acryloylation and grafting of starch with AA

Acryloylated starch-g-PAA superabsorbent polymer is synthesised by acryloylation of starch followed by grafting acrylic acid onto the starch ester using Fenton's reagent as initiator. The acryloylation reaction is a homogenous process which involves the use of pyridine as a nucleophilic acylation catalyst and also as a base. The hydrochloric acid formed as a by-product in the course of the reaction reacts with the excess pyridine to form pyridinium salt that is easily separated from the reaction product after dissolution in methanol [1]. The substituted starch ester is maintained at a degree of substitution (DS) value in a range of 0.8–1.00, because at higher DS more cross-linking occurs between the starch molecules which could lead to a rigidity, brittleness and poor water-dispersibility of the polymer structure [2]. The product, which is synthesised without any cross linking agent, has a low concentration of homopolymer (PAA) and shows impressive water absorption property. Grafting of vinyl monomers onto substituted starch (AS) is an efficient technique due to the presence of C=C in the starch structure which has high potential for grafting [3]. Acryloylation of starch prior to grafting is done so as to control the degree of substitution in the final product, to obtain a more uniform distribution of substituents along the starch chain and a higher conversion yield [2]. Li *et al*. [4] reported that acryloylation of starch prior to grafting with vinyl monomers enhances grafting efficiency and improves the performances such as adhesion-to-fibers and mechanical properties of grafted starch film.

3.1.2 Objectives

The objectives of the study include

- Synthesis of superabsorbents from chemically modified starch and study of the effects of acryloylation and cross-linking of starch on the superabsorbency of the final product.
- Characterisation of the product using chemical techniques such as FTIR, XRD, SEM and TGA techniques which could provide evidence for starch ester formation and grafting of AA onto its backbone.
- Study of water absorbency of the product in water, saline and under load.

- Study the effects of acryloylation and cross-linking on the grafting parameters such as grafting percentage, ratio, efficiency and amount of homopolymer in the final product.

3.1.3. Cross-linking, acryloylation and grafting of starch and AA

Chemical modification of starch was carried out using epichlorohydrin as cross-linking agent; the cross-linked potato starch was acryloylated before grafting with acrylic acid (AA) using Fenton's reagent as initiator. Cross-linking of the graft copolymers yields the formation of interconnected structure which allows trapping of large amounts of water without being dissolved. On the other hand, acryloylation of the starch before grafting produces a polymer structure with long comb-like chains that could allow water to be trapped within the network of the polymer structure [6]. This work combines the dual processes; the cross-linking of potato starch and acryloylation before grafting with acrylic acid. The epoxide easily gets deep into the starch granular structure due to its small molecular size compared to other cross-linking compounds [7]. The polymer, a cross-linked acryloylated starch grafted with acrylic acid (CAS-g-PAA), is characterised and tested for absorbency in water and saline solution. Scheme 3.1 shows the structural feature of the product with epichlorohydrin cross-linking agent acting as a bridge between the molecules of acryloylated starch-graft poly(acrylic acid). The degree of cross-linking is restricted to allow further sites for grafting reactions with acrylic acid (AA), while the degree of substituted ester (DS) is maintained in a range of 0.2–0.8 as a highly cross-linked starch would shield and hinder successful grafting of monomer onto the backbone of the starch. The optimum time for the grafting reaction and concentration of the initiator were used throughout the study.

3.2 Experimental

3.2.1 Materials

Potato starch (Sigma-Aldrich) was used as received. Acrylic acid (Sasol) was freshly distilled under reduced pressure before use. Hydroquinone (Sigma-Aldrich) was used as the inhibitor. Acryloyl chloride was prepared from benzoyl chloride (Sigma-Aldrich) using the procedure reported by Stampel *et al.* [8]. Pyridine, epichlorohydrin (99%), ferrous

ammonium sulphate (FAS) and hydrogen peroxide (30 %) (Sigma-Aldrich) were also used as received in the synthesis.

3.2.2 Synthesis of acryloyl chloride

Acrylic acid (0.5 mol, 36 g) was mixed with benzoyl chloride (1 mol, 140 g) in a flask containing hydroquinone (0.1) and distilled at a temperature of 90-100 °C. The distillate was collected in a container immersed in an ice bath containing hydroquinone (0.5 g). The product (acryloyl chloride) was redistilled using the same setup at 72-74 °C and collected as a pale yellow liquid.

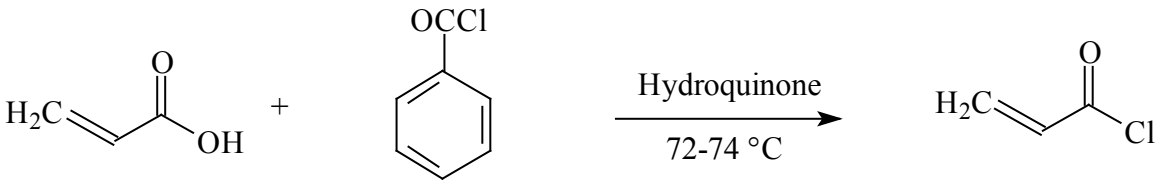

Scheme 3.1 Synthesis of acryloyl chloride

3.2.3 Synthesis of cross-linked starch

A cross-linked starch was prepared using the procedure reported by Kurakake *et al*. [6]: a slurry of potato starch (20 g) was prepared by stirring with a solvent (100 mL water/ethanol 20:80). After adding NaCl (0.15 g) and epichlorohydrin (1 mL), KOH in water (1 g in 6 mL H_2O) was gradually added over 30 min while the temperature was maintained at 50 °C. After cooling to 30 °C, Water (5 mL) and epichlorohydrin (0.3 mL) were added and stirred for 5 hrs. The reaction mixture was neutralised (2 M HCl), filtered, washed with water, acetone and methanol and dried under vacuum at room temperature.

Selected IR, ν (cm^{-1}): 1608 (O-H), 2919 (C-H), 1074 (C-H)

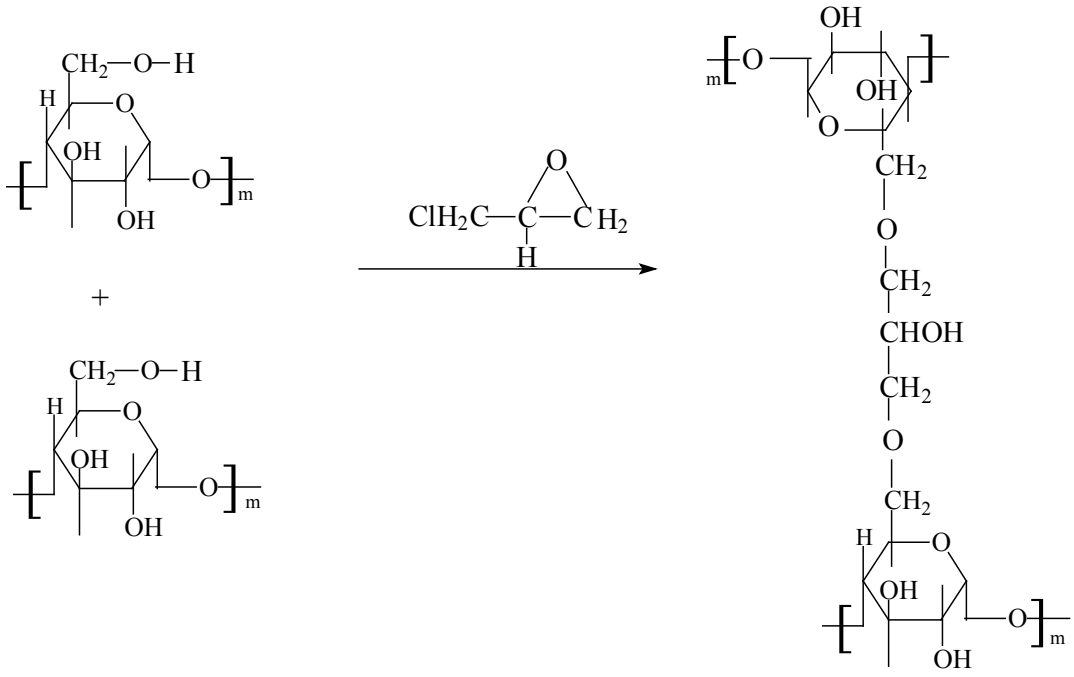

Scheme 3.2 Cross-linking of starch using EPI.

3.2.4 Acryloylation of starch

The synthetic procedure reported by Fang *et al.* [2] was used. Typically, dry starch (6 g) was added to water (80 mL) and stirred at 80 °C for 60 min to produce a slurry. N,N′-dimethylacetamide (DMA, 3 x 50 mL) was added and distilled to remove the water azeotropically at 90 °C under reduced pressure. After all the water was removed, at a time when DMA was collected as the only distillate at constant temperature, LiCl (0.3 g) was added and the temperature of the slurred-starch was allowed to cool to 60 °C. Dry pyridine (1.5 mL) and freshly prepared acryloyl chloride (1.5 mL) was added drop wise and stirred for a further 30 min at 60 °C. The final product was precipitated with acetone and dried before analysis.

Selected IR, ν (cm^{-1}): 1722 (C=O), 1616 (C=C), 2928 (C-H),

3.2.5 Preparation of graft copolymers

Acryloylated starch (5 g) was added to water (50 mL) in a three-necked round-bottomed flask and stirred while the temperature was kept at 60 °C under nitrogen. The mixture was allowed to cool. Different concentrations of Fenton's reagent and distilled acrylic acid (AA)

were added to the reaction mixture and stirred for 3 h at 30 °C. The product, acryloylated starch-poly(acrylic acid) (AS-g-PAA) was washed with ether as a light brown glue-like substance, dried at 45 °C under vacuum and crushed to finer-sized particles using a mortar and pestle.

A slurry of cross-linked acryloylated starch (5 g) was made in a three-necked round bottomed flask containing water (50 mL) at 60 °C for 45 min and under nitrogen cover to maintain an inert atmosphere. The mixture was allowed to cool to 25–30 °C. Ferrous ammonium sulphate (2.0 mmol) mixed with acrylic acid were gradually added to the flask. After stirring for 5 min, H_2O_2 (2 mL) was added and the mixture was stirred for 3 h at different temperatures in the range of 30–80 °C. The product, cross-linked acryloylated starch poly (acrylic acid) (CAS-g-PAA), was precipitated with methanol washed with ether and dried at 45 °C under vacuum to constant weight before analysis.

Selected IR, v (cm^{-1}): 3260 (O-H), 1722 (C=O), 2928 (C-H).

3.2.6 Extraction of homopolymer

The dried products obtained above were extracted with methanol in a Soxhlet extractor for 24 h to remove poly (acrylic acid) homopolymer. The pure copolymers were dried in an oven at 40 °C to constant weight.

3.2.7. Water absorbency

A gravimetric method was applied whereby polymer samples (1 g) was immersed in water (250 g), or 0.9 % saline solution (150 g) for 10 h at room temperature. The swollen polymer was separated using a 100 mesh sieve and weighed. The water absorbency Q was calculated from the relation:

$$Q\left({}^{g}/_{g}\right) = (w_2 - w_1)/w_1 \qquad (1)$$

Where Q is the water absorbency, w_1 and w_2 are the weights of dry sample and swollen gel respectively [9].

The absorbency under load (AUL) was measured using the following procedure [10]: A macro-porous sintered glass filter plate (porosity # 0, d = 80 mm, h = 6 mm) was placed in a Petri dish (d = 118 mm, h = 12 mm). The sample (1 g) was uniformly placed on the filter

paper on the sintered glass plate and a load of 500 g in a glass cylinder was placed on the dry sample of the polymer. A 0.9 % NaCl solution was added till the liquid reached the height of the filter plate (around 6 mm). The swollen particles were weighed again after 60 min. and the AUL was calculated from equation (1). The retention ability of the swollen samples were tested in a centrifuge for 60 min at a speed of 5000 rpm, at ambient temperature. The samples were weighed again and the retention ability was calculated using equation (1)[8]. In each case, three (3) runs were carried out and the average values obtained were used in calculating the water absorbency.

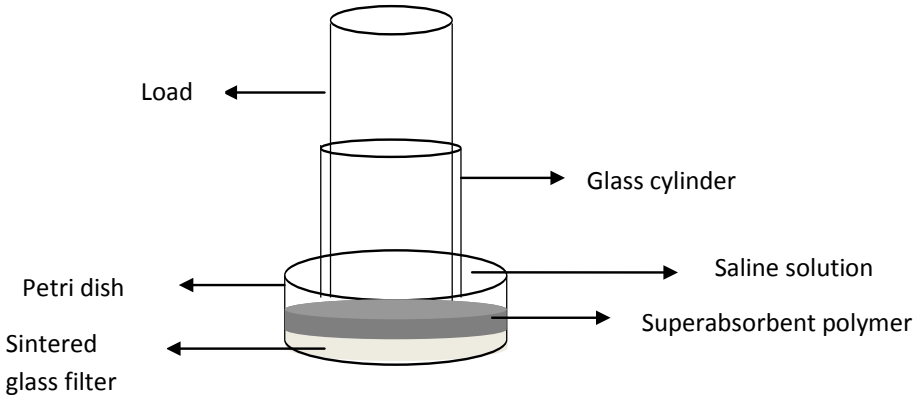

Figure 3.1 Schematic diagram showing AUL absorbency of saline solution.

3.2.8 Characterisation

3.2.8.1 FTIR analysis

A Bruker VERTEX 80 FTIR spectrometer was used to characterise the products. The infra-red spectra of the samples were recorded in absorbance mode, in the frequency range 550–4000 cm^{-1}, at room temperature, with a resolution of 4 cm^{-1}based on 32 scans and using a Bruker Platinum-Diamond ATR accessory.

3.2.8.2 Thermogravimetric analysis

The Thermal properties of the pure starch, starch ester and the graft copolymers were determined on an SDTQ 600 thermal analysis Instrument. Samples were contained within

aluminium crucibles and heated at a rate of 10 °C min^{-1} from room temperature to 500°C under flowing nitrogen at a rate of 75 mL min^{-1}.

3.2.8.3 Scanning electron microscopy

The samples were completely dried in an oven before the analyses. The solid particles were evenly distributed on SEM specimen stubs and coated with a thin layer of palladium-gold prior to analysis. The SEM images were obtained on a Quanta FEG 250 Environmental Scanning electron microscope using an accelerating voltage of 15 kV.

3.2.8.4 X-ray Diffraction analyses

The samples were processed and measured in powdered form. The X-ray powder diffraction (XRD) data were collected on a Röntgen PW3040/60 X'Pert Pro X-ray diffractometer using Ni-filtered Cu Kα radiation (λ = 1.5405 Å) at room temperature.

3.3 Results and discussion

3.3.1 FTIR analysis

FTIR results of starch is shown in Fig. 3.2(a), the absorption bands show the characteristic absorption peaks at 3266 and 1634 cm^{-1} due to O-H stretching and bending modes respectively, and 2922 and 1076 cm^{-1}due to C-H stretching and bending respectively. In Fig. 3.2(b) the AS shows important peaks at 1722 $cm^{-1}$of carbonyl absorption bands due to ester bond formation in addition to the characteristic peaks of the native starch which confirms acryloylation. In addition, a new intensive absorption band appears at 1616 cm^{-1} due to double bond vibration of C=C . These additional peaks confirm the presence of ester formation on the starch backbone and further indicates that the C=C double bond of the acryloyl group remains unreacted after the acryloylation.

The grafted product (As-g-PAA), Fig. 3.2(c) shows important peaks at around 1705 cm^{-1} due to carbonyl stretching, around 1600 cm^{-1} due to the OH bending mode, 2930 and 1077 cm^{-1} from C-H stretching and bending respectively. It is also observed that the strong OH stretching band around 3310 cm^{-1} in Fig.3.2(a) and (b) has changed shape to a broad peak in Fig.3.2(c) after the grafting reactions, as the number of hydroxyl groups in the starch ester

backbone decreases as a result of intermolecular bonds between the acryloyl groups that have substituted most of the hydroxyl groups in the starch molecules. In each case, these confirm successful grafting of the monomer onto the starch ester.

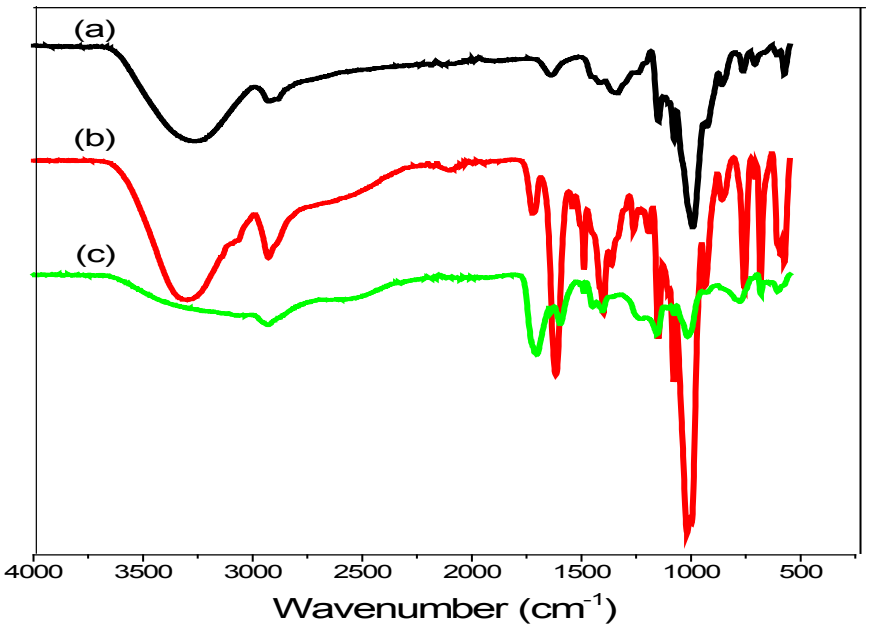

Figure 3.2 FT-IR spectra of (a) starch (b) AS and (c) AS-g-PAA.

Fig. 3.3 shows the FTIR spectra of native starch, cross-linked starch, acryloylated cross-linked starch and acryloylated cross-linked starch graft poly(acrylic acid) samples. In Fig. 3.3(a) the starch sample shows a broad band at 3260 and 1631 cm^{-1} due to O–H stretching and bending modes respectively. The C–H stretching and bending modesare observed at 2919 cm^{-1} and 1074 cm^{-1} respectively. In the cross-linked starch, Fig. 3.3(b) there is an intensive peak at 1608 cm^{-1} due to from the unreacted C=C of the starch esterand probably from the OH bending vibration of the opened epoxide ring of epichlorohydrin after the cross-linking reaction. This confirms that epichlorohydrin is covalently linked to the starch molecules via some of the OH groups. In the acryloylated product, Fig. 3.3(c), an important peak appears at 1711 cm^{-1} due to carbonyl stretching mode of the ester bond formation, and another intensive peak at 1620 cm^{-1} due to double bond vibration of C=C in cross-linked acryloylated starch. In Fig. 3.3(d), CAS-g-PAA shows absorption peak at 1722 cm^{-1} due to C=O stretching vibration

from poly(acrylic acid) (PAA), and 2928 and 1078 cm^{-1} due to C-H stretching and bending modes respectively.

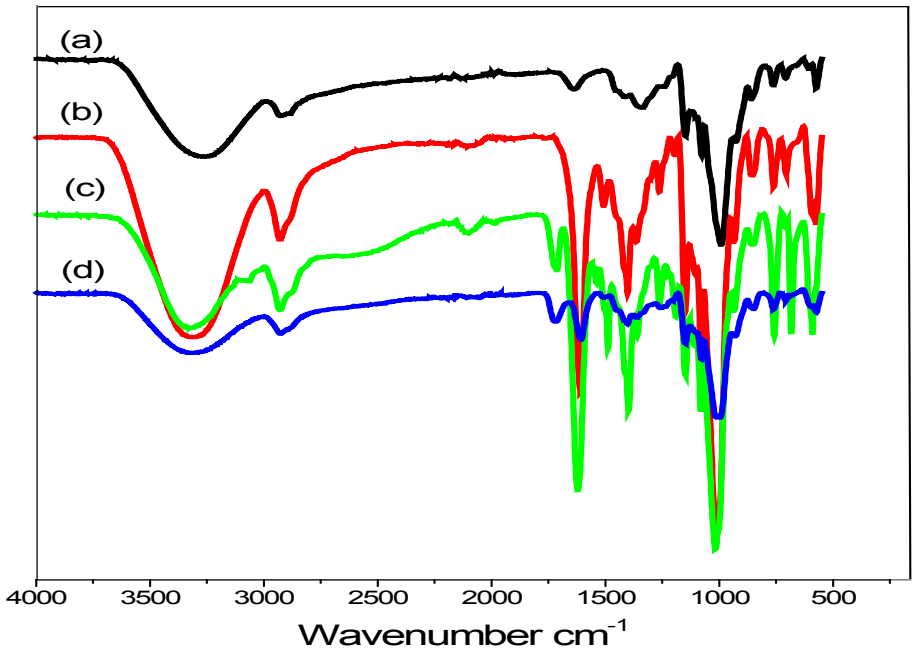

Figure 3.3 FTIR spectra; of (a) starch (b) Cross-linked starch (c) Cross-linked acryloylated starch and (d) CAS-g-PAA.

The intensity of the C=O stretching band in cross-linked acryloylated starch is reduced in the final product as a result of high cross-linking that took place after the grafting reaction. In this study, only a polymer with a maximum DS of 0.8 was obtained due to overall hindrance and limited number of free OH in the starch network that could be effectively bonded to the PAA.

3.3.2 Thermogravimetric analysis

The thermal properties of the starch, AS and AS-g-PAA was examined by TG analysis under nitrogen heated at the rate of 10 °C/min. Starch exhibits a three-step thermal behaviour: The initial slight loss in weight in Fig. 3.4 is merely due to evaporation of the absorbed moisture in the starch. The rapid decomposition is observed at a second stage resulting in a

major weight loss of 75 %; the weight derivative curve clearly shows the temperature of maximum decomposition for this stage as 300 °C. The final stage is probably due to the formation of some volatile compounds; hence very slow. The AS, Fig. 3.5, shows a similar pattern of decomposition with the starch while exhibiting a lower decomposition temperature. It started with a slow decomposition at 105 °C followed by a major weight loss at around 200 °C resulting in 43 % weight loss and the final stage was due to the formation of some compounds and their subsequent decomposition. The AS-g-PAA, Fig 3.6, shows a first decomposition pattern from 30–124 °C due to dehydration showing about 6 % weight loss. The second stage pattern of decomposition occurs at a temperature range of 180–271 °C whereby 44 % weight loss is observed. The third stage involves formation of some compounds and their slow decomposition with a char yield of 38 % at 396 °C, and this could be mainly due to cross-linked grafted AS-g-PAA copolymer. Generally, there is a relatively high thermal stability of the grafted product over non grafted starch.

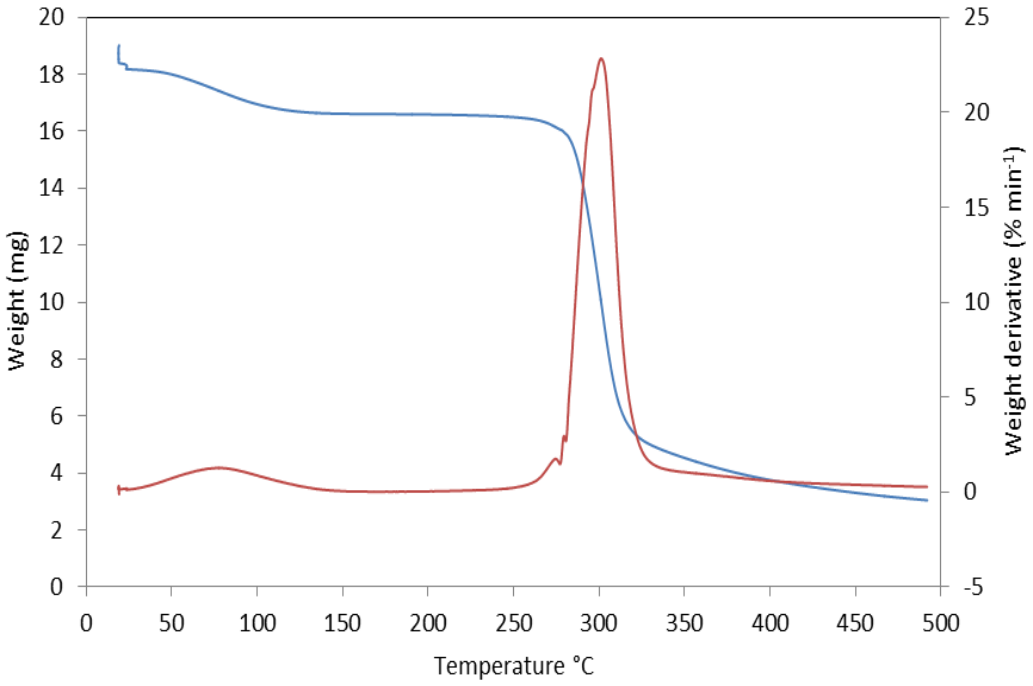

Figure 3.4 **Thermal analysis curve of starch.**

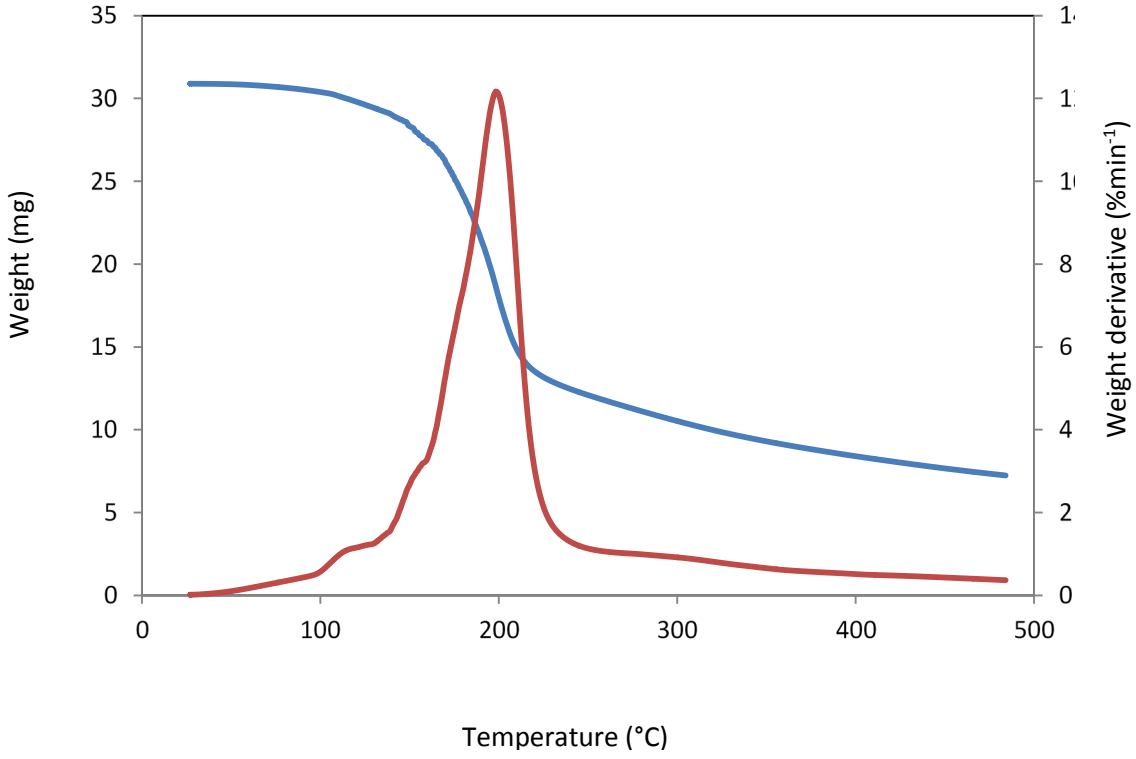

Figure 3.5 **Thermal analysis curve of AS**

This agrees with the findings reported in the literature [11–13]. The variations observed in the thermal stability of starch, AS and AS-g-PAA clearly indicates that starch has undergone a successful chemical transformation to form a new product (AS-g-PAA).

The thermal stability and the degradation pattern of cross-linked starch, the cross-linked ester and the graft copolymer were analysed by TG analyses. The cross-linked starch exhibits a three-step degradation pattern (Fig. 3.7). The first stage of decomposition is due to the evaporation of absorbed moisture which results in a slight loss in weight. At around 178 °C there is rearrangement of the molecules due to swelling of starch particles and expansion of the amorphous region thereby disrupting the crystallinity [6]. The third step is rapid and accounts for the highest weight-loss (75 %) with a temperature of maximum decomposition of 282 °C as can be seen in the weight-derivative curve; this is then followed by the final stage of slow decomposition, probably, of some volatile compounds formed at higher temperature. The cross-linked acryloylated starch in Fig. 3.8 shows a slight decrease in thermal stability with a marked-difference in the decomposition pattern.

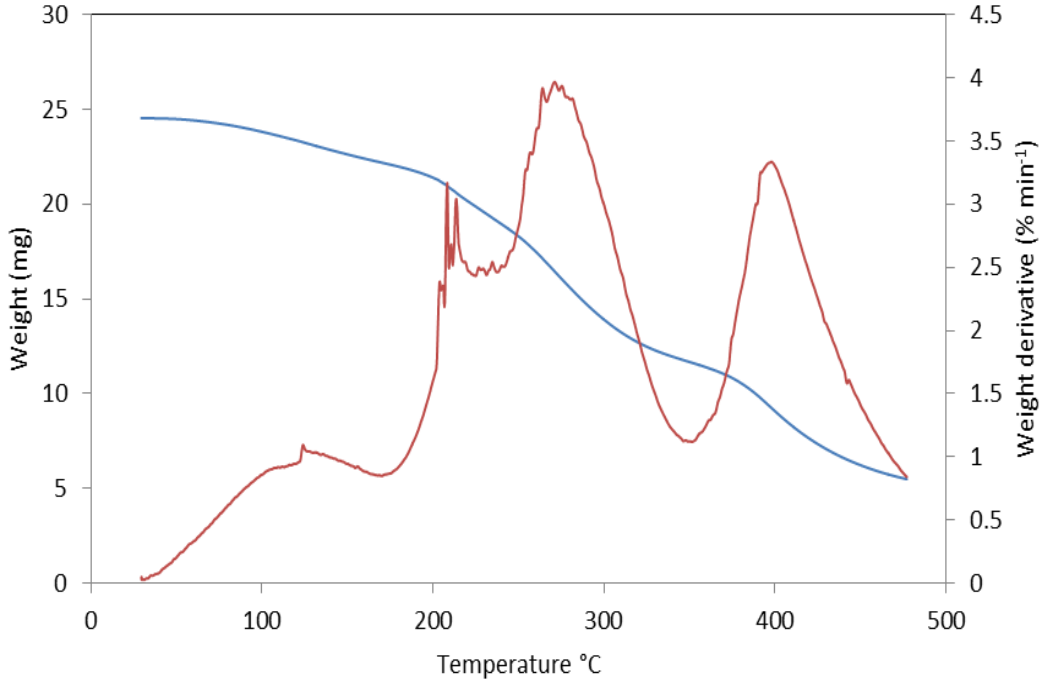

Figure 3.6 Thermal analysis curve of AS-g-PAA.

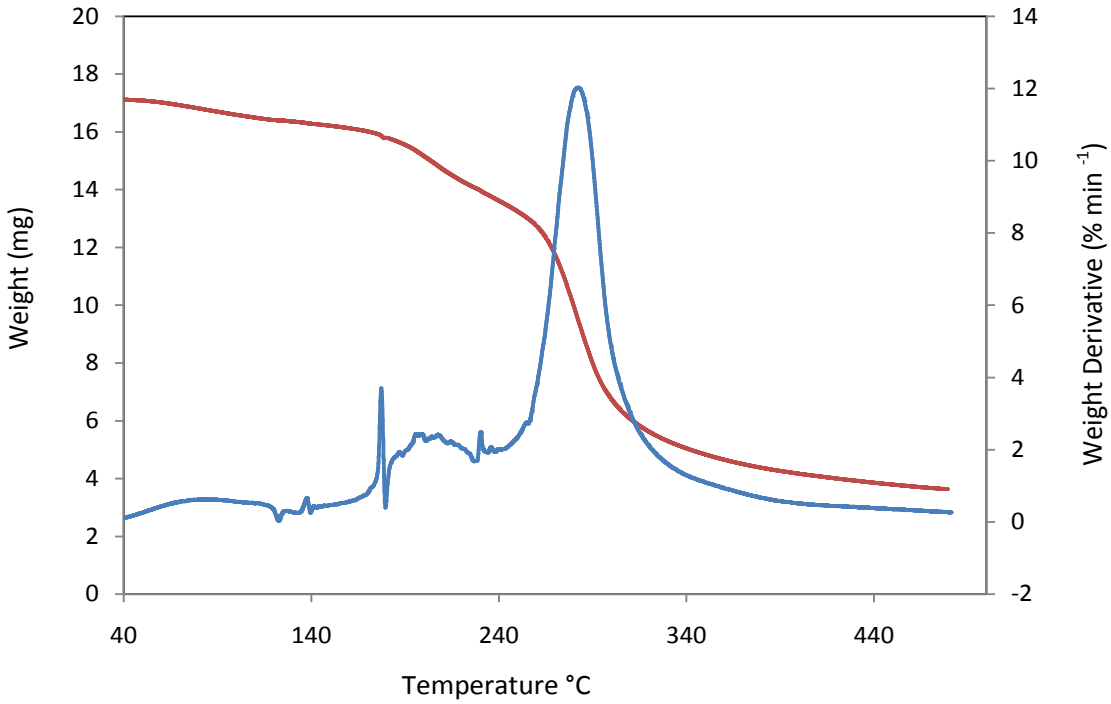

Figure 3.7 Thermal analysis curve of cross-linked starch

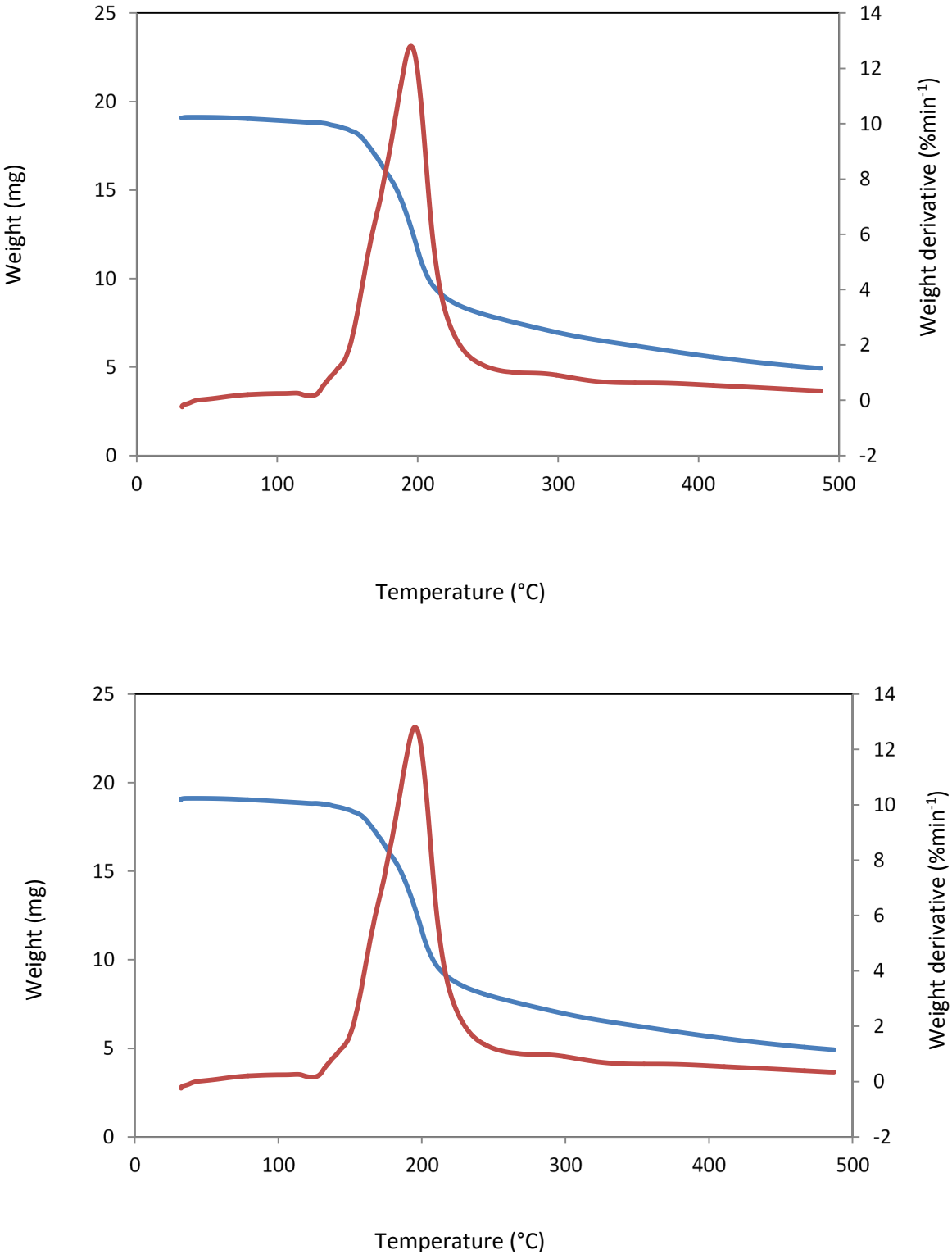

Figure 3.8 **Thermal analysis curve of cross-linked acryloylated starch.**

The thermal behaviour of cross-linked acryloylated starch (due to decrease in the hydrogen bonds in the cross-linked starch network as a result of acryloylation) shows lower thermal stability than the starch, with a temperature of maximum decomposition at 200 °C. The final stage could be due to the formation and decomposition of some compounds formed at higher temperature. The thermal behaviour of CAS-g-PAA in Fig. 3.9 shows initial decomposition due to the absorbed moisture, followed by usual rearrangement of the polymer molecular structure, similar to what is observed in cross-linked starch sample, at 180 °C, followed by decomposition at 265 °C resulting in 53 % loss in weight. Moreover, decomposition is observed at a much higher temperature, 370 °C, with a char yield of 40 %. The final stage is the formation of some compounds and their slow decomposition. These thermograms, apart from proving that a grafted product was obtained, clearly show that chemical modification of starch affects its thermal behaviour.

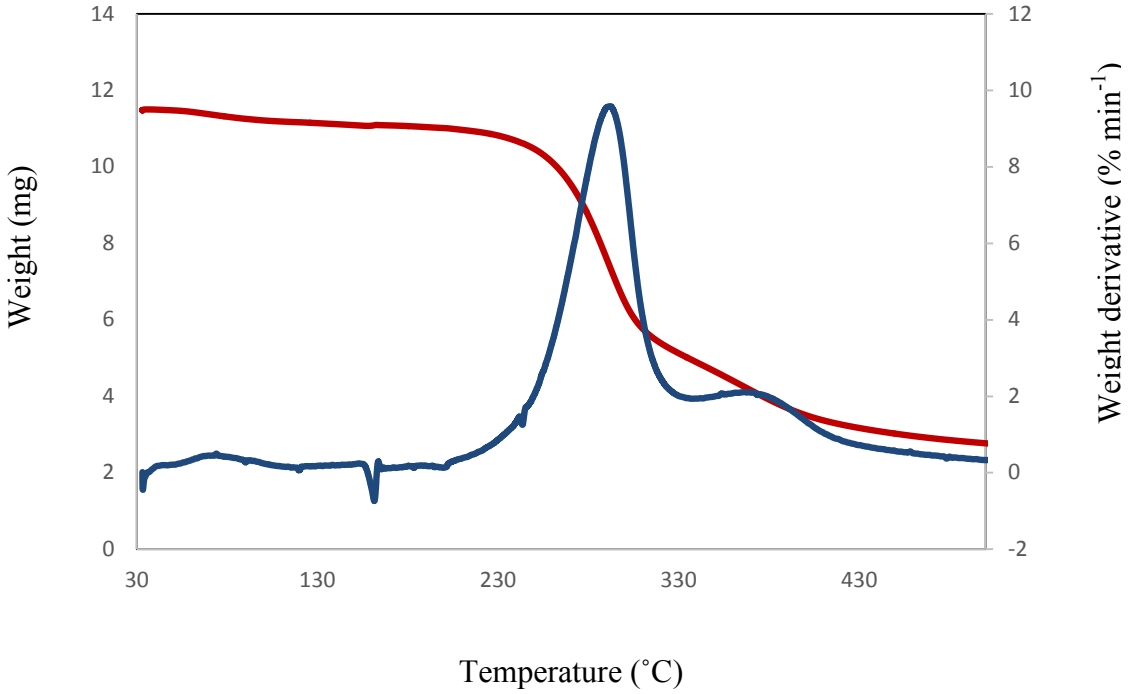

Figure 3.9 Thermal analysis curve of CAS-g-PAA.

3.3.3 SEM analysis

The SEM photographs of starch, AS and AS-g–PAA are shown in Fig.3.10. The surface morphology of both the starch granules, AS and AS-g-PAA were analysed. Ungrafted starch

granules have an irregular shape and varied particle size with a smooth surface as is shown in Fig. 3.10(a), which is disrupted after acryloylation (Fig. 3.10b). The graft copolymers have a different surface morphology. In Fig. 3.10(c), the change in granular structure of the starch to a thick-coated rough surface of the product confirms grafting of poly (acrylic acid) onto the starch matrix. The surface morphology of starch, cross-linked starch, cross-linked acryloylated starch and CAS-g-PAA are shown in the SEM images in Fig. 3.11. The irregular oval shape of the granular starch with a smooth surface can be clearly seen in Fig 3.11(a). In Fig 3.11(b and c), starch cross-linked with epichlorohydrin shows a different surface morphology which at higher magnification shows a rough surface compared to the native starch. Acryloylation of cross-linked starch forms rather a rough surface which results from the acryloyl groups chemically bound with the cross-linked network of starch, which can be clearly seen in Fig 3.11(d).

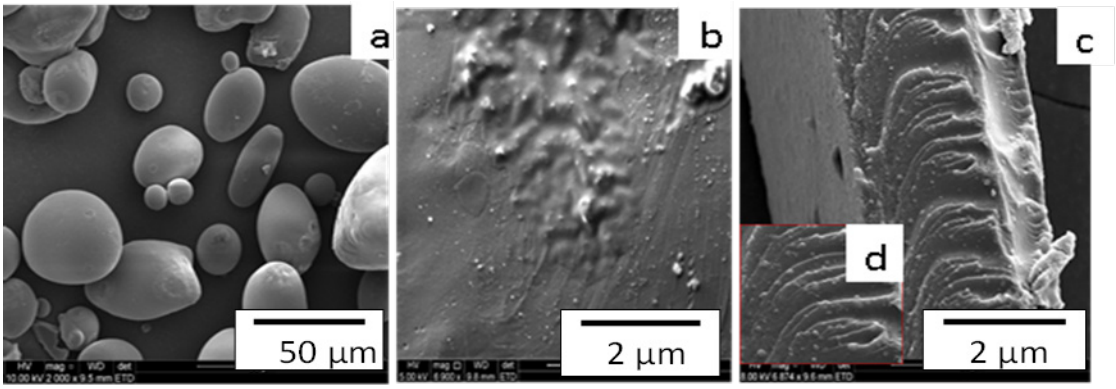

Figure 3.10 SEM images of (a) starch(b) AS (c) AS-g-PAA and (d) magnified AS-g-PAA.

After the grafting of poly (acrylic acid) onto the cross-linked starch ester (cross-linked acryloylated starch), the entire surface changes to a different morphology; a coarse surface with a more definite morphological structure of a thick polymeric coating of poly(acrylic acid) onto the cross-linked acryloylated starch is seen in Fig 3.11(e). In each case, however, the change in morphology from one chemical process to the other confirms a successful molecular transformation of the starch structure into a cross-linked network, followed by ester formation of the cross-linked starch and its copolymerisation reaction with acrylic acid.

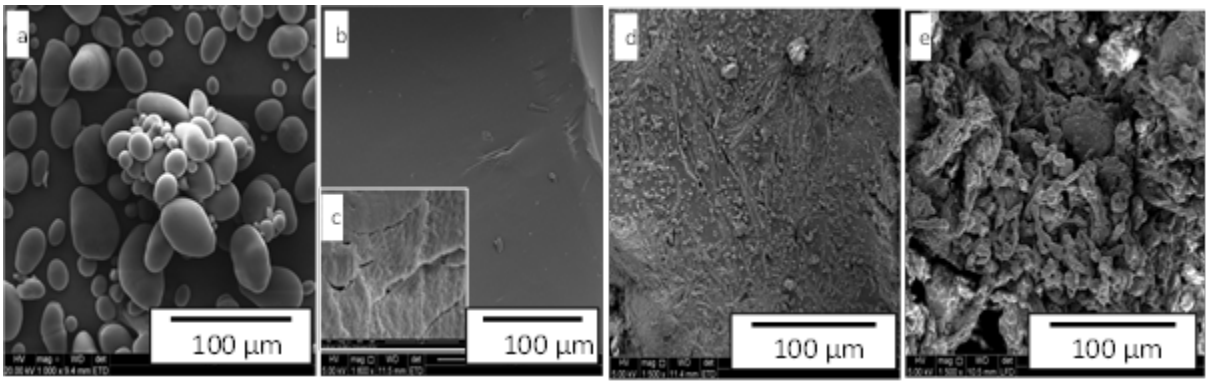

Figure 3.11 **SEM images of (a) starch (b) cross-linked starch (c) magnified granular cross-linked starch surface (d) cross-linked acryloylated starch (e) CAS-g-PAA.**

3.3.4 X-ray diffraction analysis

The XRD measurements were carried out on starch, AS and AS-g-PAA in powdered form. From Fig. 3.12, the semi-crystalline nature of the granular starch, which Athawale and Lele [14] reported to have been due to the amylopectin fraction in the starch, is altered after grafting. In Fig. 3.12(a) the starch shows the four sharp crystalline peaks in the range of 5600 counts between 2θ values of 10-25°, however, the crystalline peaks have disappeared into a single sharp peak in the AS (Fig. 3.12b). In the grafted product, AS-g-PAA, Fig. 3.12(c), the peaks were compressed into a single broad peak. Therefore, there is an overall disorrientation of the semi-crystalline structure of granular starch after undergoing chemical modification (acryloylation and grafting) into an amorphous substance (AS-g-PAA). The change in the crystallinity of the starch not only confirms grafting, but further shows that both components of starch, i.e. amylose and amylopectin, do take part in the grafting process.

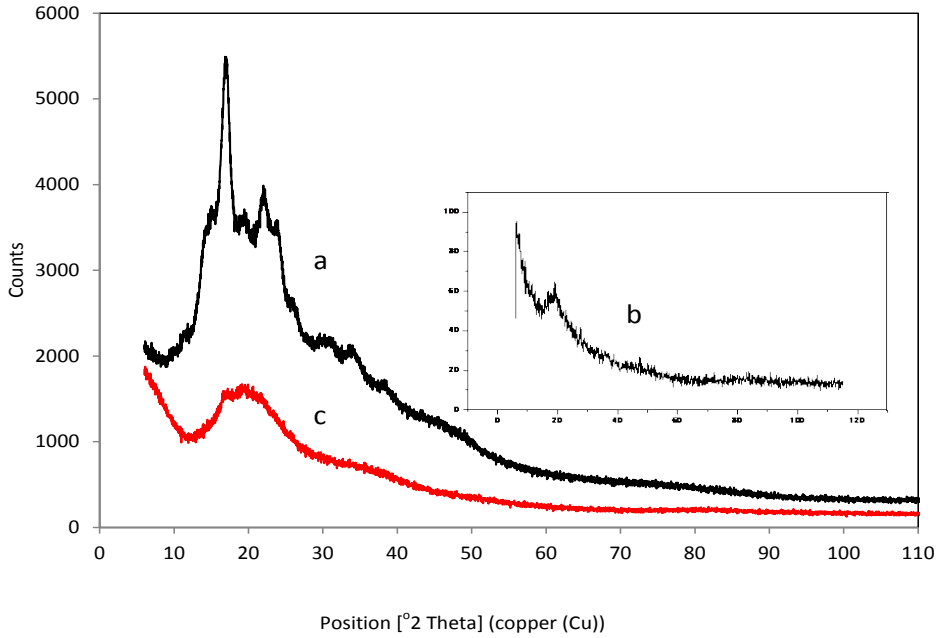

Figure 3.12 XRD spectra of (a) starch (b) AS and (c) AS-g-PAA.

3.3.5. Superabsorbency

3.3.5.1 Effects of amount of monomer on superabsorbency

Generally, an increase in the monomer concentration increases the absorbency of the polymer samples to a certain extent. At higher concentrations of the monomer, large number of the AA molecules are grafted onto the starch backbone to form a hydrophilic structure in the polymer that could absorb a large amount of water as can be seen in Fig.3.13. An excessive amount of AA leads to the formation of more homoplymers which sheilds the starch radical and blocks further grafting onto starch. This could also lead to an increase in the amount of self cross-linking reactions, hence decreasing the ability of the polymer to absorb and retain a high amount of water due to the formation of a stiff and rigid structure as reported in literature [9,15]. The highest water absorption in this study was noticed at AS to AA ratio of 1:3. The grafted polymer obtained when the AS to AA ratio of 1:3 was used has a 60% weight increase to the starting material (after extracting the homopolymer), as against 12% weight increase obtained when the starch to AA ratio is 1:1. Table 3.1 shows the effect of monomer content on the amount of copolymer obtained.

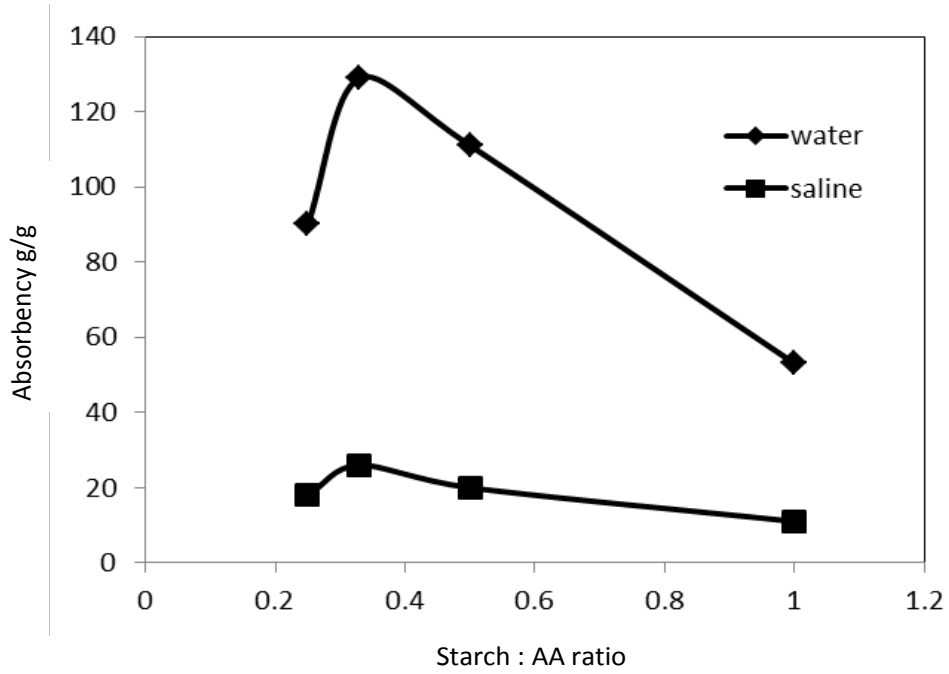

Figure 3.13 Effect of monomer content.

Table 3.1 Effect of amount of monomer on graft copolymer yield

AS:AA ratio	Weight of AS (g)	Weight of AS-g-PAA (g)	% weight added
1:1	5	5.60	12
1:2	5	6.88	37
1:3	5	8.02	60
1:4	5	6.30	26

3.3.5.2. Effect of initiator content

An increase in the amount of initiator (to a certain level) shows a slight increase in the water absorbency of the polymer in both water and saline solution as shown in Fig.3.14. Initial increase in the concentration of the initiator increases the chance of hydrogen abstraction from the starch backbone, and chain transfer reaction of the copolymer chain with

starch backbone leads to the increase in the grafting yield. At higher concentration of the initiator there is a decrease in the degree of polymerisation because too many radicals are produced which facilitate an increase in the termination rate between the free radical species produced and the starch macroradicals or with the growing polymer chains. Hence, the uneven comb-like hydophilic sites expected to be formed on the starch backbone are mostly absent in the polymer, which results in lower absorbency as shown in Fig. 3.14. The absorbency initially increases with initiator concentration (up to 2 mmole of FAS), but decreases when the concentration was increased to 2.5 mmole, this is because the grafting yield decreases at higher concentrations of the initiator and low-molecular weights polymers are produced with reduced-swelling.

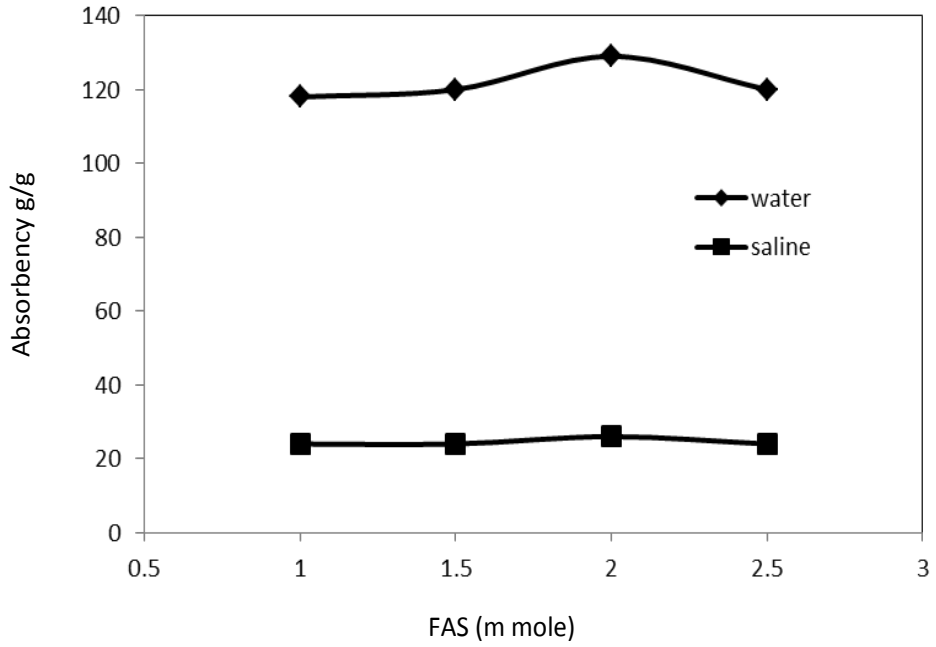

Figure 3.14 Effect of initiator content.

3.3.5.3 Effect of the degree of neutralisation

The observed increase in the degree of neutralisation in this experiment conforms to the previous works in the literature [12,16,17,18], whereby the water absorbency is proportional to the degree of neutralisation. In this work the maximum absorption capacity was obtained at 80 % neutralisation of all the samples as can be seen in Fig. 3.15. From Flory's description of the water absorption mechanism in equation (2) below, it could be that the increase in the

ability of increased absorbency up to 80 % (pH 5.6) neutralisation in this work comes from the structural feature of the polymer chains which hinders the screening effect of sodium ions of the negatively charged carboxyl groups up to this level.It is generally observed that the polymer samples have a lower water absorbency in saline solution compared to water. In saline solution the Na^+ in the solution hinders the mutual repulsion of the negatively charged carboxyl groups thereby hampering further expansion of the polymer network. The overall relationship between the presence of ions in the solution and the water absorbency is expressed by Flory's equation [9] :

$$\varphi^{5/3} = [(i/2\, v_u S^{*1/2})^2 + \left(\frac{1/2 - X_1}{v_1}\right) \div \left(v_e/V_0\right)] \quad (2)$$

Where φ is the degree of swelling, i/v_u is the charge density of the polymer, S^* is the ionic strength of the swollen solution, $\frac{1/2 - X_1}{v_1}$ is the polymer-solvent affinity, v_e/V_0 is the cross-linking density.

The equation describes how the presence of ions (ionic strength) in aqueous solution affects water absorbency; the absorbency decreases in saline solution due to the ionic strength of the solution. The superabsorbent property of polymers results from the hydrophilic polar groups present in the polymer network which becomes hydrated upon contact with water. Hennick and Nostrum [19] describe the effect of swelling activity that results from the primary bound water and the hydrophilic groups as leading to exposure of the hydrophobic groups in the polymer into an interaction with water molecules forming secondary bound water. The polymer network itself allows more water to be trapped within its matrix due to osmotic pressure from the network chains, while the covalent bonds and the cross-linked structure limit the expansion to a certain level. Neutralisation of the carboxylic groups in the polymer chains leads to the formation of ionic ($–COO^-$) groups which exercise electrostatic repulsion further increasing the expansion of the polymer network which allows more water to be trapped.

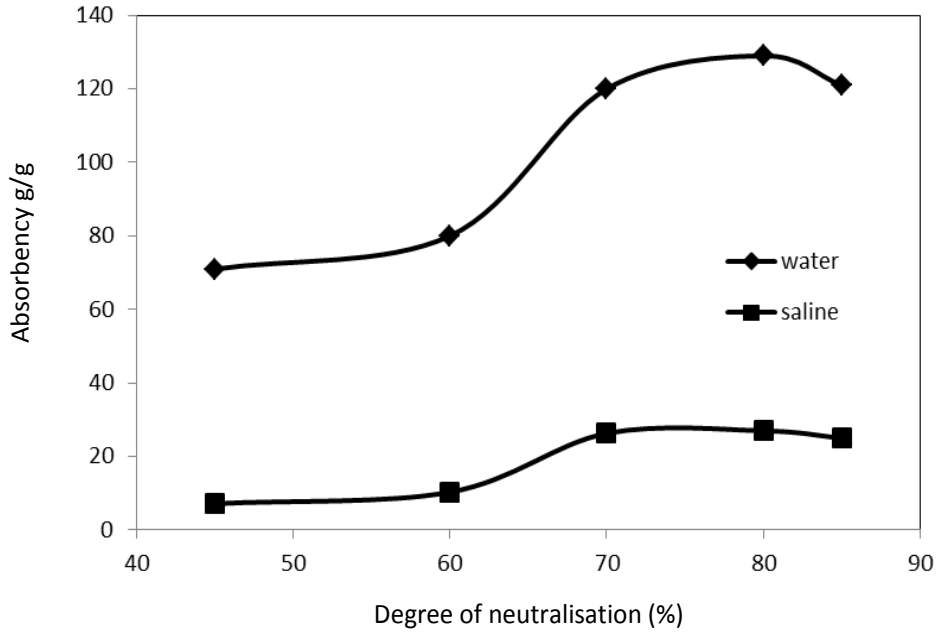

Figure 3.15 Effect of degree of neutralisation.

3.3.5.4 Water retention

Li *et al.* [7] reported that a swollen hydrogel could contain free water which is not bound with the polymer; it is mobile and easily lost. So it could be said that the water retention test determines the amount of water that is properly bound to the polymer matrix. The ability of the polymer sample to absorb and retain water and saline solution was tested on a centrifuge. The swollen polymer sample was centrifuged for 60 minutes at a speed of 5000 rpm, at ambient temperature, the net weight of the sample was calculated and the retention ability was calculated using equation (1) [16]. Table 3.2 shows the retention ability of different samples with different water absorption capacity. All the samples show impressive ability to retain water even at the highest absorption capacity. A polymer sample with absorbency value of 127 g/g was able to retain water up to 97 % and could absorb 18 g/g of saline solution under pressure. The water absorption and retention capacity, especially under load, of the polymer could be useful in agricultural applications and in personal hygiene products.

Table 3.2 Water retention ability of samples.

Degree of neutralisation (%)	Water absorption (g/g)	Saline soln. absorption(g/g)	Saline soln. AUL (g/g)	Retention (%) water	Retention (%) saline solution
45	71	7	4	100	100
60	80	10	6	100	100
70	120	26	16	98	98
80	127	27	18	97	97
85	121	25	16	98	98

3.3.5.5 Superabsorbency of CAS-g-PAA

The samples prepared at different reaction conditions show different levels of absorbency in water and in saline solution. Generally, polymer samples prepared from cross-linked acryloylated starch with more substituted acryloyl groups (Higher DS) have the highest absorbency.

The acryloyl groups are spread across the cross-linked starch ester forming a long chain of poly(acrylic acid) randomly distributed in the polymer matrix with a favourable network structure of more hydrophilic groups. This accounts for better ability of the polymer to absorb large amounts of water within its frame structure. In Table 3.3, the absorbency in water and saline solution of the samples increases proportionally with the DS, thus confirming what's explained above. In addition, there are excellent retention ability and high values of absorbency under load (AUL) of all the samples with different DS compared to results obtained with a polymer prepared from the native starch ester [5]. As mentioned earlier, a cross-linked starch has increased stability to acid, heat treatment and to shear forces. Due to the aforementioned properties associated with the polymer, the samples have remarkable ability of absorbing water under pressure and with good retention ability.

Table 3.3 Superbsorbency of different samples of CAS-g-PAA.

DS of CAS-g-PAA samples	Degree of neutralisation (%)	Absorbency in water (g/g)	Absorbency in saline (g/g)	AUL (g/g) Saline	Retention (%) saline
0.2	20	17	4.0	3	100
0.2	40	29	8.0	6	100
0.2	60	33	12	9	100
0.2	75	49	14	11	100
0.2	80	43	13	11	100
0.5	20	38	12	9	100
0.5	40	45	13	11	100
0.5	60	54	16	12	100
0.5	75	71	20	16	100
0.5	80	60	18	15	100
0.8	20	47	14	11	100
0.8	40	54	16	12	100
0.8	60	61	18	15	100
0.8	75	99	28	24	100
0.8	80	75	22	17	100

In this study the neutralised cross-linked acryloylated starch-g-poly(acrylic acid) sample prepared from cross-linked acryloylated starch with DS 0.8 was able to absorb 99 g/g and 28 g/g of water and saline solution respectively. On the other hand, the maximum absorption of 99 g/g was obtained from a polymer sample of CAS-g-PAA with 75 % neutralisation. In fact, increasing the degree of neutralisation of the polymer samples increases the absorbency of all the polymer samples up to a certain level when excessive amount of Na^+ screens the –COO groups and hinders the electrostatic repulsion and expansion of the overall polymer network. In Table 3.3 further neutralisation of the sample above 75 % accounts for a decrease in absorbency from 99 g/g to 75 g/g due to the screening effect of Na^+ explained earlier.

3.3.6 Grafting parameters

3.3.6.1 Effect of acryloylation

Table 3.4 shows the grafting parameters obtained at different level of DS. The GE %, PG %, and GR % increase proportionally with the DS. This is because the presence of more acryloyl groups in the starch means more active sites, as the vinylic sites are the potential bonding points with the acrylic acid monomer after the action of radical initiator. Although the starch ester, cross-linked acryloylated starch, has a limited range of DS due to cross-linked nature of the starch (0.2–0.8), the difference is quite noticeable in affecting the grafting parameters.

The polymer, CAS-*g*-PAA, synthesised from cross-linked acryloylated starch with a DS of 0.2 has the lowest value of GE %, PG %, and GR % and has a higher amount of homopolymer percentage. 78 %, 52 %, 34 % and 21 % were the values obtained for GE, GR, PG and HP respectively. The highest grafting percentage of 49 %, efficiency of 91 % and grafting ratio of 96 % were obtained when the DS was 0.8 and a minimum amount of HP (8.6 %). It can be seen that an increase in acryloylation agents (starch: pyridine: acryloyl chloride) facilitates an increase in the acryloyl substituent group on the cross-linked starch backbone, hence higher grafting yield. The starting material is a cross-linked starch, therefore some of the free OH groups in the starch are substituted with the cross-linking agent (epichlorohydrin) as a result of bridging reaction between the cross-linker and the starch molecules (Scheme 3.1) and there is an increase in the steric hindrance between the molecules of starch leading to a limited number of acryloyl groups per average glucose unit. As a result, acryloyl starch ester with a maximum degree of substitution (DS) of 0.8 was obtained in this study.

Table 3.4 Effect of DS on copolymerisation; at 60 °C and 3 h reaction time.

Run	DS	PG %	GR%	GE %	HP%
1	0.2	34	52	78	21
2	0.5	40	68	83	16
3	0.8	49	96	91	9.0

Table 3.5 Effect of Temperature on graft copolymerisation; DS 0.8; At 3 h reaction time.

Run	DS	Temp (˚ C)	PG %	GR%	GE %	HP%
1	0.8	30	33	52	77	19
2	0.8	50	41	89	85	11
3	0.8	60	49	96	91	9.0
4	0.8	80	37	60	81	15

3.3.6.2 Effect of temperature

From Table 3.5, HP% decreases with increase in the temperature from 30–60 °C, thereafter it increases again. On the other hand, there is an increase in the grafting parameters such as ratio and percentage, as it leads to a more effective mobility of the reacting species (acrylic acid) in the reaction vessel and the swelling ability of the starch particles [12,20]. From Arrhenius equation (2); an increase in temperature can increase the grafting rate and homopolymerisation at the same time, but it is noteworthy that the activation energy of grafting polymerisation is much greater than that of homopolymerisation, hence, increasing the temperature can improve the grafting efficiency [21]. At higher temperatures (in this case 80 °C) the rate of formation of surface radicals becomes high which leads to premature termination of the radicals, and a polymer with a low percentage add-on and efficiency is produced as can be clearly seen in the Table. For this reason 60 °C is taken as the optimum temperature in the graft copolymerisation for determining the effect of other reaction variables

$$k = Ae^{(-E/RT)} \tag{3}$$

3.3.6.3 Amount of acrylic acid (AA)

Table 3.6 shows the effect of adjusting the amount of acrylic acid ratio on the grafting efficiency, percentage grafting, grafting ratio and the amount of homopolymer produced along the cross-linked acryloylated starch graft poly(acrylic acid). Initial increase in the amount of acrylic acid increases the GE %, PG % and GR %, as the rate of grafting process depends on the amount of monomers that could get to the substrate. Higher amount of AA monomers results in the decrease of the grafting parameters; this can be ascribed to the chain

transfer to excess monomer molecules in the vicinity of growing ends of grafted chains [14]. In fact, among the different ratios of monomer to substrate selected in this study, the highest percentage of homopolymer and the lowest grafting percentage and grafting efficiency were obtained when the acrylic acid amount is lowest; GE %, PG %, GR % and amount of homopolymer in the run were 14%, 61%, 16 % and 38 % respectively.

Table 3.6 Effect of amount of monomer on graft copolymerisation, DS 0.8, temperature 60 ˚C.

Starch:AA ratio	PG %	GE%	GR%	HP%
1:1	14	61	16	38
1:2	25	68	35	15
1:3	49	91	96	9.0
1:4	47	88	90	10

3.4 Conclusions

In this work, superabsorbent polymers of starch grafted with acrylic acid has been prepared without the aid of a cross-linking agent. The product was prepared by acryloylation of starch followed by grafting with acrylic acid using Fenton's initiation system. By varying the starch to the monomer ratio and amount of the initiator up to a certain concentration, a highly absorbent polymer product with good retention capacity was obtained. A sample with absorption capacity of 127g/g and 27g/g for water and 0.9% saline solution respectively was formed without the use of cross-linking agent. The product shows a gradual increase in the absorbency with a degree of neutralisation up to 80 % (pH of 5.6) and a good retention capacity (97 %) which could be associated with the molecular structure of the product and nature of distribution of the hydrophilic ends in the polymer.

Controlled-cross-linking reaction of potato starch with EPI allowed successful acryloylation reaction of varying DS onto the starch network. The presence of double bonds in the CAS was confirmed by FTIR, SEM and thermal properties of the sample and its availability for grafting reactions. The final product, CAS-g-PAA, produced from successful polymerisation of the ester with AA using Fenton's reagent as initiator, was characterised and

was proved to have impressive water and saline absorbency, especially under pressure. The temperature of the reaction and amount of AA were observed to affect the grafting parameters with the optimum temperature of 60 °C and 1:3 of starch to AA ratio. The superabsorbency was found to be affected by the degree of acryloylation and neutralisation of the polymer samples. Generally, there is an improved PG, GE, GR and low amount of HP in all runs of the experiment compared to similar grafting reactions of starch and PAA. In this study, the superabsorbency is not so high, but the remarkable water retention ability and appreciable absorbency under load may make the polymer to be of importance applications in pharmaceutical and agricultural purposes.

3.5 References

[1] Fang J.M., Fowler P.A., Tomkinson J., Hill C.A.S. *Carbohydr. Polym.* 2002, 47:245–252

[2] Fang J.M., Fowler P.A., Hill C.A.S. *J. Appl. Polym. Sci.* 2005, 96:452–459

[3]Patil D.R., Fanta G.F. *J. Appl. Polym. Sci.* 1993, 47:1765–1772

[4] Li M., Zhu Z., Pan X. *Starch/Stärke* 2011, 63:683–691

[5]Mohammed A.D., Young D.A., Vosloo H.C.M. *Starch/Starke* 2014, 66:1–7

[6] Kurakake M., Akiyama Y., Hagiwara H., Komaki T. *Food Chem.* 2009, 116:66–70

[7]Li A., Wang A., Chen J. *J. Appl. Polym. Sci.* 2004, 92:1596–1603

[8] Stampel G.H., Cross, R.P., Mariella R.P. *J. Am. Chem. Soc.* 1950, 72:2299–2300

[9] Lanthong, P., Nuisin, R., Kiatkamjornwong, S. *Carbohydr. Polym.* 2006, 66:229–245

[10]Ramazani-Harandi M.J., Zohuriaan-Mehr M.J., Yousefi A.A., Ershad-Langroud A., Kabiri K. *Polym. Test*. 2006, 25:470–474

[11]Weaver M.O., Montgomery R.R., Miller L.D., Sohns V.E. *Starch/Stärke* 1997, 29:410–413

[12] Athawale V.D., Rathi S.C. *Rev. Macromol. Chem. Phys*. 1999, 39:445–480

[13] Sandle N.K., Singh O.P., Verma I.K. *Angew. Makromol. Chem.* 1984, 121:187–193

[14] Athawale V.D., Lele V. *Carbohydr. Polym.* 2000, 41:407–416

[15] Chen J., Zhao Y. *J. Appl. Polym. Sci.* 2000, 75:808–814

[16] Zhang J., Yuan K., Wang Y., Gu S., Zhang S. *Mater. Lett.*2007, 61:316–320

[17] Hua S., Wang A., *Carbohydr. Polym.* 2009, 75:79–84

[18] Chen J., Zhao Y. *J. Appl. Polym. Sci.* 1999, 74:119–124

[19] Hennink W.E., Nostrum C.F. *Adv. Drug Deliv. Rev.*2002, 54:13–36

[20] Sacak M., Oflaz F. *J. Appl. Polym. Sci.* 1993, 50:1909–1916

[21]Zhu J., Deng J., Cheng S., Yang W. *Macromol. Chem. Phys.* 2006, 207:75–80

Chapter 4

Synthesis of High Performance Superabsorbent Glycerol Acrylate cross-linked Poly (acrylic acid)/Poly (acryloylated starch) Copolymers

4.1 Introduction and objectives

4.1.1 Superabsorbent Glycerol acrylate cross-linked poly (acrylic acid)

The chemical modification of glycerol is often required in chemical industries to better suit its properties to specific applications. Modified glycerol may find application in the synthesis of important products such as polyethers, esters, alkyd resins, ethers, acetals, and ketals. Roice *et al*. [1] have reported the synthesis of a mechanically stable polymeric support resin by radical polymerisation of glycerol dimethacrylate and methyl methacrylate. By the introduction of functional and reactive groups into the polymer structure, a flexible network structure that allows unhindered diffusion of reagents and solvents through its matrix was obtained. Thus, a polymeric resin with a wide range of applications was synthesised.

Acrylic acid is found to be used mostly in the form of its polymer and accounts for 80–85% of raw materials needed in the manufacture of superabsorbents [2]. The interconnectivity of the structural network of superabsorbent polymers enables them to absorb a large quantity of water without getting dissolved via hydrogen bonds [3]. The commonly used cross-linking agents utilised in the synthesis of superabsorbent PAA include 4,4'- divinylazobenzene [4], N,N′-methylene-bis-acrylamide [5], ethylene glycol dimethacrylate [6] and sucrose [7]. Other techniques such as photo-cross-linked polymers are also reported [8]. The cross-linking compounds form a bridge by forming an ester or ether intermolecular linkages between the hydroxyl groups on the polymer matrix [9] and without compromising the hydrophilicity of the polymer. Among the range of compounds used as cross-linking agents, those with smaller and more active bonding sites are preferred, as they easily get bonded and form the intermolecular bridge between the polymer molecules [10]. Cross-linking of polymers is one of the processes used in enhancing the physico-chemical properties of polymer products.

4.1.2 Objectives

The objectives of the study are:

- Synthesis of glycerol acrylate (GA) by acryloylation reaction with acryloyl chloride.
- Study the synthesis of cross-linked poly (acrylic acid) using various proportions of glycerol acrylate as cross-linking agent.

- Study the effects of the amount of cross-linking density in the product (GA-PAA) and the degree of neutralisation on absorbency of the polymer samples.
- Synthesis of acryloylated potato starch and graft copolymerisation of the product with acrylic acid, using different proportions of glycerol acrylate as cross-linking agent and Fenton's reagent as initiator.
- Study the effect of the cross-linking agent by varying the % density of glycerol acrylate in the total reaction mixture.

4.1.3 Superabsorbent glycerol acrylate cross-linked poly (acryloylated starch) (AS-g-PAA-GA)

The cross-linking of the graft copolymers yields the formation of interconnected structures that allows the trapping of a large amount of water without being dissolved. In the previous work reported [3], the acryloylation of the starch before grafting produced a polymer structure with a long comb-like chains that could allow water to be trapped within the network of the polymer structure. A maximum absorbency of 127 g/g was obtained from the polymeric structure containing the PAA molecules roped on the starch backbone without the aid of a cross-linker. This work, however, entails the use of glycerol acrylate as a cross-linker whereby a molecular bridge is formed between the comb-like structures of grafted PAA onto the starch backbone and the study of the effects of cross-linking on the superabsorbency. The thermal and structural properties of the copolymer are also compared to the product reported having been obtained previously by the authors [3]. 0, 1, 2, 5% cross-linking density was used to produce the copolymer, acryloylated starch-g-acrylic acid/glycerol acrylate (AS-g-PAA-GA)

4.2 Experimental

4.2.1 Materials

Potato starch, glycerol, ferrous ammonium sulphate, benzoyl chloride, pyridine and hydrogen peroxide (30%) (Sigma-Aldrich) were used as received. Acrylic acid (Sasol) was freshly distilled under reduced pressure before use.

4.2.2 Analytical techniques

The FTIR analysis of the samples was carried out using a Bruker VERTEX 80 FTIR spectrometer. The infra-red spectra of the samples were recorded in absorbance mode, at a frequency range of 550–4000 cm^{-1}, at room temperature, with a resolution of 4 cm^{-1} based on 32 scans and using an ATR Bruker Platinum-Diamond accessory. Thermal properties of the polymer samples were determined on an SDTQ 600 thermal analysis Instrument. Samples were contained within aluminium crucibles and heated at a rate of 10 °C min^{-1} from room temperature to 500 °C under flowing nitrogen at a rate of 75 mL/min.

The Scanned electron images were obtained on a Quanta FEG 250 Environmental Scanning electron microscope using an accelerating voltage of 15 kV.

XRD analysis of the samples was processed and measured in powdered form. The diffraction patterns were recorded on a Röntgen PW3040/60 X'Pert Pro X-ray diffractometer, using Ni-filtered Cu Kα radiation (λ = 1.5405 Å) and scintillation counter at 40V and 40mA at ambient temperature. All the samples were scanned at 2θ diffraction angles ranging from 0°–120°. The powdered samples with uniform surfaces were exposed to X-rays, and the scattering angles of the diffracted X-rays with respect to the angle of the incident beam were measured.

Three samples of cross-linked poly(acrylic acid)(GA-PAA 0.8, GA-PAA 2.0, GA-PAA 5.0) were selected for characterisation as the polymer samples containing 5.0% and 10% cross-linking density show no noticeable difference in the analytical results. Poly (acrylic acid) was also synthesised using the same procedure without a cross-linking agent so as to make a proper comparison of the added properties after cross-linking reactions.

The second phase of the study is the acryloylated starch poly (acrylic acid) cross-linked with the same cross-linking agent as above. The samples are designated as; AS-g-PAA, AS-g-PAA1, AS-g-PAA2, AS-g-PAA5 for 0, 1, 2 and 5 % cross-linking density respectively.

4.2.3 Synthesis of acryloyl chloride

Acryloyl chloride was prepared using the procedure described in 3.2.2 above.

4.2.4 Acryloylation of glycerol

Glycerol acrylate was prepared using the acryloylation procedure reported by Mohammed *et al.*[3]. Nitrogen gas was purged into a three-necked round bottom flask containing glycerol (7.3 mL). Freshly prepared acryloyl chloride (24.0 mL) and dried pyridine (24.1 mL) were

slowly introduced into the flask and stirred for 45 min at 50 °C under nitrogen cover. Molar ratio of 1:2:2 for glycerol, acryloyl chloride and pyridine respectively were used. The product was dissolved in ether to remove the pyridinium salt produced along with the glycerol ester.

Selected IR, v (cm^{-1}): 3283 (O-H), 2935 (C-H), 1029 (C-O), 1730 (C=O)

4.2.5 Synthesis of glycerol acrylate cross-linked poly (acrylic acid)

GA-PAA was prepared in a three-necked round bottomed flask; nitrogen gas was purged into the flask to maintain an inert atmosphere, water (50 mL) containing 2.5 mmol ferrous ammonium sulphate was mixed with acrylic acid (20 mL) and glycerol acrylate (0.24–3.0 mL) were introduced into the flask. After stirring for 15 min, H_2O_2 (2 mL) was added followed by gradual addition of acrylic acid (15 mL) which makes a total volume of 30 mL acrylic acid in the mixture. The mixture was stirred for 2 ½ h, at a temperature of 60 °C under nitrogen cover. The product, GA-PAA was precipitated with methanol and dried at 45 °C under vacuum to constant weight before analysis. Scheme 4.1 shows the desired structure to be obtained in the reaction involving GA with acrylic acid to give the cross-linked product. However, mixtures of both primary and secondary acryloylated products were obtained.

Selected IR, v (cm^{-1}): 2931 (C-H), 1025 (C-O), 1720 (C=O),

4.2.6 Acryloylation of starch

Acryloylated starch with a degree of substitution (DS) value in a range of 0.8–1.0 was synthesised; as at higher DS a much more cross-linking occurs between the starch molecules which could lead to a rigid, brittle and poor water dispersibility of the polymer structure [10]. The acryloylation procedure reported by Mohammed *et al.* [3] was used in each case: dry starch (6 g) was added to water (80 mL) and stirred at 80°C for 60 min to produce a slurry. N,N′-dimethylacetamide (DMA, 3 x 50 mL) was added and distilled to remove the water azeotropically. After all the water was removed, LiCl (0.3 g) was added and temperature of the slurred-starch was allowed to cool to 60°C. Dry pyridine (1.5 mL) and freshly prepared acryloyl chloride (1.5 mL) was added dropwise and stirred for further 30 min at 60°C. The final product was precipitated with acetone and dried before analysis.

Selected IR, v (cm^{-1}): 1722 (C=O), 1616 (C=C), 2928 (C-H),

4.2.7 Synthesis of cross-linked AS-g-PAA

Nitrogen gas was purged into a three-necked round bottomed flask to maintain an inert atmosphere. Water (50 mL) containing 2.5 mmol ferrous ammonium sulphate was mixed with acryloylated starch (5 g) acrylic acid (20 g) and glycerol acrylate (0.0 –1.75 g) were introduced into the flask. After stirring for 15 min, H_2O_2 (2 mL) was added followed by gradual addition of acrylic acid (15 g) which makes a total mass of 30 g acrylic acid in the mixture. The mixture was stirred for 2 ½ h, at a temperature of 60 °C under nitrogen cover. The product, AS-g-PAA was precipitated with methanol and dried at 45 °C under vacuum to constant weight before analysis.

Selected IR, ν (cm^{-1}): 1600 (O-H), 2930 (C-H), 1016 (C-O), 1713 (C=O), 1448 (C-O-H).

4.2.8 Extraction of homopolymer

The dried product containing (AS-g-PAA) obtained above was extracted with methanol in a Soxhlet extractor for 24 h to remove the poly (acrylic acid) homopolymer. The pure copolymer, AS-g-PAA, was dried in an oven at 40 °C to constant weight.

4.2.9 Superabsorbency

The polymer samples with different cross-linking density were tested for water absorbency using a simple gravimetric method. An accurately weighed sample (1.0 g) was immersed in 500 g of water or 100 g of 0.9 % NaCl aqueous solution. The sample was allowed to remain in water or saline solution for 10 h; the swollen gel was screened through a 100 mesh sieve and weighed to determine the weight of the water absorbed by the sample. The absorbency (**Q)** was calculated using the relation:

$$\mathbf{Q = (w_2 - w_1) / w_1} \qquad (1)$$

where **Q** is the water absorbency, $\mathbf{w_2}$ and $\mathbf{w_1}$are the masses of the water-swollen sample and dry sample respectively.

The ability of the samples to absorb under load (AUL) was measured using the following procedure [12]: A macro porous sintered glass filter plate (porosity # 0, d = 80 mm, h = 6 mm) was placed in a Petri dish (d = 118 mm, h = 12 mm). The sample (1 g) was uniformly deposited on the filter paper on the sintered glass plate and a load of 500 g in a glass cylinder was deposited on the dry sample of the polymer. A 0.9 % NaCl solution was added until the

liquid reached the height of the filter plate (around 6 mm). The swollen particles were weighed again after 60 min and the AUL was calculated from equation (1). In each case, three analyses were carried out and the average values obtained were used in calculating the water absorbency. The retention ability of the swollen samples was tested in a centrifuge for 60 min at a speed of 5000 rpm, at ambient temperature. The samples were weighed again and the retention ability was calculated using equation (1) [3].

The solvent take-up of the samples was determined by dissolving 1 g each of the dry samples in a beaker containing 50 mL of solvent, the air-tight beakers containing the solvent and the samples were allowed soak for 48 hrs. The swollen samples were screened, centrifuged and the absorbed solvent was calculated from equation (1).

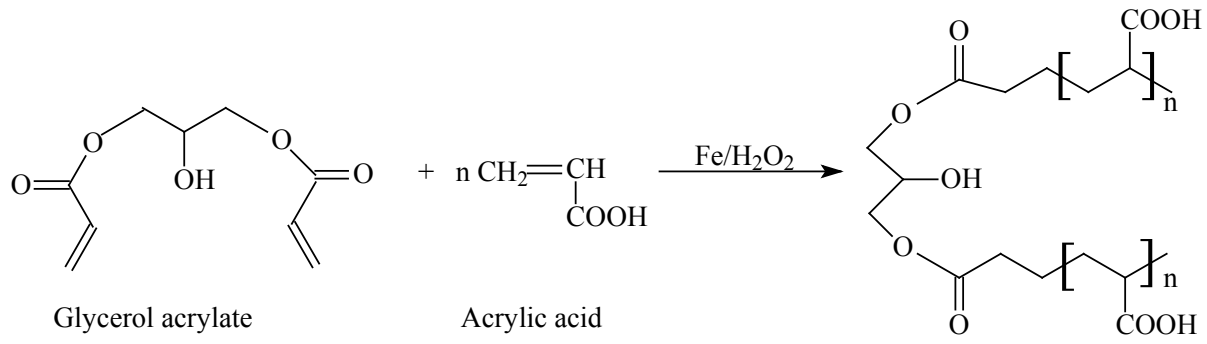

Glycerol acrylate Acrylic acid

Scheme 4.1 Synthesis of glycerol acrylate cross-linked PAA.

4.3 Results and discussion

4.3.1 FTIR analysis

The FTIR spectra of glycerol and the subsequent products obtained from acryloylation and cross-linked copolymers of PAA are shown in Fig. 4.1. The spectrum of glycerol (Fig. 4.1 a) shows absorption bands at 3282 cm^{-1} due to OH stretching vibration and 2932 cm^{-1} from dissymmetry stretching vibration of C-H. The C-O stretching and C-O-H bending vibrations are observed at 1029 and 1414 cm^{-1} respectively.

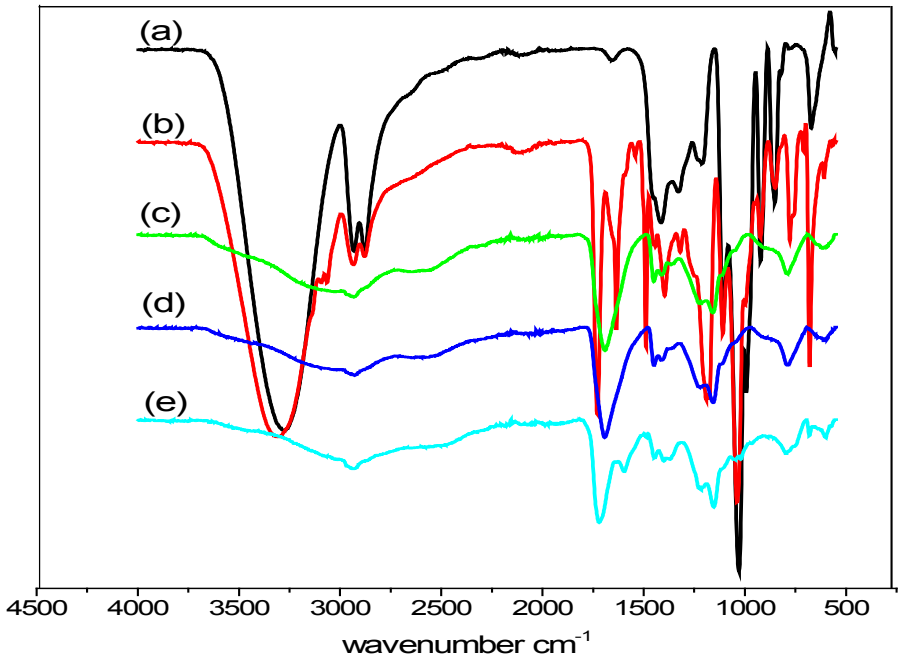

Figure 4.1 **FTIR spectra of (a) glycerol, (b) GA, (c) PAA, (d) GA-PAA0.8 and (e) GA-PAA5**

The acryloylated glycerol (GA), shows new absorption peaks at 1730 cm^{-1} due to C=O stretching mode and at 1635cm^{-1} from double bond vibration of C=C stretching of the acryloyl groups in the glycerol. These vibration peaks confirm that successful acryloylation of glycerol did take place. Fig.4.1(c) is the spectrum of PAA without any cross-linking agent; it shows a similar characteristic peak pattern with the cross-linked PAA from 0.8 % GA (Fig 4.1(d). With more amount of cross-linker, the absorption peaks show a noticeable shift in the absorption band. The C=O stretching vibration at 1691 cm^{-1} (Fig. 4.1c and d) is now shifted to 1720 cm^{-1} (Fig. 4.1e) due to the high cross-linking structure of the sample. The presence of new peaks and the shift in the existing ones confirm that glycerol acrylate has successfully played a chemical role as a cross-linker in the synthesis of PAA.

In the second phase of the work, the FTIR spectra of different samples of the copolymer containing varying densities are shown in Fig.4.2. The AS-g-PAA sample containing no

cross-linker is shown in Fig. 4.2(a). The sample shows important peaks at around 1705 cm^{-1} due to carbonyl stretching, around 1600 cm^{-1} due to the OH bending mode , 2930 and 1077 cm^{-1} from C-H stretching and bending respectively. Fig. 4.2(b) shows the spectum of the copolymer sample containing 1% cross-linking density. Abosrption peak at 2929 cm^{-1} is due to the C-H stretching vibrations, while at 1695 cm^{-1} comes from the carbonyl stretching of the acrylic groups in the copolymer. Graft copolymer samples of AS-g-PAA-GA with 2 % and 5 % cross-linking density (Fig. 4.2 c & d) show the following peaks: 2936, 2931 cm^{-1} and 1700, 1713 cm^{-1} for C-H and C=O stretching modes respectivley. The C-O stretching and C-O-H bending vibrations from the cross-linking agent are observed in all the samples, with increased intensity in Fig. 4.2(d) at 1016 and 1448 cm^{-1} absorption bands respectively. This arises from the high amount of glycerol ester in the sample. In addition, the OH bending mode around 1600 cm^{-1} in Fig. 4.2 (a) diminishes with the presence of cross-linking agent in the remaining spectra in Fig. 4.2(b), (c) & (d)

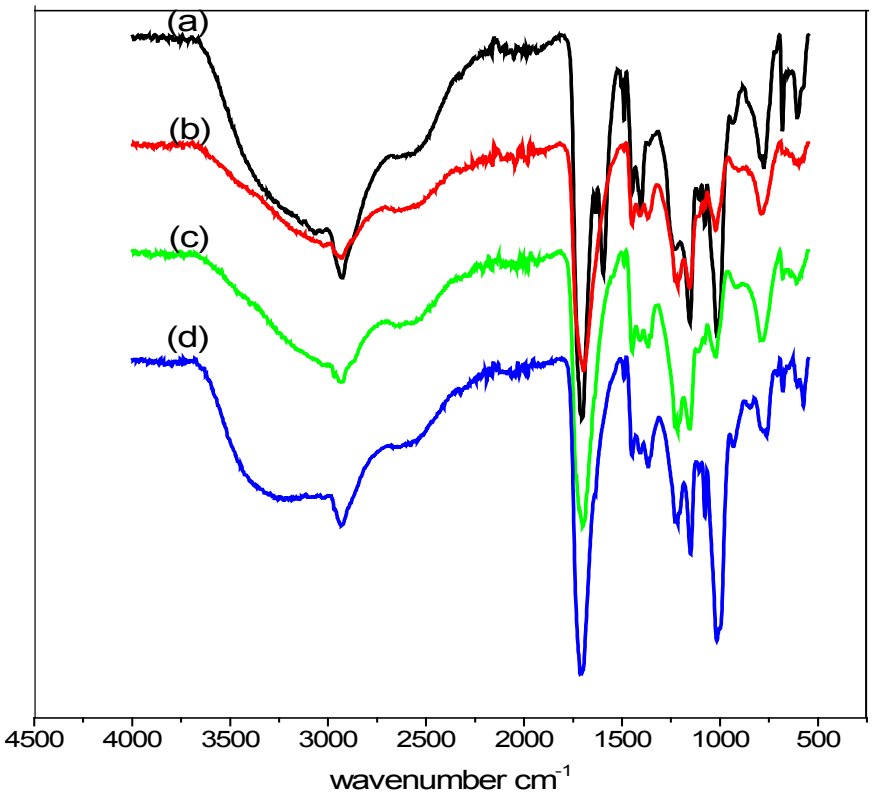

Figure 4.2 **FTIR spectra of (a) AS-g-PAA, (b) AS-g-PAA-GA1, (c) AS-g-PAA-GA2 and (d) AS-g-PAA-GA5 .**

4.3.2 Thermogravimetric analysis

The thermal analyses curves are represented in Fig.4.3 and 4.4. The thermal stability of PAA and GA-PAA 0.8 is shown in Fig 4.3. The PAA sample (Fig 4.3 a) shows initial loss in weight at about 125 °C due to the evaporation of trapped moisture in the polymer. Another weight loss of about 30 % is observed at 300 °C, followed by two successive major decompositions at 395 °C and 432 °C which results in 70 % weight loss. The final stage is the formation and decomposition of compounds formed at higher temperature. The lightly-cross-linked PAA (Fig 4.3 b) shows a similar decomposition pattern with the uncross-linked PAA (Fig. 4.3 a), but with the sample degradation occurring at a slightly lower temperatures and with a temperature of maximum decomposition at 421 °C with 70 % loss in weight. In Fig 4.4(a), the highly cross-linked PAA (GA=PAA 5.0) shows a different pattern of thermal stability. The initial loss in weight at 100 °C with 7 % loss in weight is followed by another important decomposition at 254 °C with a weight loss of 23 %. The temperature of maximum decomposition was observed at 398 °C with a weight loss of 63 %. Close examination and comparison of the three samples show a slight decrease in the thermal stability of the samples with increase in the cross-linking density. Fig.4.4 (b) shows the TGA curves of PAA, GA-PAA0.8 and GA-PAA5.0 samples. The slight decrease in the thermal stability with an increase in the cross-linking density in the polymers is clearly seen in the TGA curves of the three samples. The trend in the samples results from the disruption and decrease in the intermolecular hydrogen bonds between the PAA molecules due to the cross-linking reaction that hinders or bonded with the free OH in the acrylic acid monomers [11,13].

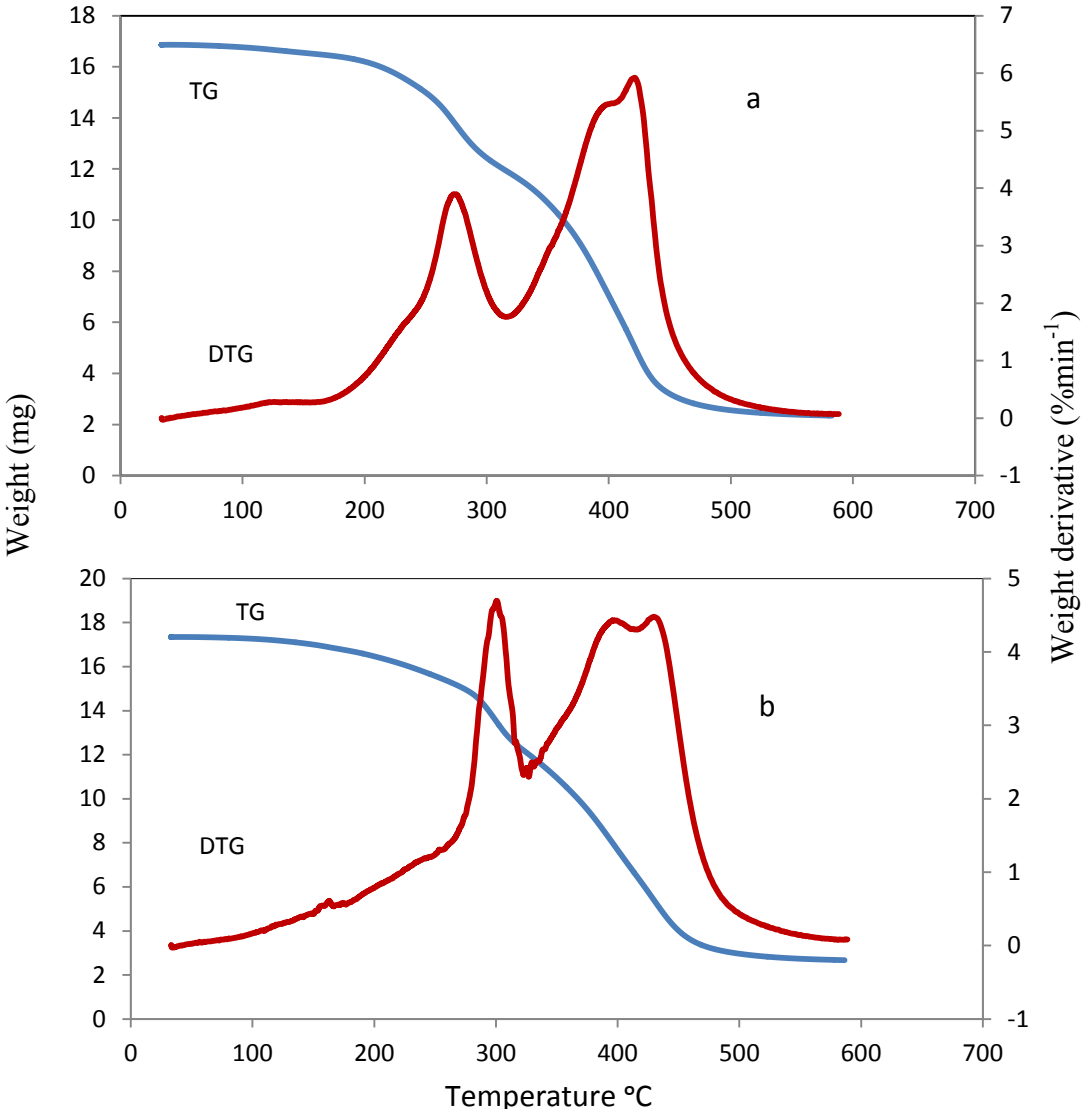

Figure 4.3 **Thermal analysis curve of a, PAAand b, GA-PAA0.8.**

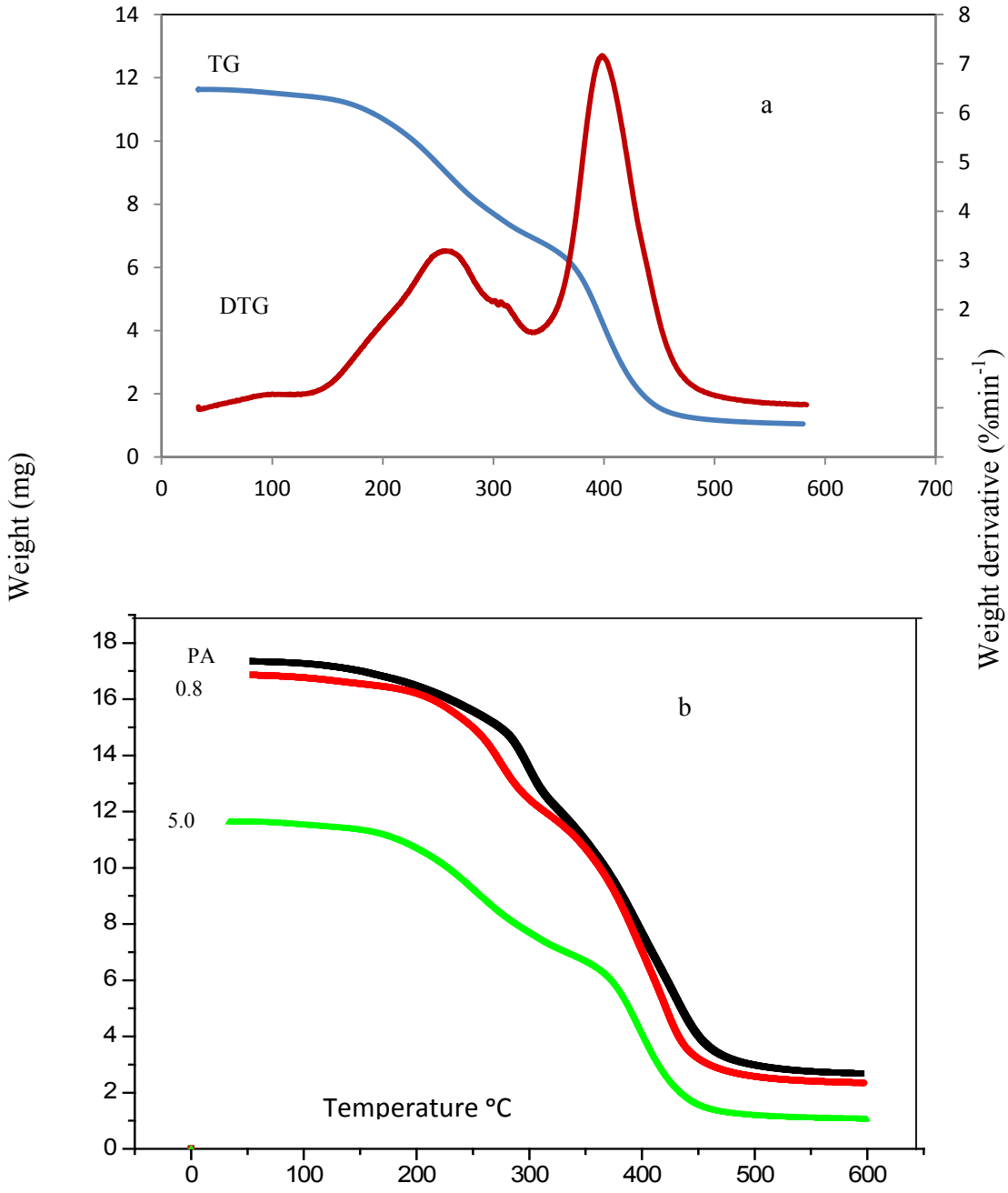

Figure 4.4 Thermal analysis curve of a, GA-PAA5.0 and b, TGA curves of PAA, GA-PAA0.8 and GA-PAA5.

4.3.3 SEM analysis

The SEM images of the PAA, GA-PAA0.8 and GA-PAA5.0 samples are shown in Fig.4.5. The surface morphology of the samples differs based on the presence and density of the cross-linker. The thick coated surface of PAA (Fig 4.5 a) changes to a rougher and noticeable

porous structure in Fig 4.5(b). These arise from the cross-linking reactions that have taken place and as a result the molecular orientation of the polymer was changed. The intermolecular spaces observed in the sample favour high absorbency behaviour of the sample as studied in this work. With an increase in the cross-linking density (Fig 4.5(c)), the morphology changes to a thicker surface with most of the structural spaces observed in Fig 4.5(b) being covered or narrowed to tinier pores. Hence, the aqueous intake was limited in the structure compared to the lightly-cross-linked PAA (GA-PAA0.8). Thus it can be deduced that the high cross-linking reactions lead to the formation of a tight interconnected structure that allows no-easy passage and entrapment of an water within the polymer matrix. The change in the morphological images (Fig 4.5 a–c) confirms that structural changes have occurred due to the intermolecular bridging reactions of the cross-linking agent with poly acrylic acid molecules.

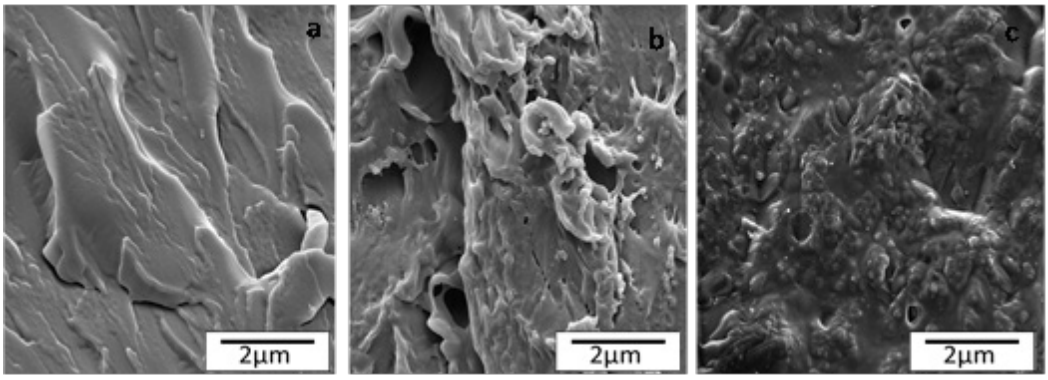

Figure 4.5 SEM images of (a) PAA, (b) GA-PAA0.8 and (c) GA-PAA5.

The cross-linked AS-g-PAA in Fig.4.6 shows the surface morphology of different samples of AS-g-PAA-GA containing a varying amount of cross-linking density. Fig.4.6(a) is the SEM image of the polymer without a cross-linking agent. The presence of PAA molecules on the surface of acryloylated starch can be clearly seen; the absence of any cross-linker causes the monomer particles to appear in a comb-like structure onto the acryloylated starch backbone. The loosely-connected structures onto the surface allows a limited amount of water to be trapped within the frame work. In the presence of cross-linker, Fig.4.6(b), the comb-like structure disappears with the formation of an interconnected network of PAA molecules onto the starch backbone. The glycerol acrylate forms a molecular bridge between the molecules of PAA thereby forming a measurable cross-linking network within the

polymer network. The cross-linking density of 1 % by mass to the total mass of the polymer sample causes the formation of a clouded surface of monomeric particles with numerous microscopic pores. The structure could allow reasonable amount of water to be trapped within the network as can be seen in the highly-magnified image of the sample in Fig.4.6(c). With high amount of the cross-linking density, Fig. 4.6(d), the highly cross-linked AS-g-PAA-GA produces a thick coated surface on the acryloylated starch backbone thereby hindering an easy passage and entrapment of water within the network. Hence, low superabsorbency. The SEM images of different samples of AS-g-PAA-GA show the effect of the cross-linking agent on the morphological features of the polymer with increase in the cross-linking density. They also show the evident features that determine the level of water and saline absorbency of the samples in that respect.

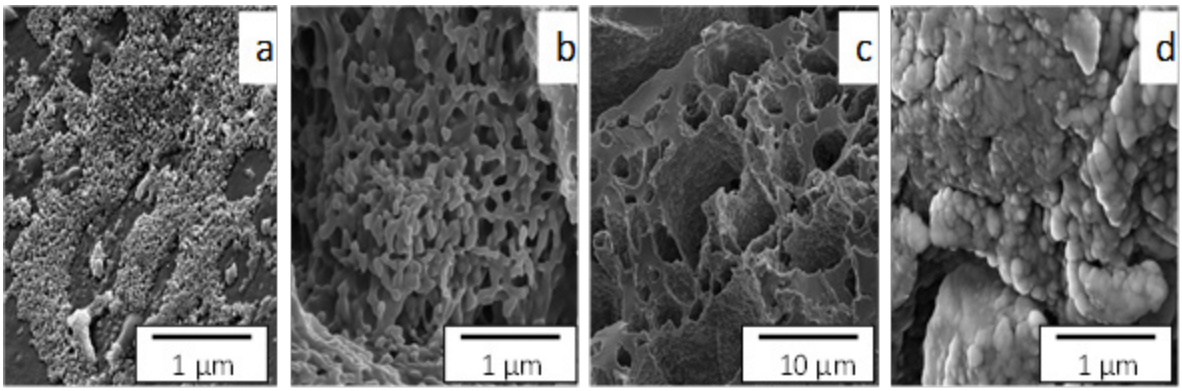

Figure 4.6 **SEM images of a, AS-g-PAA , b, AS-g-PAA-GA1,c, higher magnification of AS-g-PAA-GA1 and d, AS-g-PAA-GA5.**

4.3.4 XRD analysis

The structural orientation of PAA, GA-PAA0.8 and GA-PAA5.0 is studied from the XRD analysis. Fig.4.7 shows different diffraction patterns with an increase in the cross-linking density. The PAA samples containing no cross-linker, Fig. 4.7(a), shows an important characteristic peak at 20° and another broad peak at 40°. In the presence of GA as cross-linking agent in Fig. 4.7 (b and c), there is a shift and variation in the intensity of the characteristic peak at 20°, and the broad peak at 40° almost disappears with increasing the cross-linking density (Fig 4.7 c). These changes arise from the homogenisation of the

amorphous phase and with the disappearance of the semi-crystalline structure of PAA with increase in the cross-linking density. In addition, it shows the effect of cross-linking reaction on the structural orientation of the PAA molecules.

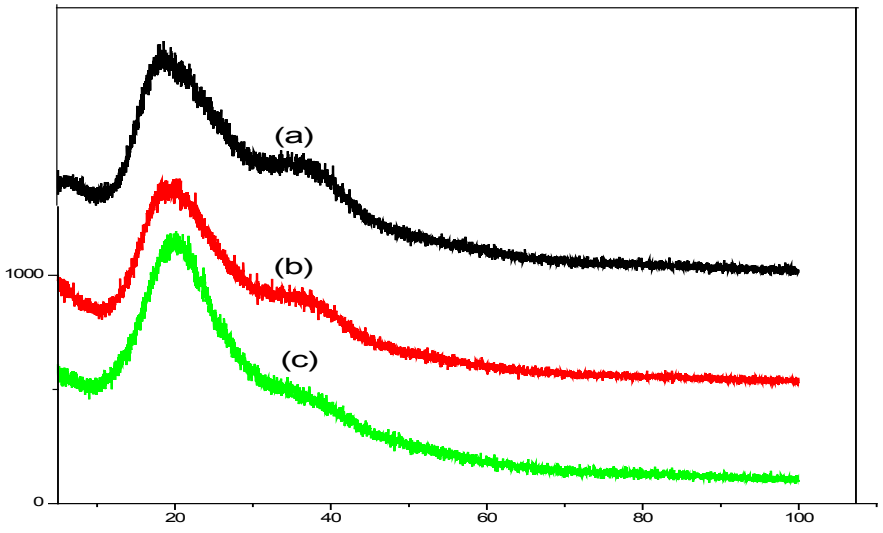

Figure 4.7 **XRD spectra of (a) PAA (b) GA-PAA0.8 and (c) GA-PAA 5.0.**

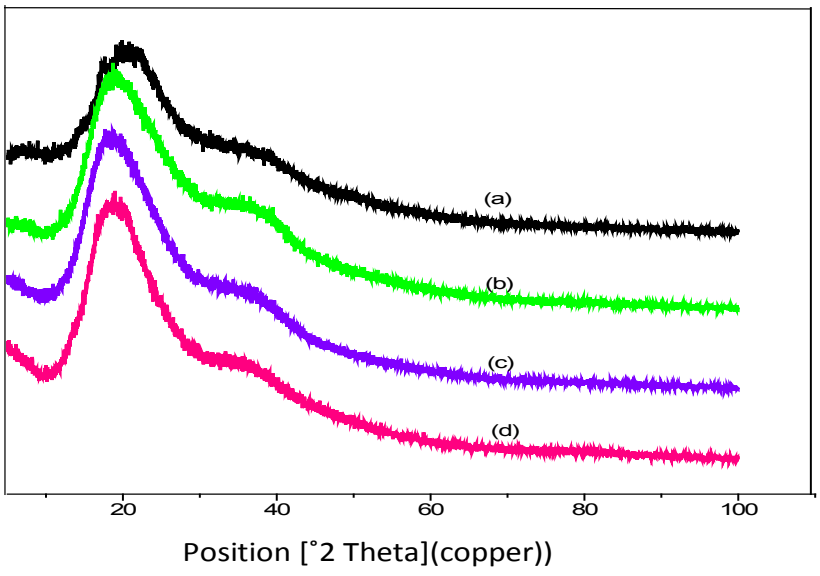

Figure 4.8 **XRD spectra of (a) AS-g-PAA, (b) AS-g-PAA-GA1 (c) AS-g-PAA-GA2 and (d) AS-g-PAA-GA5.**

On the other hand, Fig. 4.8 shows the XRD spectrum of the acryloylated starch copolymer samples with and without the cross-linking agent. The broad structure observed in AS-g-PAA, Fig. 4.8(a) at around 20˚ on the theta value changes to a more intensive peak at less than 20˚ in all the samples containing the cross-linking agent (Fig. 4.8b-d). Figure 4.8 c and d show intensive peaks at lower 2˚ values. In other words the shift is observed to be proportional with the percentage cross-linking density present in the samples. This is as a result of structural reorientation of partially crystalline molecules as a result of cross-linking reactions into an expanded and homogenised amorphous region. It, moreover, shows the effect of the cross-linking agent on the structural rearrangement of the polymer molecules. Fig. 4.8 c & d, samples containing 2 and 5 percentage cross linking density, appear to be the same in terms of the intensity and position of the diffraction peaks. This similarity in the structural feature is probably because the homogenisation and the structural rearrangement of the polymer molecules have levelled-off from 2 % cross-linking density; hence no noticeable difference is observed in the diffraction peaks.

4.3.5. Cross-linking and Superabsorbency

4.3.5.1 Water and saline absorbency

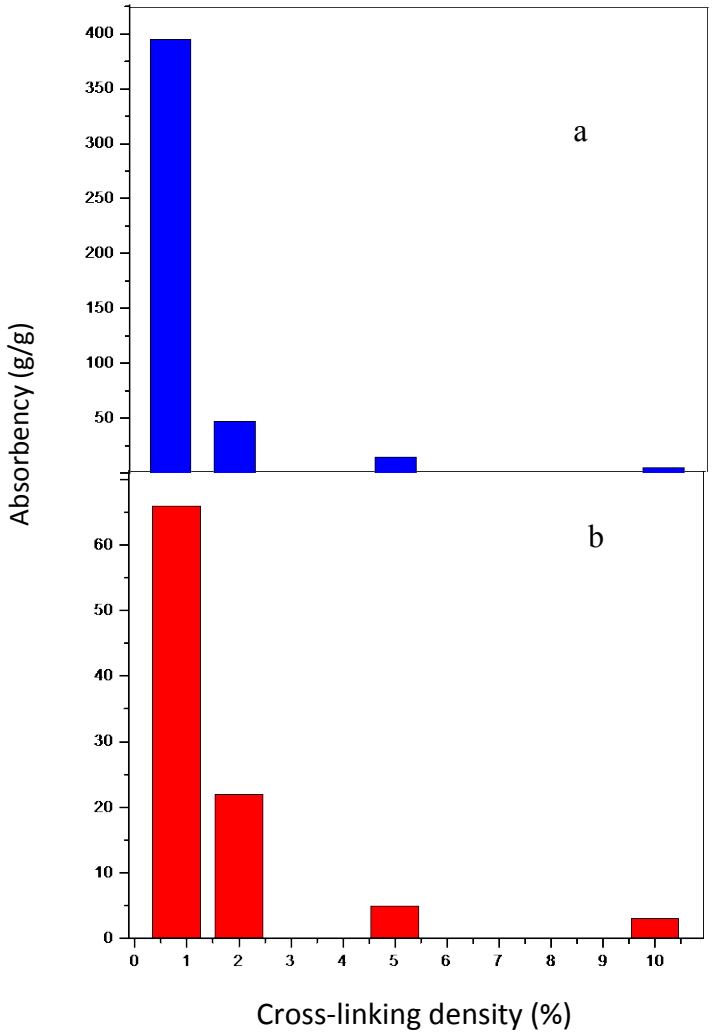

Figure 4.9 **Absorbency of GA-PAA samples of different cross-linking densities; neutralised to pH 6.5 in: (a) water and (b) saline solution.**

The samples prepared from different cross-linking densities were tested for water and saline absorbency. The cross-linked network structure of the polymer facilitates large amount of water to be trapped within its matrix via osmotic pressure from the network chains, while the covalent bonds and the cross-linked structure limit the expansion to a certain level. The superabsorbent polymers contain hydrophilic polar groups in the polymer network which becomes hydrated upon contact with water. The swelling activity of superabsorbent polymers results from the primary bound water and the hydrophilic groups as leading to exposure of the hydrophobic groups in the polymer into an interaction with water molecules forming

secondary bound water [14]. Fig 4.9 shows the absorbency of cross-linked poly (acrylic acid) samples of different cross-linking density; the absorbency decreases with the cross-linking density, with the lightly cross-linked PAA (GA-g-PAA0.8) having the highest absorbency of 395 and 66 g/g for water and saline solutions respectively. Samples containing high cross-linking density leads to the formation of a tightly interconnected structure with little intermolecular spaces for entrapment of water. That is why the samples containing 5 and 10 % cross-linking density could only absorb 15 and 09 g/g of water and 5 and 3 g/g saline respectively. All the samples, moreover, have the ability to absorb aqueous saline solution under load.

Table 4.1 Water retention and absorbency under load (AUL) of different samples of GA-PAA having different cross-linking density.

GA-PAA samples	Absorbency in saline (g/g)	AUL (g/g) Saline	Retention (%) saline
GA-PAA 0.8	66	11	100
GA-PAA 2.0	22	7	100
GA-PAA 5.0	15	5	100
GA-PAA 10	9	3	100

Table 4.1 shows the ability of each sample (GA-PAA) prepared from different cross-linking densities to absorb under load. Like water absorbency, there is significant absorbency of samples with low cross-linking density, with all the samples showing excellent water retention ability. Table 4.2 shows the percentage water retention and AUL of GA-PAA0.8 samples at different degrees of neutralisation. The samples show impressive retention ability at different absorbency values. The sample containing the highest volume of water was able to retain up to 97% of the same volume after centrifuging for 30 min, while samples with lower absorbency values could retain 100 % of the absorbed water in their matrix after centrifuging. This property is explained based on the amount of loosely retained and mobile water contained in the polymer samples, as the free water is not bound with the polymer and is easily lost [3].

Table 4. 2 Effect of neutralisation on the absorbency GA-PAA samples.

GA-PAA samples	Degree of neutralisation (pH)	Absorbency in water (g/g)	Absorbency in saline (g/g)	AUL (g/g) Saline	Retention (%) saline
GA-PAA 0.8	2.0	44	13	11	100
GA-PAA 0.8	3.5	53	15	13	100
GA-PAA 0.8	4.5	68	22	18	100
GA-PAA 0.8	5.5	107	41	38	99
GA-PAA 0.8	6.5	395	66	47	97
GA-PAA 0.8	7.5	388	64	45	97

4.3.5.2 Effect of neutralisation

The effect of neutralisation on absorbency was tested by using varying degrees of neutralised and non-neutralised samples. The sample with the highest swelling capacity was selected and further neutralised at different pH to determine the optimum pH level for the superabsorbent samples. Sample GA-PAA0.8 had the highest swelling ability and was thus taken for further tests. Neutralisation of the carboxylic groups in the polymer chains leads to the formation of ionic ($–COO^-$) groups which exercise electrostatic repulsion, further increasing the expansion of the polymer network and resulting in more aqueous material to be trapped within the matrix. In this study, the optimum neutralisation level of pH 6.5 was obtained. Table 4.2 shows a proportionate increase in the swelling ability of the samples with pH increase. Initial increase in the neutralisation of the samples leads to a simultaneous increase in the electrostatic repulsion between the negatively charged carboxylate groups, hence a more expanded network polymer structure. Excessive neutralisation, however, of acidic protons leads to excessive amounts of Na^+ which exercise a screening effect on the –COO groups, thus limiting further electrostatic repulsion and expansion of the polymer network structure.The slight decrease in the absorbency from 395 g/g at pH 6.5 down to 388 g/g at pH 7.5 could not be explained otherwise. A similar trend is observed in the AS-g-PAA sample of the cross-linked PAA with the glycerol ester. A pH level of 6.5 of the polymer sample was found to absorb the highest amount of water. Table 4.3 shows the effect of neutralisation on the absorbency of the samples. The same pattern is observed whereby an

initial increase favourably increases the absorbency while an excessive amount of the alkali causes decrease in absorbency. The absorbency is quite low in samples with a low pH but increases with an increase in the degree of neutralisation up to the optimum level of 6.5 where the sample absorbes 330 g/g and 58 g/g for water and saline sample, respectively. A pH increase to 7.5 decreases both the water and saline absorbency, respectively.

Table 4.3 Effect of degree of neutralisation on water and saline absorbency of AS-g-PAA-GA samples

GA-PAA samples	pH	Absorbency in water (g/g)	Absorbency in saline (g/g)	AUL (g/g) Saline
AS-PAA-GA1	2.5	40	11	4
AS-PAA-GA1	3.5	51	12	5
AS-PAA-GA1	4.5	135	20	12
AS-PAA-GA1	5.5	220	38	21
AS-PAA-GA1	6.5	330	58	27
AS-PAA-GA1	7.5	302	50	24

4.3.5.3 Solvent uptake

The absorbency test was carried out on solvents with different polarity. Fig.4.10 shows the pattern of absorbency of GA-PAA0.8. The highest absorbency is observed in DMF and the least in hexane. A remarkable uptake of 1700 % of DMF was obtained. Although there is no noticeable difference in the % uptake of other solvents selected for the test, it shows that the value of the dielectric constant of the solvent could determine their uptake capacity. Fig.4.10 shows the pattern of solvent uptake in the following order DMF>DCM>Ethyl acetate>Hexane, with the pattern following the polarity and dielectric constant of the solvents. The solvent uptake property shows that the cross-linked polymer could find further application in solvent entrapment, especially on polar solvents with high dielectric constant.

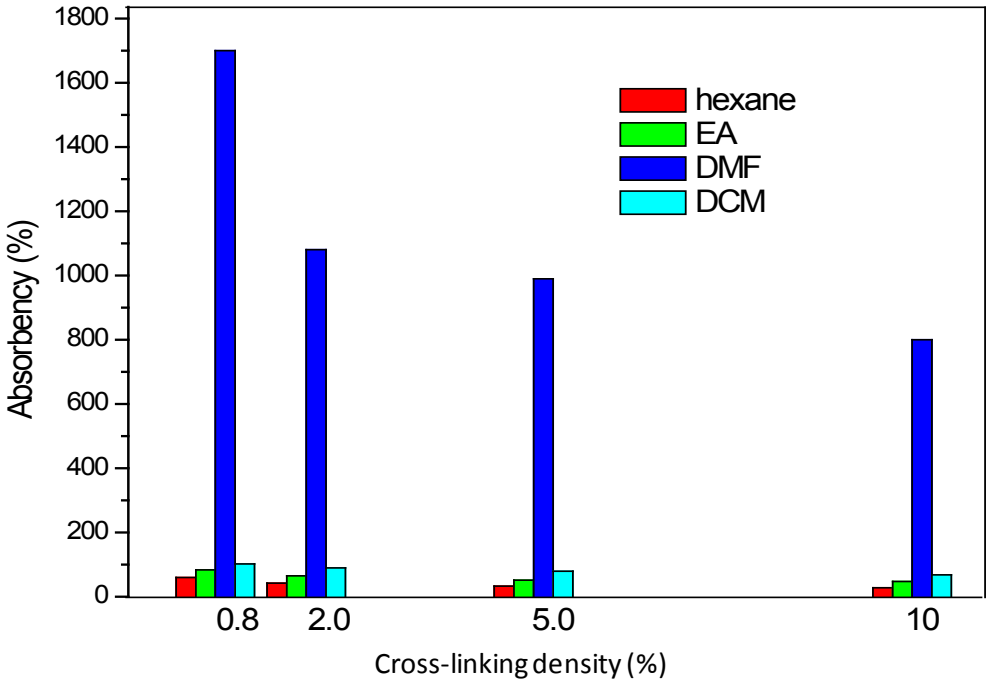

Figure 4.10 Solvents intake of GA-PAA samples of different cross-linking densities

4.3.5.4 Effect of cross-linking

Fig. 4.11 shows the water absorbency of different samples of AS-g-PAA-GA containing different cross-linking densities. The sample containing no cross linker could absorb up to 127 g/g of water, while in the presence of 1 % cross-linker, the sample was found to absorb the highest amount of water (330 g/g). The cross-linked network structure causes large amount of water to be trapped within the polymer matrix via osmotic pressure from the network chains. Excessive increase in the cross-linking density, however, decreases the absorbency of the polymer samples. The tightly interconnected structure formed with high cross-linking density limits the amount of water that can be trapped within the polymer network. This could be clearly seen in the samples containing 2 and 5 % cross-linking densities with water absorbency of 255 and 42 g/g, respectively.

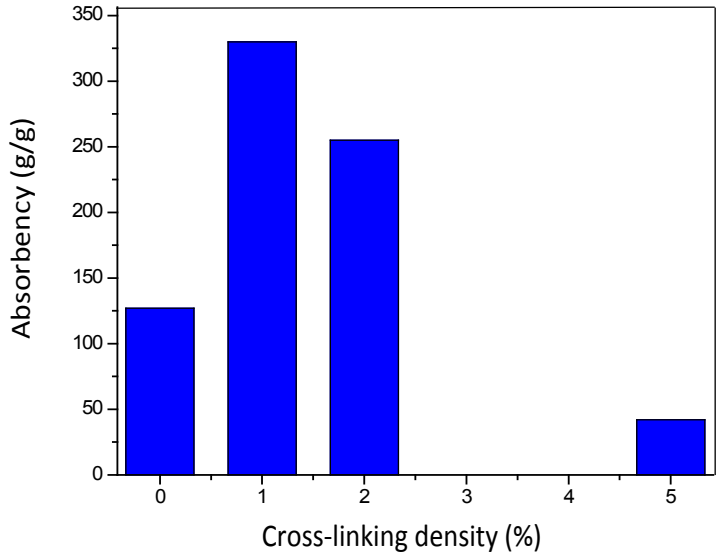

Figure 4.11 Water absorbency of AS-g-PAA containing different cross-linking densities.

4.3.5.5 Saline absorbency and absorbency under load

Fig. 4.12 shows the ability of the AS-g-PAA samples to absorb a saline solution. Like water absorbency, the amount of saline solution trapped in the polymer samples increases with the presence of cross-linking agent. Excessive amounts of cross-linking density, however, hampers further absorption due to the reasons explained above.

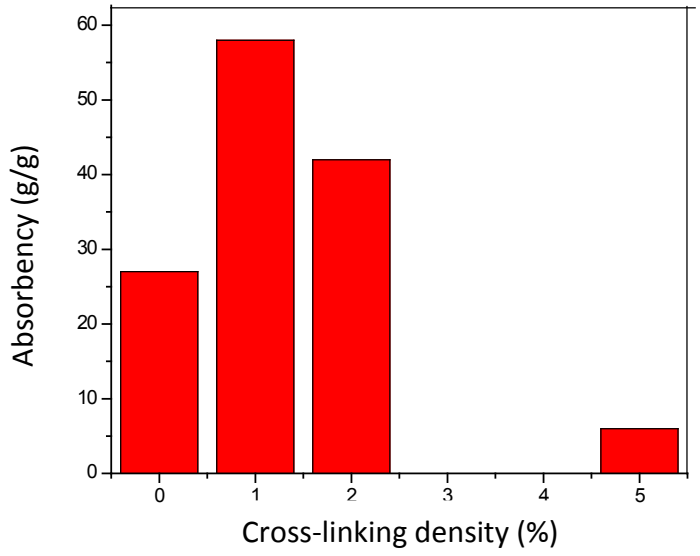

Figure 4.12 Saline absorbency of different samples of AS-g-PAA

Fig.4.12 shows the saline absorbency of each sample. The polymer sample with 1 % cross-linking density (AS-g-PAA-GA) could absorb 58 g/g of saline solution, while the sample with the highest cross-linking density could only absorb 6 g/g.

The AUL follows the same trend (Table 4.4); whereby the highest amount of saline solution absorbed was 25 g/g and the least was 3 g/g for AS-g-PAA-GA samples containing 1 % and 5 % cross-linker, respectively. This shows that all the samples' superabsorbency is determined by the amount of the cross-linking density. The retention ability of each absorbed sample of the AS-g-PAA was tested. Table 4.4 shows all the samples of AS-g-PAA-GA having an impressive water retention ability; the AS-g-PAA-GA1 sample with an absorbency of 330 g/g could retain 97 % of that mass of water, while samples with higher cross-linking density and lower absorbency values could retain 99-100 % of the absorbed water in their matrix after centrifuging.

Table 4.4 AUL of different samples of AS-g-PAA neutralised to pH 6.5.

AS-g-PAA samples	Water Retention (%)	Saline Retention (%)	AUL (g/g)Saline
AS-g-PAA	97	100	18
AS-g-PAA-GA1	97	100	27
AS-g-PAA-GA2	99	100	22
AS-g-PAA-GA5	99	100	03

4.4 Conclusions

Superabsorbent cross-linked poly (acrylic acid) was successfully synthesised using different amounts of glycerol acrylate as a cross-linking agent. The presence of double bond in the glycerol ester was confirmed by FTIR, XRD, SEM and thermal properties of the sample. The final product, glycerol acrylate cross-linked poly (acrylic acid) produced from successful polymerisation of acrylic acid using Fenton's reagent as initiator, was characterised and proved to have a remarkable water and saline absorbency and easy uptake of solvents. Neutralisation of the polymer up to a pH of 6.5 increases the absorbency in both the water and saline solution. Moreover, the structural features and absorbency of the samples

were affected by the cross-linking density in the polymer. The XRD shows a slight change in the crystallinity of the polymer with high cross-linking density.

On the other hand, the superabsorbency of acryloylated starch graft poly(acrylic acid) has been impressively improved by using glycerol acrylate as cross-linking agent. Due to the formation of a structural network of chains via the cross-linking reaction, the comb-like chain of poly(acrylic) acid on the starch ester backbone was now transformed into a cross-linked network and bridged by glycerol ester molecules that absorb more water within the polymer matrix. The amount of cross-linking density present determines the absorbency as well as the structural properties of the polymer sample. Similarly, the amount of Na^+ generated from neutralisation of the cross-linked copolymer plays a significant role in water and saline absorbency.

4.5 References

[1] Roice M., Subhashchandran K.P., Gean A.V., Franklin J., Rajasekharan Pillai V.N. *Polymer* 2003,44:911–22

[2] Nemec J.W., Bauer W. ‘‘Acrylic Acid and Derivatives’’ in ECT 2000, 3rd ed., Vol. 1, pp. 330–54

[3] Mohammed A.D., Young D.A., Vosloo H.C.M. *Starch/Stàrke* 2014, 66:1–7

[4] Kakoulides E.P., Smart J.D., Tsibouklis J. *J. Control. Rel.*1998, 54:95–109

[5] Jin S, Liu M, Zhang F, Chen S, Niu A. *Polymer* 2006, 22:1526–32

[6] Chansai P, Sirivat A, Niamlangs S, Chotpattnanont D, Viravaidya-Pasuwat K. *Int. J. Pharm.* 2009, 381:25–33

[7] Garcia-Gonzalez N., Kellaway I.W., Anguiano-Igea H.S., Delado-Charro B., Oteo-Espinar F.J., Blanco-Mendez J. *Int. J. Pharm.* 1993, 100:65–70

[8] Sheikh N, Jalili L, Anvari F. *Radiat. Phys. Chem.* 2010, 79:735–39

[9] Koo S.H., Lee K.Y., Lee H.G. *Food Hydrocolloids* 2010, 24:619–25

[10] Kurakake M., Akiyama Y., Hagiwara H., Komaki T. *Food Chem.* 2009, 116:66–70

[11] Krumova M., Lopez D., Benavente R.,Mijangos C., Perena J.M. *Polymer* 2000, 41:9265–72

[12]Ramazani-Harandi M.J., Zohuriaan-Mehr M.J., Yousefi A.A., Ershad-Langroud A., Kabiri K. *Polym. Test*. 2006, 25:470–74

[13] Pieróg M., Ostrowska-Czubenko J., Gierszewska-Drużyńska M. *Prog. Chem. App. Chitin Deriv*. 2012, 17:67–74

[14] Hennink W.E., Nostrum C.F. *Adv. Drug Deliv. Rev.* 2002, 54:13–36

Chapter 5

Graft Copolymerisation of Acrylic acid onto Starch Using Oxy-Catalyst/Aluminium Triflate as Initiators

5.1Introduction and Objectives

5.1.1. Use of oxy catalyst as initiator

The choice of an initiator plays a fundamental role in determining how effective a free radical polymerisation process takes place with respect to the polymer yield, rate and the amount of homopolymers. CAN was found to be the most efficient initiator in free radical grafting of vinyl monomers onto starch in terms of a high yield and with the least amount of homopolymers [1,2]. In the free radical initiation using CAN, there is a direct formation of starch macro radicals before the step of propagation; however, because of the metallic nature of cerium, being a heavy metal which can find its way into the polymer product, and being expensive, other initiator compounds are preferred [2]. Sughara *et al*. [3], however, reported that CAN was found to be an unsuitable initiator in the graft copolymerisation of acrylic acid onto starch. They further reported that acrylic acid (AA) is the least reactive when compared with other vinyl monomers such as acrylonitrile (AN) and acrylamide (AM). Alternatively, redox initiators are preferred to other substances for generating free radicals in grafting vinyl monomers onto natural polymers such as starch, cellulose, and wool [4–6].

In an attempt to get a new and better catalyst to generate $^{\cdot}OH$ radicals for reaction with acrylic acid, Hydrogen Link Canada provided us with a proprietary catalyst capable of generating $^{\cdot}OH$ radicals from H_2O_2; No details of the structure or active components of the catalyst were provided, and due to the agreement, we did not analyse the catalyst. The oxy catalyst was used in grafting AA onto starch using aluminium triflate as a co-catalyst in different reaction conditions. The reaction system is found to have some advantages over ferrous ammonium sulphate (FAS), these include easy recoverability (for reuse) of the initiator and its insensitivity to pH. In order to improve the grafting yield of the product, aluminium triflate ($Al(OTf)_3$), a Lewis acid, was used as co-catalyst. $Al(OTf)_3$ is readily applicable in polymer science due to its constituent properties that allows solubility in water, easy handling, reusability and it is appreciably friendly to the environment [7].

This work, the first of its kind, explores the synthesis of the starch copolymer of AA (Starch-g-PAA) using oxy-catalyst/H_2O_2 and aluminium triflate as co-catalyst at different ratios and under different reaction conditions. Grafting parameters, (percentage add-on, amount of homopolymers and efficiency) were also studied in each case. The catalyst was used separately, before the incorporation of the triflate, to initiate grafting onto the starch at different conditions.

5.1.2 Objectives

The objectives of the study include:

- Synthesis of starch grafted with poly(acrylic acid) (starch-g-PAA) via free radical polymerisation using a new radical initiator. Oxy-catalyst, which is a ˙OH generating catalyst from H_2O_2, would be used for the first time as initiator with aluminium triflate as co-catalyst.
- Study the effects of the amount of co-catalyst, temperature, starch to monomer ratio and time of the reaction on grafting properties such as the percentage add-on (% add-on) and the grafting efficiency (GE %).
- Characterisation of the samples with Fourier transform infra-red spectroscopy (FTIR), scanning electron microscopy (SEM), X-ray diffraction analysis (XRD) and thermogravimetric analysis (TGA).

5.2 Experimental

5.2.1 Materials

Potato starch, ferrous ammonium sulphate (FAS) and hydrogen peroxide (30 %) (Sigma-Aldrich) were used as received. Acrylic acid (Sasol) was freshly distilled under reduced pressure before use. Oxy-catalyst (a black powder) produced by Hydrogen Link Inc. Canada and aluminium triflate (Aldrich) were also used as received in the synthesis.

5.2.2 Graft polymerisation procedure

Dried potato starch (5 g) was stirred in water (150 mL) for about 30 min to form a uniform slurry by heating at 80 °C in a 250mL three-necked round bottomed flask equipped with a reflux condenser. The mixture was allowed to cool to 25–30 °C. Nitrogen gas was purged into the mixture to maintain an inert atmosphere. Oxy-catalyst (0.05–1.5 g) were introduced into the mixture and stirred. AA (10 mL) was gradually added. H_2O_2 (2 mL) was added to the mixture and stirred for specific periods and temperature. The reaction product was precipitated with acetone, washed with distilled water and dried at 40 °C in a vacuum oven for 24 h. The same experiment was repeated using oxy-catalyst (0.25 g) and varying amounts of $Al(OTf)_3$ (0.05–1.5 g), at a temperature of 60 °C. AA (5–15 mL) were introduced into the

mixture and stirred for 4 h. The product was separated as above and dried to constant weight before analysis.

Selected IR, ν (cm^{-1}): 3260 (O-H), 2919 (C-H), 1015 (C-O), 1700 (C=O)

5.2.3 Extraction of homopolymer

The dried product obtained above was extracted with methanol in a soxhlet extractor for 24 h to remove PAA homopolymer. The pure copolymer, starch-g-PAA, was dried in an oven at 40 °C to constant weight.

5.3 Results and discussion

All the samples of starch grafted with acrylic acid (starch-g-PAA) were characterised using FTIR, XRD, TGA and SEM analyses. Two samples of the starch-g-PAA and the starch sample were taken to represent the general behaviour of the polymer with respect to the amount of co-catalyst. From the analytical results obtained, there isn't any marked difference in the polymer samples synthesised with 0.00, 0.05, 0.1 and 0.25 g of $Al(OTf)_3$ as co catalyst. Likewise, the samples prepared using 0.5, 1.0 and 1.5 g of the co-catalyst appear to have the same pattern of analytical results.

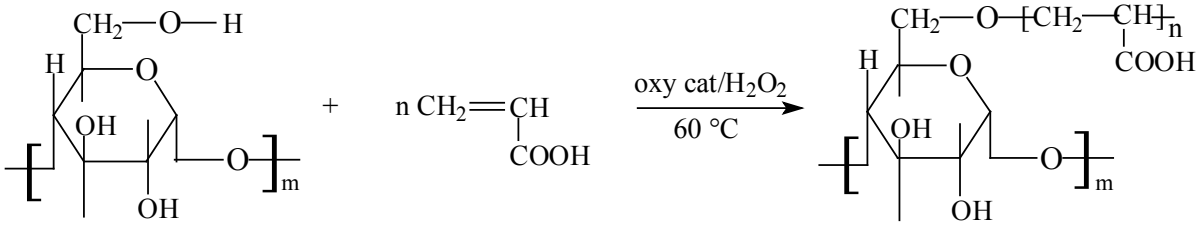

Scheme 5.1 Grafting acrylic acid onto starch using oxy-catalyst.

5.3.1 X-ray diffraction analysis

The XRD measurements of the starch and the samples are shown in Fig. 5.1. Like cellulose, starch contains both crystalline and amorphous regions. The X-ray pattern of the

crystalline polymer shows sharp peaks associated with the region of three-dimensional order and the diffused features that are characteristics of the molecularly disordered substances coexisting within it [8]. The semi crystalline structure in the granular starch is due to the amylopectin ratio in the starch particles [9] and exhibits four sharp characteristic crystalline peaks which can be clearly seen in Fig. 5.1(a). There is also an acute diffraction peaks in the range of 2θ values of 15–25°. All the grafted products, Fig. 5.1(b and c), show a broad dispersion peaks at 2θ = 20°. The only noticeable difference is the intensive peak with higher counts in Fig. 5.1(b) that arises from the higher % add-on of grafted PAA onto the backbone. This shows the overall disorientation of the starch structure in the grafting process, and as a result, the semi crystalline structure of the granular starch is lost to an amorphous polymer after grafting.

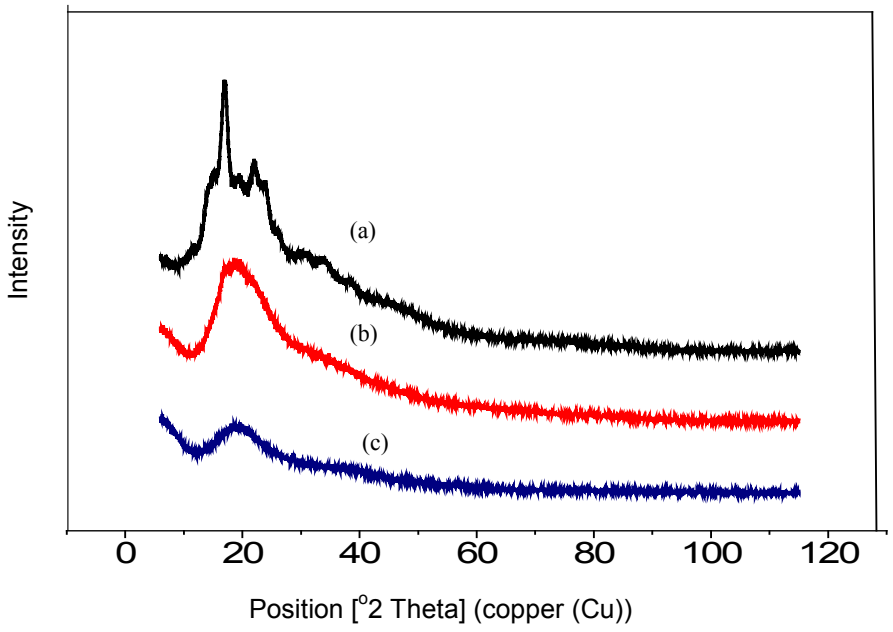

Figure5.1 XRD spectra of starch and samples of starch-g-Poly (AA) initiated by Oxy-catalyst at different amounts of $Al(OTf)_3$; (a)starch (b) Starch-g-PAA, 1.0 g $Al(OTf)_3$ and (c) 0.25 g of $Al(OTf)_3$.

5.3.2 FTIR analysis

Fig. 5.2 shows the FTIR spectra of starch and starch-g-PAA samples. In Fig. 5.2(a) the starch sample shows a broad band at 3260 and 1631 cm^{-1} due to O–H stretching and bending

mode respectively. While the C–H stretching and bending modes are observed at 2919 cm^{-1} and 1074 cm^{-1}respectively. All the grafted starch polymer samples show additional peaks around 1700 cm^{-1}, even after the removal of the homopolymer (PAA), due to the C=O stretching vibration from poly(acrylic acid) (PAA). At lower amount of the co-catalyst (0.00 – 0.25 g), the peak attributed to C=O stretching vibration is less intensive, as can be seen in Fig. 5.2(b), at 1715 cm^{-1} . This is due to the low amount of PAA grafted onto the starch. In Fig. 5.2(c), an increase in the amount of the co-catalyst from 0.5 –1.5 g, the C=O stretching peak becomes intensive at 1700 cm^{-1}. Hence, an evidence that large amount of PAA was chemically bound to the starch

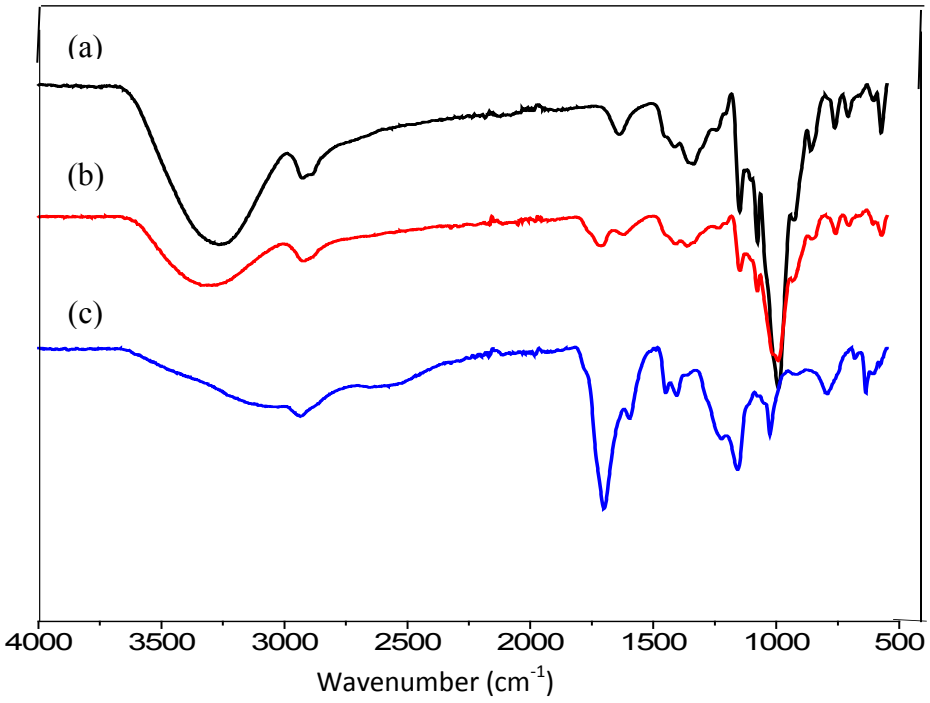

Figure 5.2 **FT-IR spectra of ; (a) starch (b) starch-g-PAA, 0.25 g $Al(OTf)_3$ and (c) starch-g-PAA, 1.0 g $Al(OTf)_3$.**

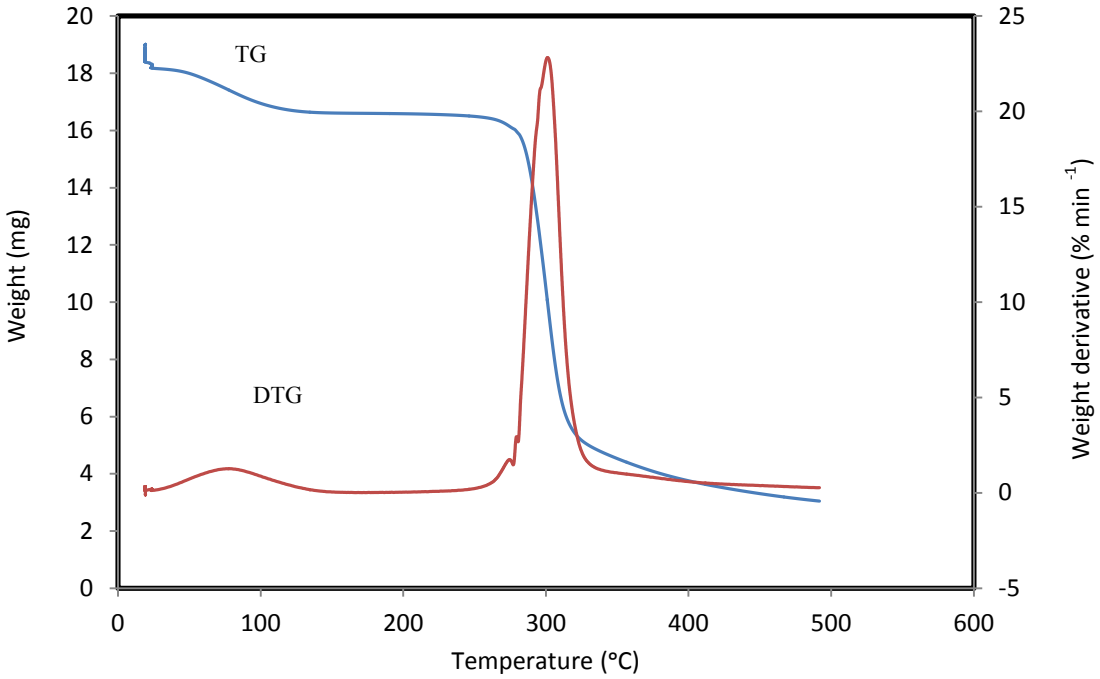

Figure 5.3 Thermal analysis curve of starch.

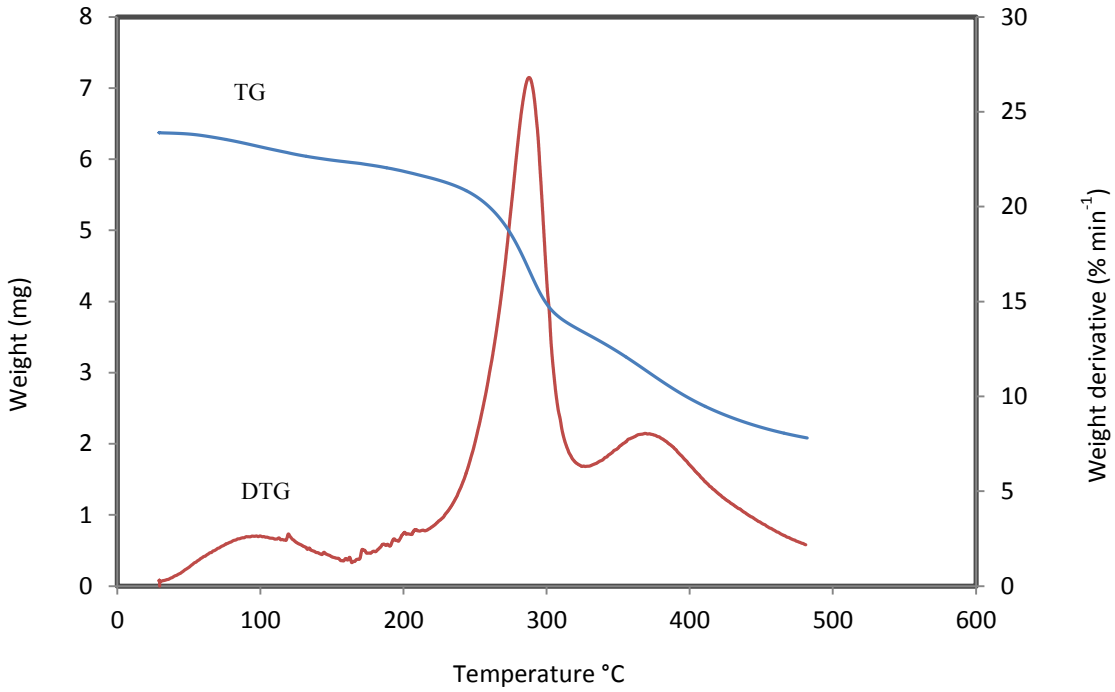

Figure 5.4 Thermal analysis curve of starch-g-PAA, 1.0 g $Al(OTf)_3$.

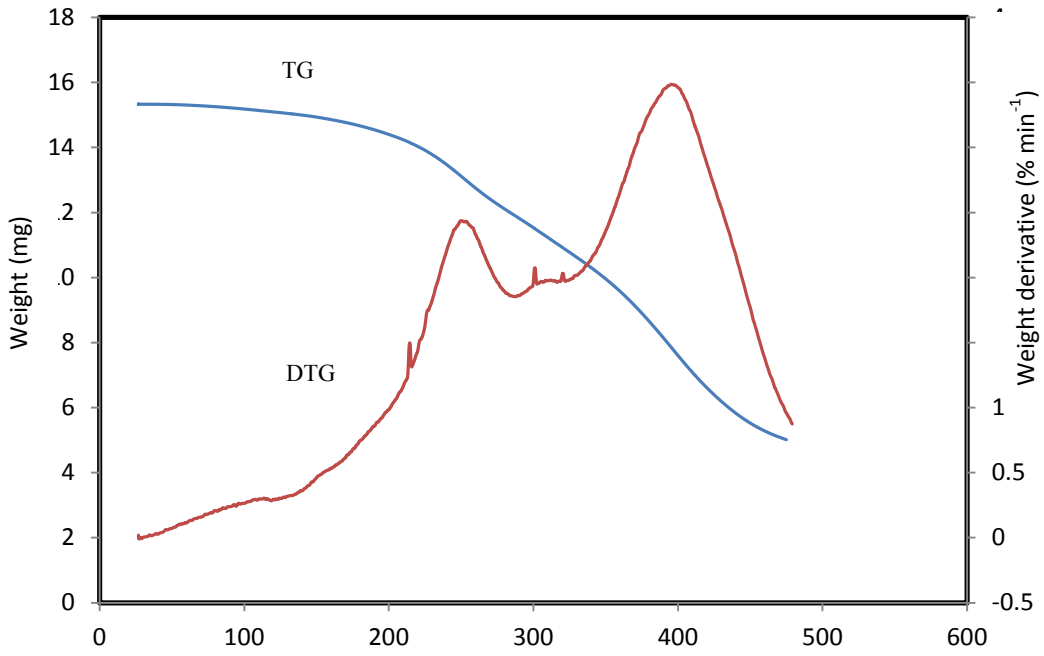

Figure 5.5 Thermal analysis curve of starch-g-PAA, 0.25 g $Al(OTf)_3$.

5.3.3 Thermogravimetric analysis

The thermal stability and the degradation pattern of starch and the starch-g-PAA samples were analysed. Fig. 5.3 shows the thermal analysis curve of starch which exhibits a three-step degradation pattern. The first stage of decomposition is due to the evaporation of the absorbed moisture which results in a slight loss in weight. The second step is rapid and accounts for the highest weight loss (75 %) with a temperature of maximum decomposition at 300 °C as can be seen in the weight-derivative curve. All the grafted products show a slight increase in thermal stability with a marked-difference in the decomposition pattern. Fig. 5.4 shows the thermal behaviour curve of starch-g-PAA grafted with oxy catalyst and 0.25 g of $Al(OTf)_3$. Due to the low add-on and grafting efficiency of the grafted product, the polymer shows a similar pattern of decomposition with the starch, with a temperature of maximum decomposition at 295 °C that results in a weight loss of 45 % and followed by decomposition at 327 °C. At higher % add-on in Fig. 5.5 the thermal stability and change in the decomposition pattern of the sample containing 1.0 g co-catalyst become apparent. The initial 3 % loss in weight at 118 °C is due to evaporation of the absorbed moisture, followed by decomposition at 250 °C resulting in 22 % loss in weight. Decomposition is observed in Fig. 5.5 at a much higher temperature, 396 °C, with a weight loss of 50 %. The final stage could

be the formation of some compounds and their decomposition. This trend in the thermal decomposition patterns, apart from proving that a grafted product was obtained, clearly show that grafted polymers with higher add-on show a relatively higher thermal stability than those with low add-on.

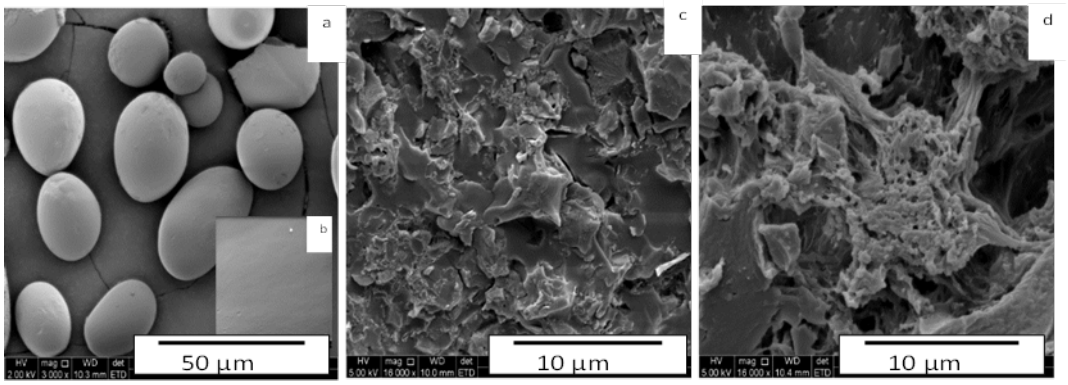

Figure 5.6 SEM images of (a) starch (b) magnified granular starch surface (c) starch-g-PAA, 0.25 g $Al(OTf)_3$ and (d) starch-g-PAA, 1.0 g $Al(OTf)_3$.

5.3.4 SEM analysis

The surface morphology of starch and starch-g-PAA are shown in Fig. 5.6. The irregular oval shape of the granular starch with a smooth surface can be clearly seen in Fig 5.6(a and b). After grafting of PAA onto the starch, the smooth surface changes to a different morphology which is apparently dependent on the level of grafting. Fig 5.6(c) shows the surface morphology of the starch-g-PAA with low % add-on as a coarse surface, but changed to, Fig 5.6(d), a more definite morphological structure of a thick polymeric coating of PAA onto the starch when the % add-on and GE were high.

5.3.5 Grafting parameters

Table 5.1 shows the % add-on, GE % and amount of homopolymers (HP) obtained in each synthetic method under different reaction conditions. It was discovered in this experiment that the use of oxy-catalyst only as the ˙OH generating species for grafting AA onto starch is quite inefficient. At a lower temperature and a low amount of the catalyst, no grafted product was obtained between AA and the starch. The grafted product with a low % add-on, GE %

and a high amount of homopolymers could only be synthesised when the temperature was increased to 50 °C and the amount of catalyst to 0.25 g. These drawbacks and limitations of the catalyst identified in this experiment triggered the use of $Al(OTf)_3$ as co-catalyst.

Table 5.2 shows the grafting parameters obtained when the oxy-catalyst is used with $Al(OTf)_3$ as co-catalyst. 0.25 g of the Oxy-catalyst was used throughout the experimental runs because it was found to be the optimum amount in the first phase of the experiment. Increasing the amount of the $Al(OTf)_3$ facilitated a sequential increase in the % add-on and efficiency. The highest add-on, 47 %, was obtained when 1.0 g of $Al(OTf)_3$ was used for 3 h, with GE of 82% and 19% PAA (homopolymer).

5.3.5.1 Increase in temperature

Table 5.1 shows the effect of temperature on the grafting parameters. An increase in temperature increases the percentage grafting and efficiency of the polymerisation process up to a certain level (60 °C) when excessive heat disfavours the polymerisation reaction. Increase in temperature leads to a more effective mobility of the monomer species (AA) and causes the swelling of the starch particles [9–10], which causes a more effective interaction with the active monomers. The rate of surface radical formation becomes high with temperature increase up to a level when excessive heat causes a higher rate of surface radicals formation which consequently leads to a premature termination. This explains why at a temperature of 80 °C, in this work, the grafting parameters are not effectively favoured, as polymer products of low add-on and efficiency are produced. Generally, an increase in temperature can increase the grafting rate and homopolymerisation at the same time, but it is noteworthy that the activation energy of grafting polymerisation is much greater than that of homopolymerisation. Hence, an increase in temperature can improve the grafting efficiency [11]. This is why 60 °C is taken as the optimum temperature in the graft copolymerisation involving the co-catalyst in the second round of the experiment.

5.3.5.2 Increase in time

The effect of time on the grafting parameters can also be seen in Table 5.1. At a shorter period of the polymerisation process, 2 h in this experiment, there was no grafting reaction. This problem is attributed to the fact that the gradual rise in the temperature to the grafting level (50 °C) requires a span of time for the particles to be active enough to facilitate the

grafting reaction. This is why in this study the shortest expected time for a free radical polymerisation to yield any product is 3 h, while the optimum time is 4 h. On the other hand, an increase in the reaction time to a certain level did not facilitate a higher % add-on or GE %. In Table 5.1, the time increase from 4 h to 8 h shows a levelling off in the grafting parameters with a time increase. The levelling off property can be explained on the basis of progressive consumption of the monomer and the initiator with time [1].

Table 5.1 Effect of oxy-catalyst, time and temperature on graft copolymerisation.

Run	Oxy-catalyst (g)	Time (h)	Temp. (°C)	Add-on (%)	GE (%)	HP (%)
1	0.05	2	30	0.0	0.0	0.0
2	0.10	2	30	0.0	0.0	0.0
3	0.25	2	30	0.0	0.0	0.0
4	0.50	2	30	0.0	0.0	0.0
5	1.00	2	30	0.0	0.0	0.0
6	0.25	3	30	0.0	0.0	0.0
7	0.10	3	50	0.0	0.0	0.0
8	0.25	3	50	6.0	34	65
9	0.50	3	50	6.0	36	63
10	0.25	3	60	9.0	45	55
11	0.25	3	80	7.0	40	62
12	0.25	4	60	14	59	41
13	0.25	5	60	14	60	40
14	0.25	8	60	15	62	37

5.3.5.3 Amount of catalyst and co-catalyst

The first phase of the experiment shows the general trend of grafting ability of the oxy-catalyst when it was used without the co-catalyst. Since it was observed that its efficiency is relatively low, the amount at which the amount starts levelling off (0.25 g) is used throughout in the further experimental runs along with the co-catalyst ($Al(OTf)_3$). Table 5.1 shows the initial increase in the add-on and GE % on the grafting level with a varying amount of the catalyst. At certain amount of the catalyst, the grafting parameters start to level off.

Table 5.2 Effect of $Al(OTf)_3$ on graft copolymerisation; 4 h reaction time; at 60°C.

Run	Amount of $Al(OTf)_3$ (g)	Colour of the dry product	Add-on (%)	GE (%)	HP (%)
1	0.00	Green	14.1	59.4	41.6
2	0.05	Green	13.9	59.6	40.4
3	0.10	Green	16.5	63.8	36.1
4	0.25	Light-green	30.5	75.1	24.9
5	0.50	Light-green	39.8	80.3	19.7
6	1.00	Pale-yellow	47.0	82.8	17.2
7	1.50	Brown	42.7	80.5	19.5

In Table 5.2, a similar trend was observed where an initial increase in the amount of co-catalyst led to a higher % add-on and GE % before they started decreasing. 1.0 g of $Al(OTf)_3$ was the optimum level discovered in this experiment. A % add-on of 47 and GE% of 82 were obtained. When the amount of the co-catalyst was adjusted to 1.5 g, the add-on and the GE dropped down. This trend can be explained from the fact that a high amount of the catalyst would release more free-radicals which would make hydrogen abstraction and chain transfer reaction at a faster rate, hence more GE and add-on. At a higher amount of the catalyst and co-catalyst, the rate of termination increases whereby the growing chains on the starch became terminated by the excess initiators or by the reaction of the free radicals of the starch with either the catalyst or the $Al(OTf)_3$ and therefore leads to a lower % add-on and GE %.

5.3.5.4 Amount of AA

Table 5.3 shows the effect of the starch to monomer ratio on the GE, add-on and the amount of homopolymers produced along the starch-g-PAA. A gradual increase in the amount of AA increases both the GE and % add-on, as the grafting yield and rate depends on the supply of the monomer molecules to the starch substrate. That is why at a lower concentration of the monomer (AA), there is more homopolymer formation than the add-on and the GE. In this study, the highest percentage of homopolymers, the lowest % add-on and GE % were obtained when the AA amount is lowest. The add-on, GE and the amount of homopolymers in the run were 17.1%, 64.2% and 34.5 %, respectively. On the other hand, an

excessive amount of monomer to starch ratio decreases the GE and % add-on and more homopolymers are produced. This drawback could result from the high rate of collision between the AA molecules which could block further grafting of the AA onto the starch by forming a layer of PAA onto the starch backbone.

Table 5.3 Effect of amount of monomer on graft copolymerisation.

Starch:AA ratio	Add-on (%)	GE (%)	HP (%)
1:1	17.1	64.2	34.5
1:2	23.3	70.8	27.7
1:3	47.1	82.3	19.2
1:4	40.4	73.9	26.1

5.4. Conclusions

Starch grafted with AA was synthesised using an oxy-catalyst as initiator and $Al(OTf)_3$ as co-catalyst. At optimum conditions, starch-g-PAA copolymer with an add-on % of 47 and GE of 82% was synthesised. Lower grafting parameters, however, were obtained when the oxy-catalyst was used only. The grafting process was found to be time and temperature dependent at some stage in the experiment. The analytical techniques used in the characterisation of the products provided evidence of both grafting, but showed a marked difference with an increase in the % add-on and GE %. Although the true chemical behaviour of the catalyst was not disclosed, in comparison with other free radical initiators, a polymer product with lower grafting parameters was synthesised. The study, however, proved that the catalyst could serve as a substitute for ferrous ammonium sulphate as an initiator catalyst in free radical formation.

5.5 References

[1] Athawale V.D., Lele V. *Carbohydr. Polym*. 2000, 41:407–411

[2] Li M., Zhu Z., Pan X. *Starch/Starke* 2011, 63:683–691

[3] Sugahara Y., Ohta T. *J. Appl. Polym. Sci.* 2001, 82:1437–1443

[4] Lagos A., Reyes J. *J. Polym. Sci*. 1988, 26:985–991

[5] Bianco G., Gehlen M.H. *J. Photochem. Photobiol. A*. 2002, 149:115–119

[6] Meshram M.W., Patil V.V., Mhaske S.T., Throat B.N. *Carbohydr. Polym*. 2009, 75:71–78

[7] Amer I., Young D.A. *Polymer* 2013, 54:505–512

[8]Chauhan A., Singh B. *Int. J. Polym. Anal. Charact*. 2011, 16:319–328

[9] Athawale V.D., Rathi S.C. *Rev. Macromol. Chem. Phys.*1999, 39:445–480

[10] Sacak M., Oflaz F. *J. Appl. Polym. Sci.*1993, 50:1909–1916

[11] Zhu J., Deng J., Cheng, S. and Yang W. *Macromol. Chem. Phys.* 2006, 207:75–80

Chapter 6

Synthesis of Xanthates from Glycerol and Starch for Removal of Heavy Metal Ions

6.1 Introduction and objectives

6.1.1 Introduction

Heavy metals such as lead, cadmium and copper pose serious environmental hazards to the environment. The expansion of the human population, human activities, scientific and technological advancement is responsible for the introduction of lethal substances to our ecosystem. Water is one of the greatest media through which pollution gets its way into the whole planet. Many ways are considered in limiting the effects of these hazardous materials to the environment. One of these techniques is the treatment of wastewater from either domestic or industrial effluent. The strategy involves the ultimate treatment of the wastewater to make it fit for drinking, or in some cases the removal of deadly contaminants present in the wastewater that might be directly hazardous to the environment [1].

Since the dawn of modern technology, several techniques have been employed in the removal of heavy metals from wastewater, these include precipitation, flotation, solvent extraction, adsorption, membrane processing, and electrolytic methods [2]. All these techniques are met with some limitations which range from high cost of the materials to operational costs. Patterson [3] reported that one of the widely used techniques is the precipitation using hydroxides to form heavy metal hydroxide precipitates. Due to the safety concern of this technique, its application is followed by the processes of solidification and stabilisation that are needed for the released metal hydroxide in the environment. Another technique, a heavy metal scavenging process using xanthates, is considered a promising technique [4] and requires a low-cost of operation. The efficiency of the technique depends on the formation of insoluble complexes with the heavy metal ions, and unlike the sulphide precipitation technique, the use of xanthates is not associated with the problem of residual sulphide in the treated water [5].

In this study, insoluble starch (ISX) and fully substituted glycerol xanthates (GX) were synthesised and used in the removal of Cu, Cd and Pb from wastewater. The efficiency of each xanthate at different conditions was investigated. The use of starch xanthate has been reported to have an impressive efficiency in metal scavenging activity [2–6]. A good comparison in efficiency with alkyl xanthate, in this case butyl xanthate, was studied in this work. Glycerol polyhydroxy sodium xanthate has been used as a depressing agent in the separation of minerals due to its structural features [7]. The aim was to study the effect of a polyxanthate group per molecule of starch and glycerol on the metal scavenging activity. Apart from what earlier works emphasised on the efficiency of xanthates based on the

number of sulphur atoms per molecules of the compound, the structural feature of GX was found to play a fundamental role in the complex formation with the heavy metals. Unlike starch xanthates whereby the sulphur groups are attached to the bulky polymeric structure of the glucose units, GX is a small molecular organic compound containing a more exposed sulphide groups at spatial positions and without molecular hindrance that could be expected in starch xanthates. In the use of ISX in this study, there was further exploration of experimental conditions to maximise the effectiveness of the heavy metal removal. The increase in the amount of sulphur per average glucose unit and the suitable adjustment of pH of the mixture were investigated.

6.1.2 Objectives

The objectives of this study include the syntheses of xanthates from glycerol and insoluble starch and their effective use in the removal of Pb, Cd and Cu from aqueous solutions.

6.2 Experimental

6.2.1 Materials and methods

Glycerol, potato starch, epichlorohydrin (99 %) and carbon disulphide (Sigma-Aldrich) were used as received. The instrument used is Agilent 7500CE ICP-MS and it was run at the following experimental conditions: RF Power: 1550 W, Sample depth: 8 mm, Carrier gas: 1 L/min, Makeup Gas: 0.17 $Lmin^{-1}$, S/C Temp: 2 °C

The FTIR analysis of the samples was carried out using a Bruker VERTEX 80 FTIR spectrometer. The infra-red spectra of the samples were recorded in absorbance mode, at a frequency range of 550–4000 cm^{-1}, at room temperature, with a resolution of 4 cm^{-1} based on 32 scans and using an ATR Bruker Platinum-Diamond accessory.

The NMR analyses was carried out by dissolving a sample of GX (25 mg) in deuterated water (D_2O), and the ^{1}H and ^{13}C NMR spectra were recorded at room temperature on a 600 SB Ultra Shield^{TM} Plus NMR spectrometer equipped with an Oxford magnet (14.09 T), operating at 600 MHz.

6.2.2 GX was prepared using the following procedure:

Glycerol (1 mol) mixed with NaOH (3 mol) were stirred in a three-necked round bottomed flask for 30 min at a temperature of 35°C. CS_2 (3 mol) was added to the mixture and stirred for 14 h at 10 °C. The yellow solid was precipitated with methanol, washed with acetone and ether and dried in vacuum oven. Scheme 6.1 shows how a fully substituted glycerol xanthate is synthesised.

Selected IR, v (cm^{-1}):1430 (O-CS), 1068 (C=S), 820 (C-S), 2976 (C-H). ^{1}H NMR (D_2O) δ = 3.5-3.6 (m, -CH_3), ^{13}C NMR (D_2O) δ= 61 (CH), 72 (-CH_2-glycerol), 167 (CS).

6.2.3 Insoluble starch xanthate (ISX)

The procedure reported by Wing *et al.* [6] was used. Dried starch (20 g) was slurred in water (150 mL) containing NaCl (0.3 g) and epichlorohydrine (EPI) (1.1 mL), at a temperature of 50 °C. KOH (1.2 g) was slowly added to the reaction mixture over a period of 30 min. The reaction mixture was allowed to cool to 30 °C followed by the addition of water (5 mL) containing EPI (0.4 mL) and stirred for 16 h. NaOH (9.6–15 g) in water (50 mL) was added to the flask containing the cross-linked starch and stirred. CS_2 (3.0–5.0 mL) was added and stirred for another 16 h. The product was washed with water and acetone and dried in vacuum oven to constant weight. Scheme 6.2 shows the synthesis of starch xanthate.

Selected IR, v (cm^{-1}):1436 (O-CS), 1079 (C=S), 816 (C-S), 3241 (O-H)

6.2.4 Potassium butyl xanthate (KBX)

The procedure reported by Mohammed *et al*. [8] was used. A flask containing n-butanol (50 mL) was purged with nitrogen gas to maintain an inert atmosphere, KOH (1.12 g) was added and the mixture stirred vigorously. CS_2 (1.2 mL) was slowly added over a period of 30 min. The cloudy yellow solution was allowed to stir for 2 h until a yellow precipitate was formed. The mixture was filtered and washed with butanol and stored in a vacuum oven overnight.

6.2.5 Heavy metal removal

Three different samples of synthetic wastewater containing $Pb(NO_3)_2$, $Cd(NO_3)_2{\cdot}4H_2O$; and $Cu(NO_3)_2{\cdot}3H_2O$ (5–1000 ppm), respectively. The samples were tested to determine the metal removal efficiency using a fully-substituted glycerol xanthate at different molar ratios

of 0.3–3 (0.3, 0.5, 0.7, 1.0, 1.5, 2.0 and 3.0 for M^{2+} and the xanthate, respectively). Starch xanthate was also used in the wastewater samples containing the same concentration of the metals at different doses. The mixture was centrifuged at a speed of 200 rpm in a centrifuge for 30 minutes at room temperature and then increased to 2000 rpm for another 30 min. The insoluble complex of M^{2+} was obtained after decantation and oven-dried at 25 °C for 24 h. The solution was filtered again and the filtrate was analysed to detect the presence of metal ions using ICP-MS. There was no pH adjustment in the use of glycerol xanthates throughout the experiment. In the use of starch xanthate, however, the pH was adjusted to 6 as has been reported by Rao and Leja to be the appropriate pH for the application of starch xanthate in metal removal, as at lower pH possible decomposition of the xanthates could occur [5].

The same experiment was repeated using 100 ppm of $Pb^{2+}$to optimise the stoichiometric ratio. The stoichiometric ratio obtained was used to determine the removal of Pb^{2+}, Cd^{2+}, and Cu^{2+} at 1000, 500, 100, 50 and 5 ppm for each of the metals from aqueous medium.

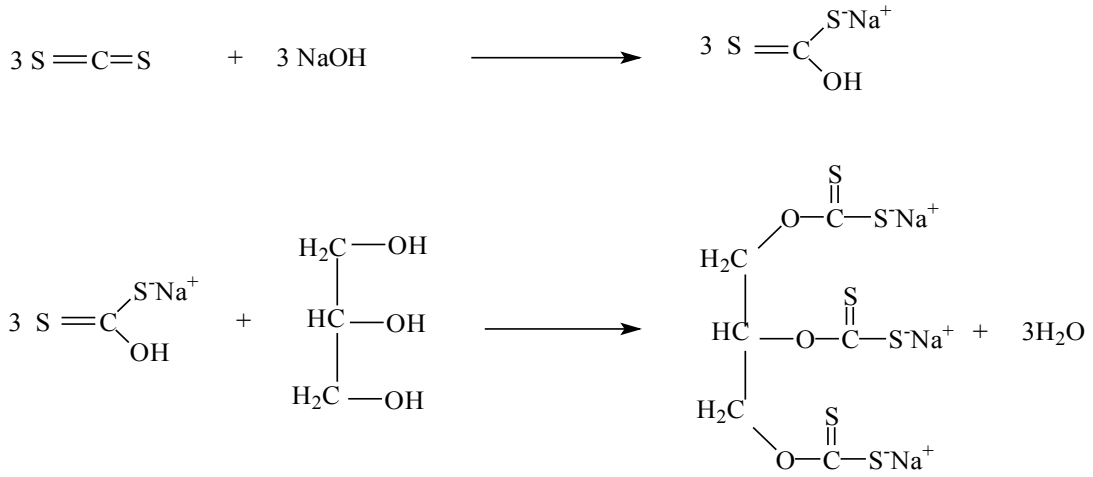

Scheme 6.1 Synthesis of GX.

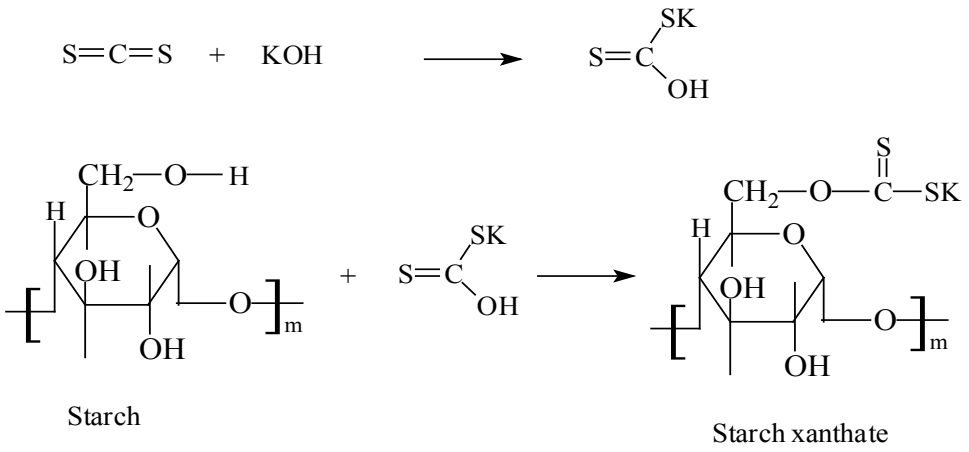

Scheme 6.2 **Synthesis of starch xanthate.**

6.3. Results and discussion

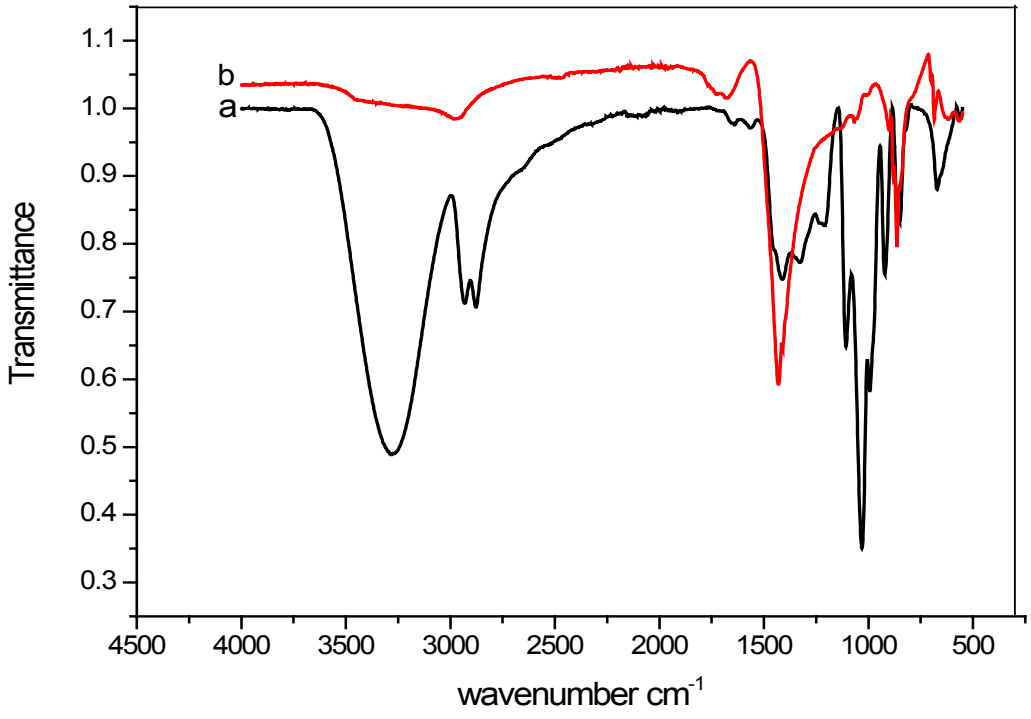

Figure 6.1 **FTIR spectrum of a, glycerol and b, GX.**

6.3.1 FTIR analysis

The FTIR spectrum of glycerol is shown in Fig.6.1(a). The absorption band at 3280 and 2930–2877 cm^{-1} is assigned to the OH and C-H stretching vibrations, respectively. In Fig 6.1 (b), in addition to the existing peaks in glycerol, the GX shows other important peaks at around 1674 cm^{-1} due to the stretching of SP^2 carbon skeleton nature, 1430 cm^{-1} due to O-CS stretching vibration, 1068 and 820 cm^{-1} due to C=S and C-S stretching modes respectively. The C-H stretching mode is now confined to 2976 cm^{-1} in GX. The disappearance of any OH stretching in the final product confirms that complete xanthation of the glycerol has been successfully achieved. In starch xanthate important peaks appear at 3241cm^{-1} due to OH stretching, 1589 and 1436 cm^{-1} are due to O-CH and O-CS stretching vibrations. The C=S stretching mode of the xanthated starch is assigned to 1079 cm^{-1}.

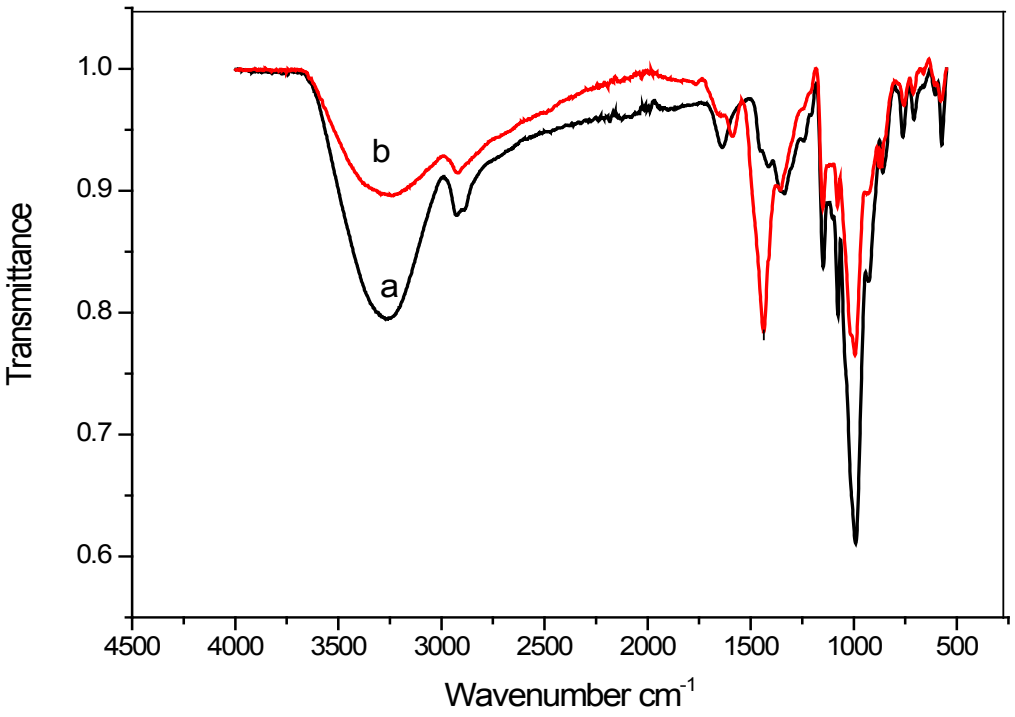

Figure 6.2 **FTIR spectra of a, starch and b, starch xanthate.**

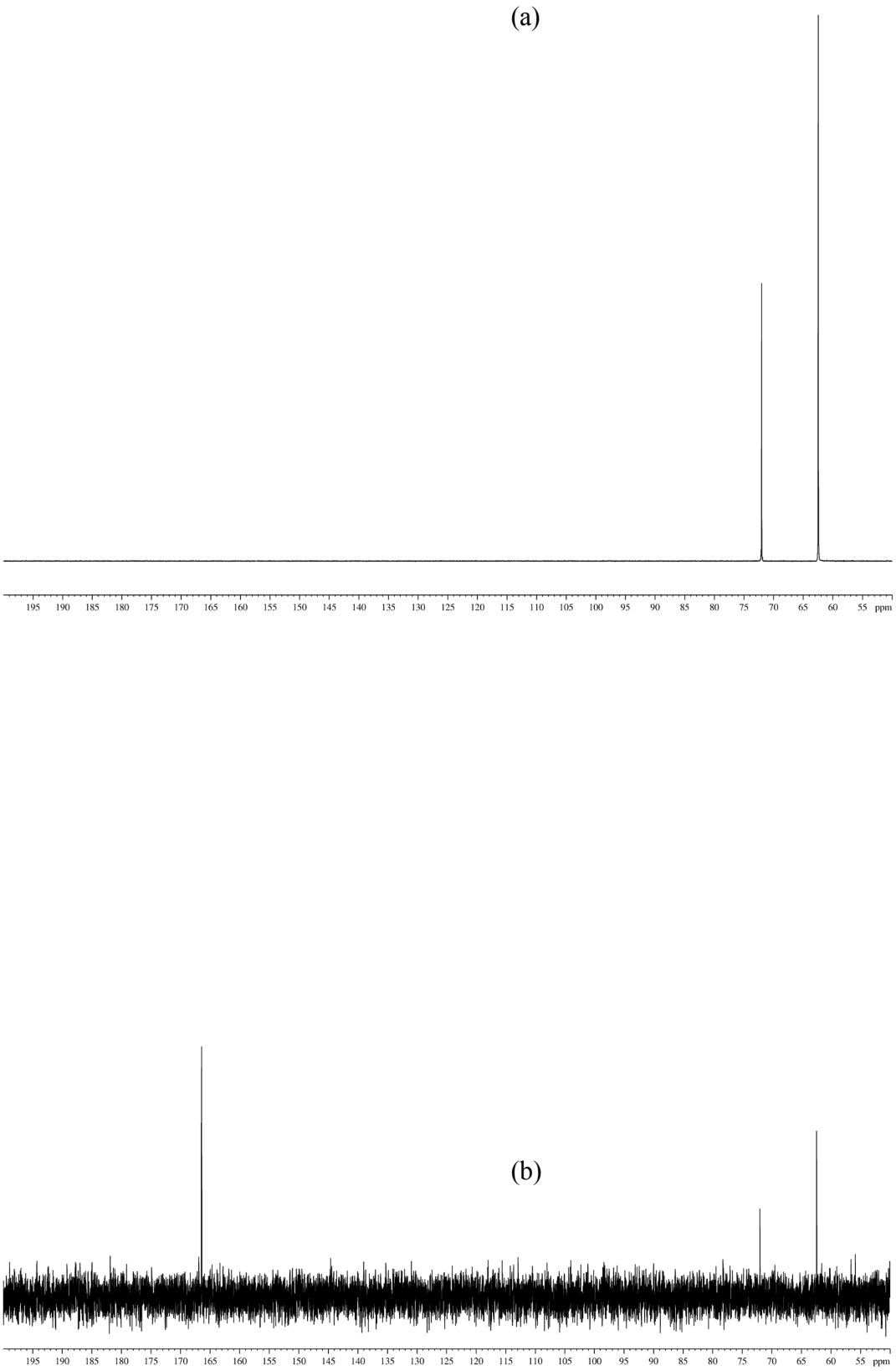

Figure 6.3 **^{13}C NMR spectra of (a) Glycerol and (b) GX.**

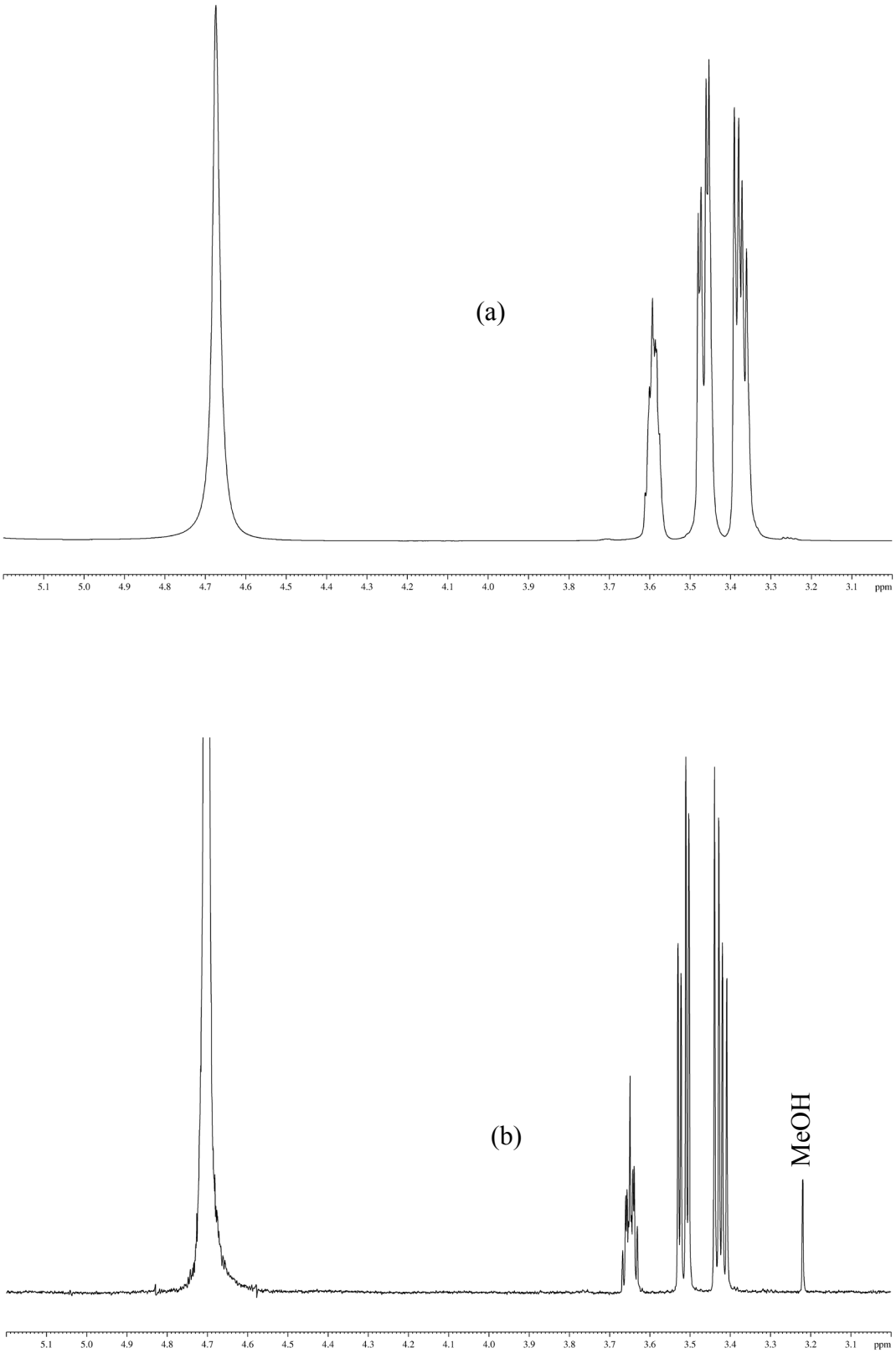

Figure 6.4 **^{1}H NMR spectra of (a) Glycerol and (b) GX.**

6.3.2 ^{13}C NMR of GX

Figure 6.3(a) isthe ^{13}C NMR spectrum of glycerol.The signals shown at 61 and 72 ppm are assigned to CH and CH_2 carbon-hydrogen bond in the glycerol; while in the xanthated glycerol, Fig. 6.3(b), a new signal at 167 ppm is due to sulphur-carbon bond (CS) from the xanthate [9,10]. This indicates a successful xanthation of the glycerol.

6.3.3 ^{1}H NMR of GX

Fig.6.4 shows the ^{1}H NMR spectrum of glycerol before and after xanthation. There are proton multiplet signals at 3.3 ppm and other proton multiplets at 3.5 and 3.6 ppm which correspond to the methylene group protons (Fig. 6.4a). The singlet proton signal at 4.7 ppm is due to the protons of the OH of glycerol and water. In the final product (Fig.6.4b) there is a shift in all the signals of multiplet protons at 3.6 ppm. The proton signal at 3.2 ppm is from the methanol used in washing the product.

6.3.4 Heavy metal removal of the xanthates

The metal removal ability at different experimental conditions of ISX and GX is shown in Figures 6.5 and 6.6 and Table 6.1 and 6.2. The overall efficiency of each xanthate was carefully studied and monitored at different conditions on different metal ions. From previous works, Pb and Cu were reported to have a poorer sorption ability to the scavengers when compared to Hg and Cd. The poor sorption is attributed to the following: relative atomic size, ability of the metal ion to react with the scavenging agent, charge density of the metal ion and reactivity of the metal ion [11]. The heavy metal removal ability of GX is impressively higher than ISX. Table 6.1 shows the use of ISX in the removal of Pb, Cd and Cu. The ease of complexation (with the xanthate group) and the removal of the insoluble product determine the scavenging efficiency in each case. At higher amount of sulphur:Metal ratio there is a complete removal of all the metals. Coversely, at lower amount (< 3.0) and at excessive amount (> 3.0) of sulphur:metal ratio, there is a partial removal of all the metals, with copper being the most in solution. On the other hand, lower dosage of GX is found to be effective in the complete removal of all the metals (within the detection limits) on different concentrations of the heavy metals.

6.3.4.1 Effect of treatment time on the heavy metals removal

The rate of metal removal increases with an increase in time at the beginning until all the available metal ions are bonded with the active groups in the xanthates. In Fig.6.5, the rate of metal ion removal leveled off after 20 minutes which shows that from that time all the available metal ions are taken off by the active groups of the xanthates. It, moreover, indicates that all the processes involved, from the release of mobile metal ions in the solution to the complex formation with the sulphur donor atoms of the xanthates, took a short period of time. Thus, the technique could effectively be employed in industrial application for wastewater treatment

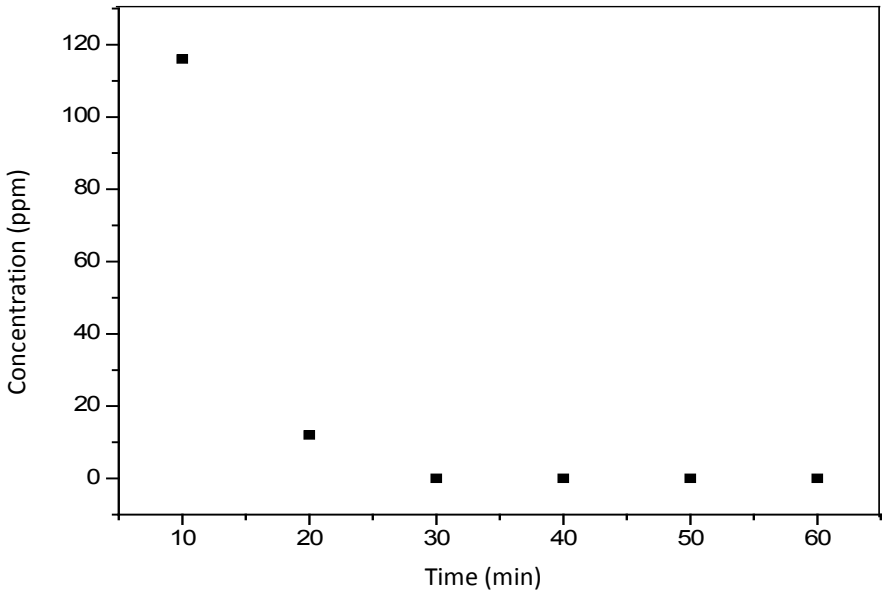

Figure 6.5 Removal of lead by GX at different contact time; 2.0 S/M^{2+}; 1000ppm of Pb.

6.3.4.2 Effect of xanthate dose on the heavy metal removal

The effect of GX dose is shown in Fig.6.6. The various M:GX molar ratios, which in other words refers to S/M ratio, show a varying role in the removal of Pb^{2+} from aqueous solution. The efficiency in Pb^{2+} removal initially increases with increase in the M:GX ratio. In Fig.6.6 the highest amount of heavy metal removal was observed at molar ratio Pb^{2+}/GX of 2, with about 100 % removal. Also, the optimum molar ratio is not affected by the pH of the

mixture. The M:GX molar ratio can best be explained on the basis of chemical interaction between the xanthate functional group (CS_2^-) in the substrate and the metal ions which results in the complexation reaction to form an insoluble metal complex compound.

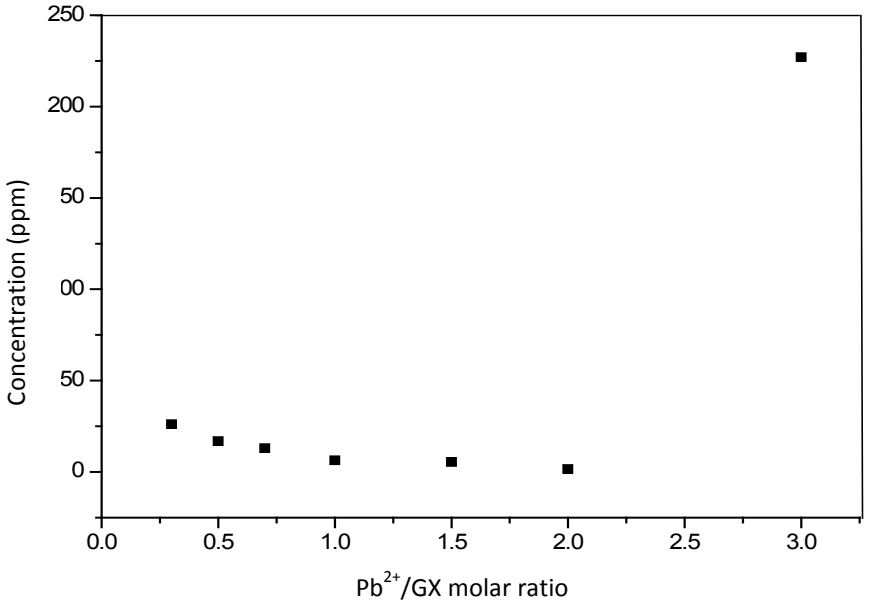

Figure 6.6 **Removal of lead by GX at different molar ratios; at 60 min contact time; room temperature. Detection limit: 0.1 ppb.**

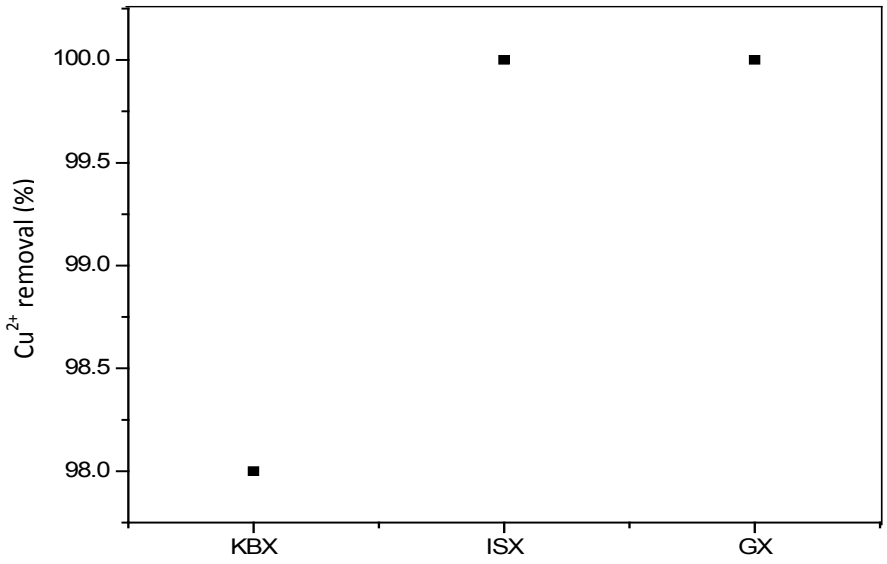

Figure 6.7 **Removal of copper by different xanthates; 1000 ppm of Cu; 60 mins contact time.**

Each sample of xanthate was used at its optimum conditions to allow a good comparison in the scavenging ability. Aqueous solution containing copper II ions was selected due to the difficulty usually encountered in its removal when compared to other metals as explained earlier. Complete removal (100 %) of copper by ISX and GX (compared to 98 % removal by KBX (Fig. 6.7)) shows that xanthates from these two sustainable products (starch and glycerol) are quite efficient in metal scavenging activity. The percentage S in the xanthate molecules determines the level of efficiency in the heavy metal removal. Generally, GX required a straightforward and simple chemical technique of synthesis, while the insoluble starch xanthate containing >5% S required much more chemical procedures of synthesis.

All what has been mentioned above could not be unconnected with the structural features of glycerol and starch. The simple molecular structure of glycerol compared with the polymeric molecular structure of starch plays a fundamental role in the effective and easy complexation with the metal ions in an aqueous mixture. This property coupled with its greater reduction ability (than from sugars) facilitates its simple xanthation and other chemical reactions that could be used in the production at higher yields of ethanol, xylitol, propionate and succinate [12].

Table 6.1 Removal of Pb, Cd and Cu at different doses of ISX; 1000ppm solution of each metal ion; 60 min contact time; room temperature. Detection limit: 0.1 ppb.

S : M^{2+} ratio	Concentration of Pb (ppm) left	Concentration of Cd (ppm) left	Concentration of Cu (ppm) left
2.0	43	27	320
3.0	< 0.1 ppb	< 0.1 ppb	< 0.1 ppb
4.0	< 0.1 ppb	< 0.1 ppb	93
5.0	12	4.0	97

Table 6.2 Removal of different concentration of Pb, Cu and Cd using a ratio of 3:1 S/M^{2+} oftwo different samples of ISX; at 60 min contact time; pH 6, room temperature and under detection limits of 0.1, 0.2 and 0.1ppb for Pb, Cu and Cd respectively.

Concentration (ppm)	% sulphur	Concentration of Pb (ppm) left	Concentration of Cd (ppm) left	Concentration of Cu (ppm) left
1000	5.3	113	93	202
500	5.3	94	67	171
100	5.3	47	41	62
50	5.3	20	11	34
5	5.3	2	2	3

The GX in this experiment contains poly xanthate groups per molecule, which probably acts as a bidentate ligand in the complex formation with the metal ions. At a higher amount of M:GX molar ratio, the free metal ion remains in solution as unreacted species when all the available xanthate groups are used up, hence, the metal removal efficiency becomes low. On the other hand, a low molar ratio of M:GX (excess GX) also results in a relatively poor removal efficiency, as colloidal solution is formed which becomes difficult to separate.

In the ISX, similarly, the efficiency is enhanced with more % S in the starch molecules. The more %S the greater the availability of active groups (xanthate) ready for complexation reaction with the metal ions. Table 6.2 shows the partial removal of the metals when the % sulphur is 5.3 in the ISX. There is, however, an excellent metal scavenging activity of ISX

when the xanthation parameters were adjusted to produce a high sulphur % of 10.12 in the product. Even Cu^{2+} which could not precipitate out easily from an aqueous mixture at a lower percentage of sulphur was completely removed (within the detection limit). This could be explained based on what has been stated above. The amount of sulphur in xanthates determines the bonding and complexation power with the heavy metal ion. Moreover, both the GX and ISX have structural features that could accommodate more xanthate groups as can been seen in Scheme 6.1 &6.2.

6.4. Conclusions

Xanthates from starch and glycerol are proven to be reliable and efficient metal scavengers in aqueous media. An easy and fast complexation reaction between the heavy metal ions and the sulphur atoms in the xanthate, followed by precipitation of the insoluble metal complex shows how effective and reliable these xanthates are. The structural features of xanthates from these sustainable substances could allow more xanthate groups to be synthesised in their structures. This explains why they are more efficient in metal scavenging activity than common alkyl xanthates, like butyl xanthate. In this study, moreover, glycerol xanthate is found to be the most effective, as lower dosage is required and not dependent on pH like the insoluble starch xanthate and the alkyl xanthates.

6.5 References

[1] Brostow W., Pal S., Sing R.P. *Mater. Lett.* 2007, 61:4381–4384

[2] Guo L., Zhang S., Ben-ZhiJu B., Yang J., Quan X. *J. Polym. Res*. 2006, 13:213–217

[4] Chaudhari S., Tare V. *J. Appl. Polym. Sci.*1999, 71:1325–1332

[3] Patterson J.W. Proceeding 36th annual industrial waste conference, Purdue University, West Lafayette, Indiana 1981, 579–602

[5] Chang Y.K., Shih P.H., Chiang L.C., Chen T.C., Lu H.C., Chang J.E. *Environ. Inform. Arch*. 2007, 5:684–689

[6] Wing R.E., Doane, W.M., Russel C.R. *J. Appl. Polym. Sci.* 1975, 19:847–854

[7] Dao-ling X., Yue-hua H., Wen-qin Q., Ming-fei H. *J. Cent. South Univ. Technol.* 2006, 6:678−682

[8] Mohamed A.A., Kani I., Ramirez A.O., Fackler J.P. *Inorg. Chem.* 2004, 43:3833–3839

[9] Gorgulu A.O., Celikkan H., Arslana M. *Acta Chim. Slov.* 2009, 56:334–339

[10] Dominiak K., Ebeling H., Kunze J., Fink H. *Lenzinger Ber.* 2011, 89:132–141

[11] Mostafa K.M., Samarkandy A., El-Sanabary A.A. *J. App. Polym. Sci.* 2009, 112:2838–2846

[12] Dharmadi Y, Murarka A, Gonzalez R. *Biotechnol. Bioeng.* 2006, 94:821–829

Chapter 7

Miscellaneous Applications

Part of this chapter has been reported in:

(i) Materials Letters 114 (2014) 63-67

(ii)Superlattices and Microstructures 70 (2014) 98-108

7.1. Introduction and objectives

7.1.1 Other uses of modified resources

The approach of testing derivatives for various different applications is one of the ways that lead to new discoveries. For this reason derivatives of starch and glycerol were screened for their ability to remove heavy metal salts from water. This paved the way to determine whether the metal complexes could be used to produce nanoparticles suitable for different catalytic processess.

7.1.2 Objectives

This objectives of the research include the following:

- Study the use of starch graft coplymers as capping agents in the synthesis of nanoparticles whereby an *in situ* process takes place from the complex formation to graft copolymerisation up to the production of nanoparticles.
- Application of xanthates synthesised in the research as sulphur-donor group in the synthesis of heavy metal complexes for nanoparticles production.

7.1.3 Synthesis of highly-confined CdS nanoparticles by copolymerization of acryloylated starch.

7.1.3.1 Introduction

The control of size and shape is of fundamental importance in the synthesis of nanoparticles, because the reduced size of particles within the nanometric domain is greatly associated with enhanced surface reactivity. This has been ascribed to the increased surface to volume ratio and the presence of dangling bonds [1] which generates spontaneous agglomeration. The size of particle agglomerates is always beyond the nanometer scale and affects the nanomaterial properties. Hence, construction of semiconductor nanocrystals within the matrices of a polymeric material with the aim of acting as both a capping/passivating agent for the surfaces of the nanoparticles, or for the preparation of polymer nanocomposites has generated a lot of research interest. This is due to their extensive scientific and industrial uses in areas such as light-emitting devices, non-linear optical devices, and biological labels [2].

In the use of polymers as capping agents, the functional groups of the polymeric material is very important because it affects the physical and electronic properties of semiconductor nanoparticles [3], and provides the inorganic nanocrystals with certain desirable properties, for example: stability, strong luminescence and solubility. The organic ligand molecules could also serve as linkers between the nanocrystals and appropriate anchor site, thereby enhancing their processability through favourable interactions [4]. Thus the electronic and chemical properties of a semiconductor material can be uniquely influenced by simply controlling particle size and preparative conditions employed.

There are a number of methods for the preparation of nanoparticles with specific functionalities of the capping group. The controlled precipitation of quantum-confined cadmium sulphide has been achieved in a wide range of media including surfactant micelles, vesicles, zeolites, random ionomer and ion-complexing block copolymers [5–8]. However, a very important method is the use of a polymerizable moiety as capping agent to modify the surface of the nanoparticles in order to immobilize them. Functionalization of inorganic particles with polymerizable vinyl groups which can be copolymerized with the monomers to form integrated polymeric materials has been reported [9]. A modified, dual-function copolymer host in which passivating properties are supplemented by charge transport capabilities has also been devised [6]. A radical polymerization or photopolymerization, mostly in the reverse micellar systems, has been employed [10, 11]. The processability of the resulting nanocomposite is of great importance and this is mostly related to the nature and structure of the surface ligand layer, the interaction between the inorganic core and polymer ligand layer and the structure of inorganic nanoparticles [12]. A method which has been reported as an efficient method to improve the interaction between nanoparticles and polymer is the introduction of covalent bonds between the nanoparticle surface and the polymer [13,14]. This method which occurs via polymerization of the ligand molecule could allow the nucleation and growth of the nanocrystals to occur directly inside the matrix through precursor molecules dispersed inside the matrices of the monomeric ligand.

We report here an alternative *in situ* free radical polymerization method utilizing polymerizable ligands with terminal double bonds to prepare surface stabilised and highly confined CdS nanoparticles. Starch was firstly modified to form the ester (acryloylated starch, AS), followed by the introduction of the Cd^{2+} ions, and finally an *in situ* polymerisation was initiated using Fenton's reagent in the presence of S^{2-} ions to generate CdS nanoparticle embedded within the polymer network.

7.2 Experimental

Materials: Cadmium acetate dihydrate, $Cd(Ac)_2 \cdot 2H_2O$, and sodium sulphide nonahydrate ($Na_2S \cdot 9H_2O$) were obtained from Associated Chemical Enterprise (ACE). Potato starch and hydroquinone (used as the inhibitor), pyridine, ferrous ammonium sulphate (FAS), hydrogen peroxide and benzoyl chloride were purchased from Sigma-Aldrich. Acrylic acid (Sasol) was freshly distilled under reduced pressure before use. The solvents ethanol, N,N′-dimethylacetamide (DMA), and N,N′-dimethylformamide (DMF), were purchased from Merck Chemical Company Inc.

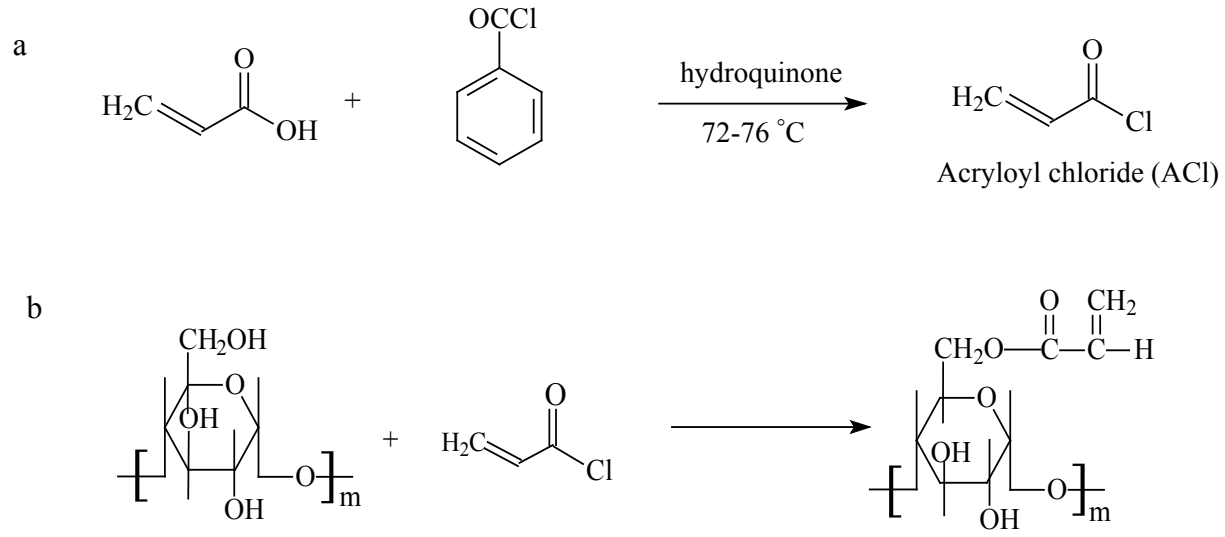

Scheme 7.1 (a) Synthesis of acryloyl chloride and (b) synthesis of acryloylated starch (AS).

7.2.1 Synthesis of acryloyl chloride and acryloylation of starch

The method of reported by Stampel *et al.* [15] was used for the synthesis of acryloyl chloride, whereby acrylic acid and benzoyl chloride were used. In the synthesis of acryloylated starch, the synthetic procedure of Fang *et al.* [16] was used. Scheme 7.1 shows the chemical steps used in the synthesis of the polymer.

7.2.2 Preparation of poly acryloylated starch copolymer-CdS

Water (50 mL) was added to acryloylated starch (5 mmol) and heated to 60 °C to form slurry. Cadmium acetate in distilled water (1.0 mmol, 2.5 mL) was added drop wise to the

acryloylated starch slurry. After all the cadmium acetate had been added, the mixture was continuously stirred under nitrogen while temperature cooled to room temperature. To this, 0.65 mmol of $Na_2S{\cdot}9H_2O$ (in 2.5 mL distilled water) was added drop wise and stirring was continued for 1 h at room temperature. Finally, free radical polymerization was initiated by the addition of Fenton's reagent, 25 mmol and 0.01 mol of ferrous ammonium sulphate (FAS) and H_2O_2respectively, to the reaction mixture and stirred for 3 h. The product was washed with ether and dried under vacuum at 45 °C. The same run was repeated for 1.5 and 2.3 mmol of cadmium acetate and 0.98 and 1.5 mmol of sodium sulphide respectively. The same concentration of acryloylated starch (5 mmol) was maintained throughout the run to obtain samples AS(5):CdS, AS(3.3):CdS, and AS(2.2):CdS respectively, reflecting the ratio of the acryloylated starch (AS) to the cadmium sulphide (CdS) nanoparticle.

7.2.3 Characterization

The absorption spectra and photoluminescence of the samples were measured on spectrophotometer and spectrofluorimeter respectively. Structural characterization was carried out by TEM and SEM analyses. FT-IR spectra were recorded on ATR mode. Detailed information on the analytical techniques used in this experiment is discussed in the supporting document.

7.3 Results and discussion

CdS quantum dots were prepared using pre-synthesized functionalized ligands containing a terminal double bond, under room temperature. A Schematic diagram of a possible growth mechanism of CdS quantum dots is shown in Scheme 7.2. The formation of CdS quantum dots capped by acryloylated starch could be described as follows: a lone pair of electrons of the oxygen atom of acryloylated starch attached to the surface of the Cd^{2+} ion and confined its size. Upon the introduction of the sulphide ion (S^{2-}), CdS was formed confined to the size of the quantum dots due the affinity of the oxygen. The oxygen atom forms a co-ordinative bond with the surface of CdS probably due to its chemisorption properties. Finally, intramolecular cross-linking reactions were engendered between CdS macromonomers (containing C=C groups). The [AS]: $[Cd(ac)_2]$ molar ratio was altered from 5 to 2.2, while the $[Cd(ac)_2]$:$[Na_2S]$ ratio was held constant at 1.5.

An increase in size were observed with decrease in the [AS]:[$Cdac_2$] ratio. The observed increase in particle size with decreasing ligand to precursor concentration ratio is supported in literature [17–19], and is consistent with the proposed competitive binding mechanism [20].

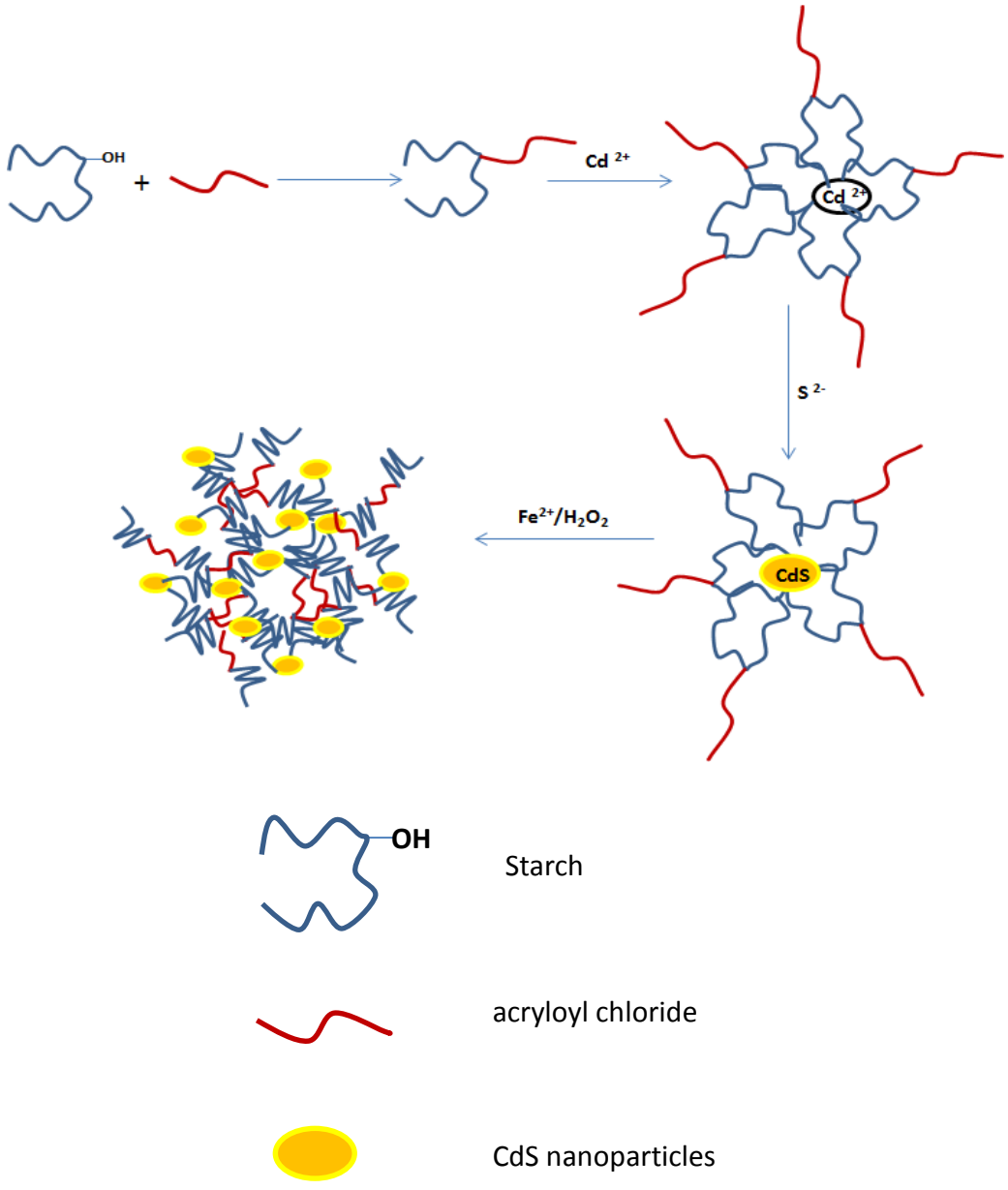

Scheme 7.2 Fabrication of PAS-CdS networks.

7.3.1 Optical properties

The absorption spectra of the PAS-CdS are shown in Appendix A1. All the spectra exhibit a well-defined absorption feature (peak) at ≈358 nm which is significantly blue-shifted

relative to the peak of absorption of bulk CdS (515 nm) [21], and indicates a pronounced role of quantum confinement [22]. In the PAS-CdS nanopatricles, the PAS formed passivation layers due to coordination interactions between the oxygen atoms of starch and CdS, thus prevent conglomerating of CdS particles and act as a quantum well. Therefore, AS encapsulation provides a restricted environment for the formation of the CdS nanocrystallites [23]. The reduction in size causes the electronic excitations to shift to higher energy, and the oscillator strength is concentrated into just few transitions due to changes in the density of electronic states [24].

The well-defined maximum at ≈358 nm is assigned to the optical transition of the first excitonic state. In the quantum confinement range, the extent of the blue shift in the excitonic peak of the nanoparticles is a function of the size. Generally, the band gap of the particles increase, as a result of quantum confinement of the photo generated electron-hole pairs. This results in the shift of absorption peak to lower wavelength, as the particle size decreases [25]. The significant blue shift clearly indicated a high degree of confinement of the synthesized nanoparticles.

The band gap energy was obtained from the absorption spectra (equation 1) and the shift in the band gap energy was utilized to calculate the particle radius (*r*), using the effective mass approximation [26], using the equation (1)

$$E^* = \frac{hc}{\lambda_c} \tag{1}$$

Where λ_c = wavelength of a photon of light propagating through the sample (distance/wave, usually m), and *c* is the speed of light

$$\Delta E_g = E_g^{nano} - E_g^{bulk} = \frac{h^2}{8r^2}\left(\frac{1}{m_e^*} + \frac{1}{m_h^*}\right) - \frac{1.8e^2}{4\pi\varepsilon\varepsilon_o r} \tag{2}$$

where m_e^* and m_h^* are the effective masses of an electron and a hole in the bulk CdS (m_e^* = 0.21= m_0, m_h^*= 0.80 = m_0) [25]. E_g^{nano} and E_g^{bulk} are the band gaps for the nanosized and bulk CdS (2.42 eV). ε = relative permittivity of CdS, 5.6 [27].

The estimated particle sizes obtained from the absorption spectra are given in Appendix B, Table 1. Particle sizes varied from 3.04 to 3.32 nm as the precursor concentration is varied from 1.0 to 2.3 mmol at a fixed stabilizer concentration of 5 mmol. The increase in particle

size with higher precursor concentration could be due to the increased concentration of the reactants (i.e. particles per given volume), and the surface area which resulted in a higher number of reaction sites. The greater the frequency of total collisions, the higher the reaction rate which could result in fast particle growth and aggregation.

The photoluminescence spectra of the samples AS(5):CdS, AS(3.3):CdS, and AS(2.2):CdS, showed emission peaks at about 575 nm (Appendix A, Fig. (B). the variation of the capping agent concentration appears to have no effect on the emission maxima. Similar observations have been reported whereby increasing particle concentration in the synthesis does not significantly alter the photoluminescence quantum yield [28]. However, a closer observation indicates that the samples at higher concentration displayed a shoulder peak at approximately 465 nm. The peaks are much shorter than the onset of absorption of ≈ 515 nm for bulk CdS, and may be assigned as band-edge emissions from particles of different sizes [25]. The absence of the band edge emission peak in the sample with higher concentration of starch-CdS ratio may be attributed to the reduction in particle size, and improvement in particle size distribution at higher concentration of the capping agent. This is consistent with the observation that the band edge emission decreases with decreased particle size at lower precursor concentrations [29]. It has been reported that in the intermediate case of distribution, which is neither too broad nor too narrow, appropriate excitation energy can excite several nanocrystals simultaneously producing a photoluminescence spectrum which contains more than one peak [25]. The photoluminescence spectra showed that increasing the molar concentrations of Cd^{2+} increased the intensity of the spectra. This could be ascribed to enhancement of the number of S^{2-} vacancies due to excess Cd^{2+} ions. The unchanged position suggests that the defect concentrations is not very high in the AS/CdS system, because the PL peak will red-shift with decreasing the amount of sulphur vacancies if the defect concentration is enough [23,30].

7.3.2 Structural properties

Appendix C1, Figure (a and b) show the TEM images of CdS nanoparticles at different precursor to polymer ratios. The morphology indicates that the nanoparticles are clearly well identified and are spherical. At higher capping group concentration, the nanoparticles are well dispersed and no effective aggregation of bulk particles is formed, indicating effective capping of PAS on the nanoparticle surfaces. However, the images at lower ratio indicate the setting in of agglomeration which may be due to increase in the concentration of the

nanoparticles. The reason for the appearance of aggregates of CdS nanoparticles may be due to static attraction of their surface groups [31]. Nanoparticles have higher surface atoms compared to the bulk molecules. In this process, PAS lowers the surface energy of the nanoparticles. The TEM images showed that the ratio of PAS to CdS plays an important role in enhancing the monodispersed property of CdS nanoparticles. From the TEM images, the sizes of the nanoparticles from [PAS]:[$Cdac_2$] = 5 is approximately 3.5 nm, while the size at lower ratio (b) is approximately 4 nm. A little increase in size of particles compared to the obtained values from UV could be due to the fact that the particles shown in TEM images includes the CdS nanoparticles core and PAS macromonomer organic shell, while the calculated sizes of CdS nanoparticles via Brus's formula only refer to the inorganic cores. The images showed that, using the right polymer to precursor ratio, it is possible to identify the boundary of nanoparticle even under cross-linking polymerization. Appendix C1 (Fig. c) is a SEM micrograph, which shows the surface morphology of PAS-CdS obtained from PAS and 2 mol of the precursor compound. The image indicates that the nanoparticles are dispersed within the polymer cross-linked network as white dots and are homogenous.

7.3.3 FTIR analysis

The surface morphology of the synthesized materials was investigated using FTIR spectroscopy to confirm the capping of the particles by PAS (Fig.7.1). In Figure 7.1 (a), the IR spectrum of starch showed absorption bands at 3262 $cm^{-1}$and at 1633 cm^{-1} due to OH stretching and bending modes respectively, and at 2925 and 1074 cm^{-1} due to C-H stretching and bending respectively.

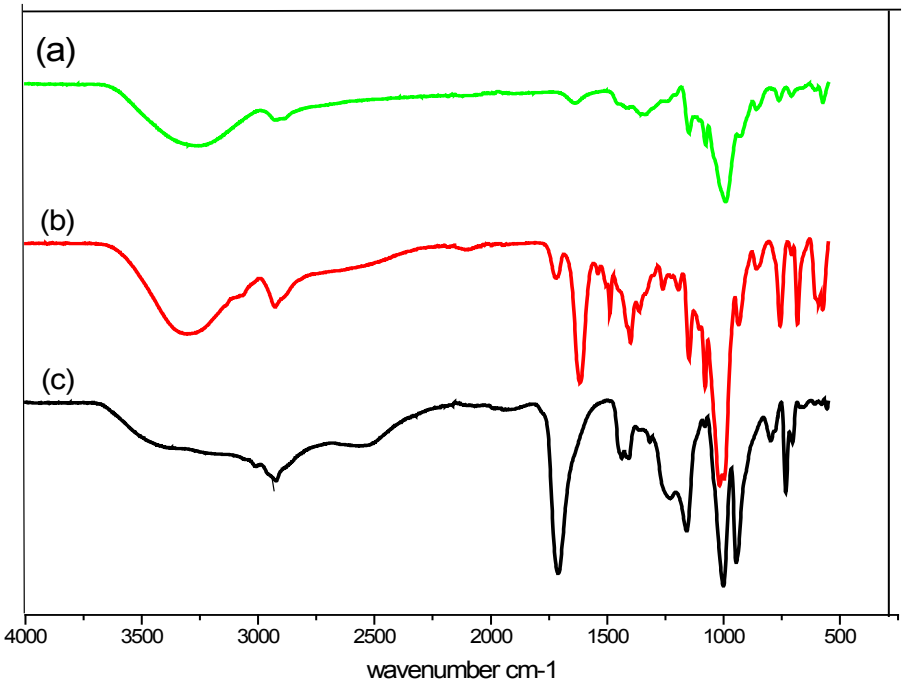

Figure 7.1 FTIR spectra of (a) starch, (b) AS and (c) PAS-capped CdS nanoparticles.

The starch ester, in Fig.7.1(b), shows additional peaks at 1721 cm^{-1} due to C=O from the ester bond formation, and an intensive peak at 1618 cm^{-1} due to C=C double bond vibration. The CdS nanoparticle capped with poly acryloylated starch (PAS), in Fig.7.1(c), showed a more intensive peak around 1710 cm^{-1} and at 2922 due to carbonyl and C-H stretching modes respectively, which confirms a successful polymerization of AS after the formation of CdS nanoparticles *in situ*. However, the broad O-H peaks around 3260 due to stretching and at 1633 cm^{-1} from the bending modes in the acryloylated starch ester Fig. 7.1(b) have almost disappeared in Figure 7.1 (c); this confirms that the hydroxyl groups in the starch ester have taken part in the bond formation with CdS nanoparticles.

7.3.4 Application of xanthate as sulphur donor group

Apart of from metal scavenging activity in aqueous medium, xanthates find application in the synthesis of complexes which serves as single source precursors to chalcogenidenanoparticles. The presence of sulphur in xanthate molecule allows the direct boding to the central metal and subsequent formation of M-S particles after thermolysis of the

compound. The ease and stability of the complexation reactionis on the fact that group 12 metals act as strong Lewis acids, and hence readily complex to electron-rich sulphur containing ligands in the principle of Hard Soft Acid Base, HSAB [29]. The complexes are importantly used in the synthesis of nanoparticles for various applications. Moreover, xanthate complexes are air-stable with reasonable volatility and readily obtained in good synthetic yields [32,33].The use of novel heteroleptic complexes of xanthate (S_2CObu) and dithiocarbamate (S_2CNMePh) in the synthesis of monodispersed spherical and hexagonal shaped ZnS and CdSnanocrystals respectively [34].

7.4 Conclusion

In conclusion, we have prepared highly confined CdS quantum dots of narrow particle size distribution using copolymerisation of acryloylated starch. The morphology and optical property of the products were investigated. The method provides an advantage over the ex-situ approach, as it allows a much better control of the particle dispersion and density, avoiding agglomeration and clustering of nanoparticles

7.5 References

[1] Fan D., Afzaal M., Mallik M.A., Nguyen C.Q., O'Brien P., Thomas P.J. *Coord. Chem. Rev.* 2007, 251:1878–1888

[2] Yang S.Y., Li Q., Chen L., Chen S. *J. Mater.Chem*.2008, 18: 5599–5603

[3] Nigel I., Pickett, O'Brien P. *Chem. Rec.* 2001, 1:467–479

[4] Xie J., Bu X., Zheng N., Feng P. *Chem.Commun*. 2005, 47:4916–4918

[5]Lu C., Cui Z., Wang Y., Li Z., Guan C., Yang B., Shen J. *J. Mater. Chem.*2003, 13:2189–2195

[6] Cheong N., Chan Y, Schrock R.R., Cohen R.E. *J. Am. Chem. Soc.* 1992, 114:7295–7296

[7] Mofftt M., McMahon L., Pessel V., Eisenberg A. *Chem. Mater.*1995, 7:1185–1192

[8] Yue J., Sankaran V., Cohen R.E., Schrock R.R. *J. Am.Chem. Soc.*1993, 115:4409–4410

[9] Fogg D.E., Radzilowski L.H., Dabbousi B.O., Schrock R.R., Thomas E.L., Bawendi M.G. *Macromolecules* 1997, 30:8433–8439

[10] Hammouda A., Gulik T., Pileni M.P. *Langmuir* 1995, 11:3656–3659

[11] Berg J.M., Claesson P.M. *J. Colloid Interface Sci.*1994, 163:289–298

[12] Guo W., Li J.J., Wang Y.A., Peng X. *J. Am. Chem. Soc.*2003, 125:3901–3909

[13] Chen S., Zhu J., Shen Y., Hu C., Chen L. *Langmuir* 2007, 23:850–854

[14] Chen L., Zhu J., Li Q., Chen S., Wang Y. *Eur. Polym. J.* 2007, 43:4593–4601

[15] Stampel G.H., Cross R.P., Mariella R.P. *J. Am. Chem. Soc.* 1950, 72:2299–2300

[16] Fang J.M., Fowler P.A., Hill C.A.S. *J. Appl. Polym.Sci.*2005, 96:452–459

[17] Nosaka Y., Yamaguchi K., Miyama H., Hayashi H. *Chem. Lett.* 1988, 17:605–608

[18] Kundu M., Khosravi A.A., Kulkarni S.K., Singh P. *J. Mater. Sci.* 1997, 32:245–248

[19] Khosravi A.A., Kundu M., Kuruvilla B.A., Shekhawat G.S., Gupta R.P., Sharma A.K., Vyas P.D., Kulkarni S.K. *Appl. Phys. Lett.*1995, 67:2506–2508

[20] Swayambunathan V., Hayes D., Schmidt K.H., Liao Y.X., Meisel D. J. *Am. Chem. Soc.* 1990, 112:3831–3837

[21] Wang W., Germanenko I., Samy El-Shall M. *Chem. Mater.* 2002, 14:3028–3033

[22] Pattabi M., Amma B.S. *Sol. Energ. Mater. Sol.*2006, 90:2377–2383

[23] Yang Y, Chen H, Bao X. *J. Crys. Growth* 2003, 252:251

[24] Alivisatos A.P. *Science* 1996, 271:933.

[25] Prabhu R.R., Khadar M.A., *Pramana J. Phys.* 2005, 65:801–807

[26] Brus L. *J. Phys. Chem.*1986, 90:2555–2560

[27] Winkelmann K., Noviello T., Brooks S. *J. Chem. Educ.*2007, 84:709–710

[28] Winter J.O., Gomez N., Gatzert S., Schmidt C.E., Korgel B.A. *Colloids Surface A*: *Physicochem. Eng. Aspects* 2005, 254:147–157

[29] Pattabi M., Amma B.S., Manzoor K. *Mater. Res. Bull.* 2007, 42:828–835

[30] Wada Y, Kuramoto H, Anand J, Kitamura T, Sakata T, Mori H. *J. Mater. Chem.* 2001, 11:1936–1941.

[31] Saravanan L., Diwakar S., Mohankumar R., Pandurangan A., Jayavel R. *Nanomater. nanotechnol*. 2001, 1:42–48

[31] Onwudiwe D.C., Ajibade P.A. *Polyhedron* 2010, 29:1431–1436

[32] Barreca D, Tondello E., Lydon D., Spalding T.R., Fabrizio M., *Chem. Vap. Depos.* 2003, 9:93–98

[33] Armelao L., Barreca D., Bottaro G., Gasparotto A., Maragno C., Sada C., Spalding T.R., Tondello E., *Electrochem. Soc. Proc.* 2003, 8:1104–1109

[34] Onwudiwe D.C., Mohammed A.D., Christien A. Strydom C.A.,Young D.A., Jordaan A. *Superlattices Microstruct.* 2014, 70:98–108

Chapter 8

Conclusions and recommendations

8.1 Conclusion

Chemical modification of these two sustainable resources, starch and glycerol, has given a versatile understanding of their applications from superabsorbent materials to metal scavenging activity, down to their usage as capping agent of nanoparticles. The aim of the research work was to add or to improve some desirable properties to the starting materials without sacrificing their needed native properties. A series of chemical techniques were employed to achieve this goal; acryloylation, grafting and xanthation were proven to be effective ways in obtaining materials for wide range of applications. However, from the stated objectives of the work in Chapter one, the following conclusion are derived:

1 Cross-linking and acryloylation of starch with acryloyl chloride and grafting with acrylic acid using Fenton's initiation system were successfully achieved. The amount of acryloylation agents determined the degree of substitution of the ester produced. Pyridine was used as a nucleophilic acylation catalyst and also as a base. The hydrochloric acid formed as a by-product in the course of the reaction reacted with excess pyridine to form a pyridinium salt that was easily separated from the reaction product after dissolution in methanol. The substituted starch ester was maintained at a degree of substitution (DS) value in a range of 0.8–1.00, because at a higher DS more cross-linking occurred between the starch molecules which could lead to a rigid, brittle and poor water-dispersibility of the polymer structure.

2 The superabsorbency of the polymers obtained from chemically-modified starch was thoroughly investigated in water, saline solution and under load. In some case solvent entrapment of the samples was tested. Moreover, the product showed a gradual increase in the absorbency with degree of neutralisation up to of 80% (5.6) and good retention capacity (97%), which could be associated with the molecular structure of the product and nature of distribution of the hydrophilic ends in the polymer, and this augurs well when compared with other works in which neutralisation did not exceed 60 or 70%. The product, AS-g-poly AA, showed a higher absorption values when compared with starch poly (AA) synthesised from direct grafting.

3 The effective use of glycerol diacrylate as cross-linking agent was studied. The glycerol acrylate was synthesised by acryloylation reaction from acryloyl chloride and pyridine, which was later used in different proportions in the synthesis of cross-linked copolymers of poly (acrylic acid) and acryloylated starch. The effect of a

cross-linker on the physico-chemical properties was also studied. A sample of GA-PAA containing 0.8 % GA was found to absorb 395 g/g and 66 g/g of water and saline solution respectively. Different solvents uptake was tested with the sample with varying capacity in different solvents. Neutralisation of the polymer up to 6.5 increased the absorbency in both water and saline solution. Moreover, the structural features and absorbency of the samples were affected by the cross-linking density in the polymer. The XRD showed a slight change in the crystallinity of the polymer with cross-linking density, on the other hand the absorbency in both water and saline solution decreased with increase in the glycerol acrylate (cross-linking agent). There was a remarkable increase in the absorbency of acryloylated starch poly(acrylic acid) containing glycerol acrylate as cross-linking agent; from 127 g/g to 330 g/g of water absorbency for the polymer sample without and with cross-linking agent respectively.

4 An alternative use of initiator radical was attempted using an Oxy-catalyst initiator in the copolymerisation of acrylic acid onto starch. The catalyst was used for the first time, instead of ferrous ammonium sulphate with hydrogen peroxide to initiate graft-copolymerisation of starch with acrylic acid with aluminium triflate as co-catalyst. The percentage add-on (% add-on) and the grafting efficiency (GE %) were quite dependent on the amount of co-catalyst, temperature, starch to monomer ratio and time of the reaction. By varying the reaction conditions, a polymer product with add-on of 47 % and GE of 82.8 % with low amount of homopolymerswas obtained. However, the catalyst had low efficiency in terms of grafting parameters when compared with Fenton's initiation system.

5 In all the chemical processes involved in the modification of starch and glycerol, there is noticeable change in thermal and structural behaviour of the starting materials. The introductions of new bonds and reorientation of the structural network as a result of the chemical transformations lead to the decrease or increase in thermal stability of the samples on one hand, and structural changes on the other.

6 Synthesis of starch and glycerol xanthates and their metal scavenging activity were studied for lead, cadmium and copper(II) ions from waste waters. Easy and fast complexation reactions between the heavy metal ions and the sulphur atoms in the xanthate, followed by precipitation of the insoluble metal complex showed how effective and reliable these xanthates are. The structural features of xanthates from these sustainable substances could allow more xanthate groups to be synthesised in

their structures.This explains why they are more efficient in the metal scavenging activity than common alky xanthates, like butyl xanthate. In this study, moreover, glycerol xanthate was found to be the most effective, as a lower dosage was required and not dependent on pH like the insoluble starch xanthate and the alkyl xanthates.

7 Miscellaneous applications of xanthates were studied, for instance, as capping agents of nanoparticles and sulphur donor species in the production of nanoparticles. A highly confined CdS quantum dots of narrow particle size distribution was synthesised using copolymerisation of acryloylated starch. The morphology and optical property of the products were investigated. The method provides an advantage over the ex-situ approach, as it allows a much better control of the particle dispersion and density, avoiding agglomeration and clustering of nanoparticles.

8.2 Recommendations for future work

Based on the research results obtained from this work, the following recommendations are postulated for future research work:

1. This research work covers the synthesis of superabsorbent copolymers from starch and poly (acrylic acid) after some series of chemical reactions: from synthesis of acryloyl chloride to acryloylation and the grafting reactions. Finally the absorbency of the polymer products is enhanced after neutralisation to the desired pH. It is however, recommended that an *in situ* option should be attempted whereby all the processes discussed above are to be carried out in a single reaction vessel so as to minimise the cost of material and time resources
2. Applications of starch and glycerol xanthates should explored with a view to the scavenging activity on other heavy metals such as platinum, palladium and rhodium from their ionic solutions. In other words, the effective usage of the xanthates as metal scavengers should be attempted on non aqueous medium, as the present work only dealt with the metal removal activity in aqueous media. In other words here is an opportunity to commercialise glycerol xanthate, since it could be effectively used in floatation and separation of different minerals and metal ions.

Appendices

Appendix A: Absorption spectra of PAS-CdS

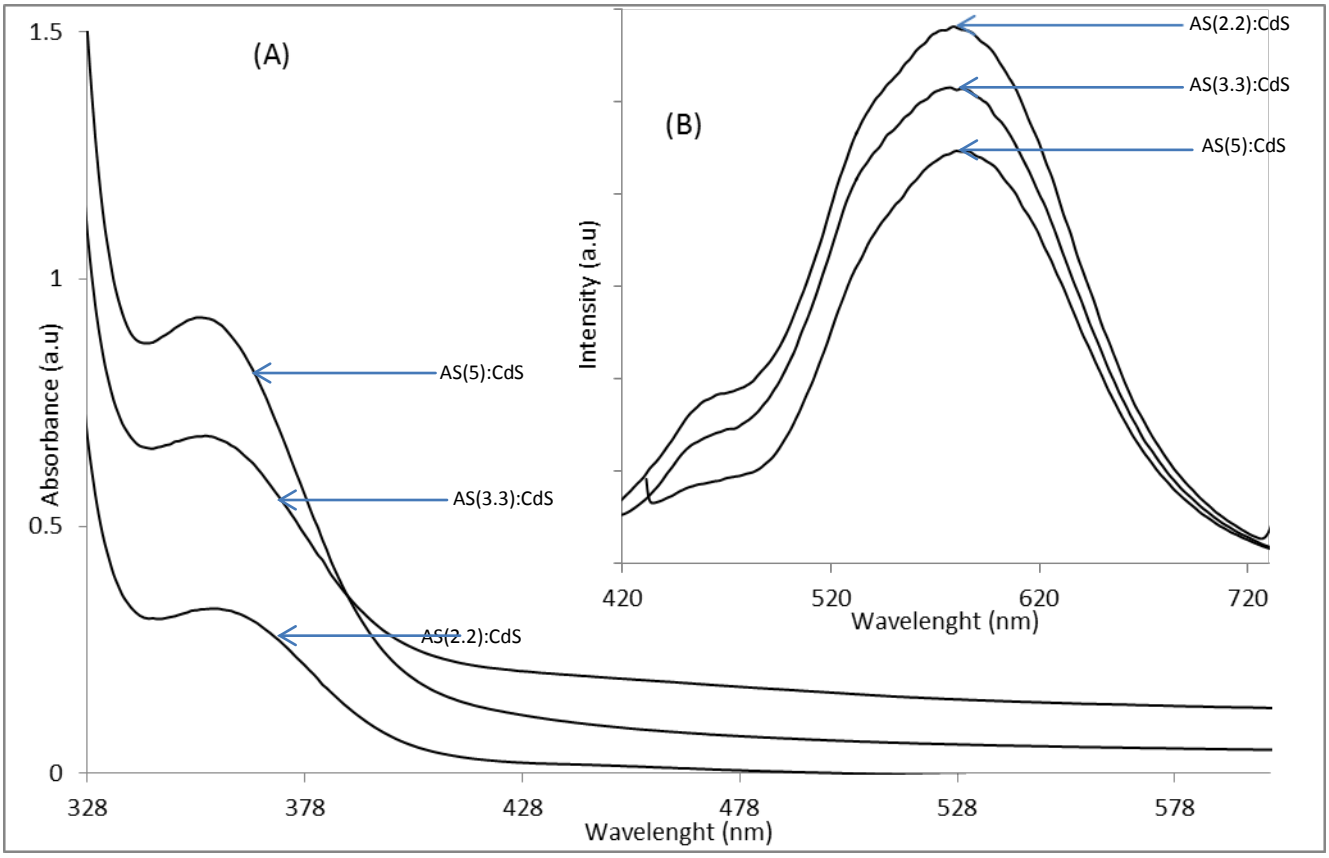

Figure A1 (A) UV and (B) Photoluminescence spectra of CdS nanoparticles stabilized by PAS macromonomers at different stabilizer to $Cd(ac)_2$ ratio.

Appendix B: Absorption spectra

Table B1. Optical band gap and the estimated particle sizes from the absorption spectra at different precursor concentration and a fixed capping group concentration of 5 mmol.

Precursor concentrations (mmol)	Band gap (eV)	Particle size(nm)
1.0	3.13	3.04
1.5	3.07	3.24
2.3	3.03	3.32

Appendix C: Structural properties of CdS nanoparticles

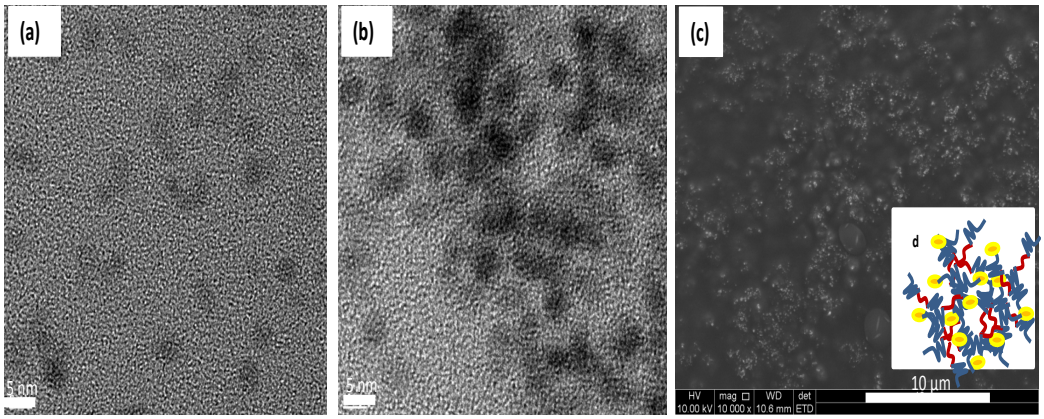

Figure C1. High maginification TEM images of (a) CdS nanoparticles stabilized by PAS macromonomers [PAS]:[$Cdac_2$] = 5: 1, (b) CdS nanoparticles stabilized by PAS macromonomers [PAS]:[$Cdac_2$]= 2.2:1, (c) SEMimages of CdS nanoparticles stabilized by cross-linking network, (d) diagram of cross-linking network.